DISSERTATION

DEVELOPMENT OF METHODS FOR ASSESSING OXIDATIVE STRESS CAUSED BY ATMOSPHERIC AEROSOLS

Submitted by

Yupaporn Sameenoi

Department of Chemistry

In partial fulfillment of the requirements

For the Degree of Doctor of Philosophy

Colorado State University

Fort Collins, Colorado

Fall 2012

Doctoral Committee:

Advisor: Charles S. Henry

Tomislav Rovis
Delphine K. Farmer
Alan K. Van Orden
Matthew J. Kipper

ABSTRACT

DEVELOPMENT OF METHODS FOR ASSESSING OXIDATIVE STRESS CAUSED BY ATMOSPHERIC AEROSOLS

Extensive epidemiological studies show strong associations between the exposure to atmospheric aerosol particulate matter (PM) in the size range of 0.1- 10 μm and health problems, including respiratory, atherosclerosis and cardiovascular diseases. However, the mechanisms of PM-induced toxicity are poorly understood. A leading hypothesis states that airborne PM induces harm by generating reactive oxygen species in and around human tissues, leading to oxidative stress. To improve understanding of this effect, methods including biological assays and chemical assays for assessing oxidative stress caused by atmospheric aerosols have been developed and are described in this dissertation. For biological assays, a cleavable tag immunoassay (CTI) was developed with an ultimate goal of measuring multiple oxidative stress biomarkers in a single run. As a proof-of-concept, the multianalyte analysis system CTI was performed in competitive, non-competitive, and mixed formats for detection of small molecules and protein biomarkers simultaneously. For chemical assays, a microfluidic electrochemical sensor and a microfluidic paper-based analytical device (μPAD) have been developed for assessing aerosol oxidative stress in an area-based exposure study and a personal exposure study, respectively. The microfluidic electrochemical sensor was used for assessing aerosol oxidative stress by measuring the oxidative activity. The sensor was coupled directly to a Particle-into-Liquid-Sampler (PILS) to create an on-line aerosol sampling/analysis system. The system offers analysis with 3 minute temporal resolution, making it the best available temporal resolution for

aerosol oxidative activity. The sensor was also used to analyze the ability of aerosols to generate hydroxyl radicals as another parameter for assessing aerosol oxidative stress. The ultimate goal of this system is to create an on-line monitoring system using a similar approach for oxidative activity analysis. As a first step toward this goal, assay optimization and system characterization in an off-line format employing flow injection analysis and amperometric detection, were carried out and presented in this dissertation. A microfluidic paper-based analytical device (μPAD) was developed for measuring oxidative activity of aerosol collected by a personal sampler. The system allows analysis with minimal sample preparation and requires 100-fold less particulate matter mass than existing analysis methods.

ACKNOWLEDGEMENTS

First of all, my Ph.D. work would have not been possible without the financial support from the Royal Thai Scholarship, Ministry of Science and Technology. The research described in this dissertation was funded by National Institute of Environmental Health Sciences (NIH grant number ES019264).

Second of all, I want to thank my advisor Dr. Charles S. Henry for his advice and role in raising me into an independent, confident, critically thinking scientist. The research in this dissertation would have not been successful without his helps. I appreciate all his contributions of time, ideas, and funding to make my Ph.D. experience productive and stimulating. I am also thankful for the excellent role model he has presented as a successful chemist and professor.

People in Henry research group both the former members and current members are acknowledged for having been a source of friendships, advice, assistance and collaboration. In particular, I would like to thank Dr. Meghan M. Mensack for her contribution on the immunoassays and microfluidic electrochemical sensor development.

Volckens research group is also gratefully acknowledged. All of on-line monitoring of aerosol oxidative activity experiments were carried out in the Volckens's lab. I would like to thank Dr. John Volckens for his valuable guidance and assistance throughout my research on chemical assay developments for aerosol oxidative activity including on-line systems and paper based devices. Dr. Kirsten Koehler and Jeff Shapiro are acknowledged for their contributions to make the on-line monitoring system for aerosol oxidative activity success. I also would like to thank Ashleigh Kayne for her helps on personal sampler set up. Taylor Carpenter is also

acknowledged for her assistance with gravimetric analysis of personal filter samples and sample collection.

Dr. Jeff Collett, Jr and Dr. Yele Sun are appreciated for their contribution and supports for the Particle Into Liquid Sampler instrument and extracted aerosol samples for the oxidative activity study.

I also would like to thank a number of people from Chulalongkorn University, Thailand who once came here as exchange students for their helps with my research. Pantila Panymeesamer and Natcha Supalakorn contributed to the paper based device for aerosol oxidative activity. Dr. Wijitar Dungchai helped teaching the electrode fabrication.

Thanks for people who helped me out to create a nice graphic abstract on the *JACS* paper. Akeapot Srifa provided his picture taken at the nuclear power plant, Florida as represent to air pollution. Piriya Wongkongkathep helped adjust the picture to make it more beautiful.

My time at Colorado State University has been made enjoyable because of new friends I have met along the way. All of them are appreciated. Thanks to all my Thai friends at CSU who have made me feel so warmth and feel so much better when getting homesick. Thanks to my classmates especially Dongmei Zhang and Brendan Tompkins for sharing and helping me throughout the course of graduate work.

Finally, I gratefully acknowledge my family for all their love, support and encouragement. For my grandparents and my parents who raised me with their love, care and always believed in my abilities and supported me in all my pursuits. For my brother who always cheered me up in every direction I go. And for my husband, Sarayuth Ajvanishchakul, I want to thank him for all his faithful love, support, patience and understanding. Even being so far away

during my time as a graduate student, he has been joining me every moment of happiness and sorrow.

This work is dedicated to my grandparents, Manee and Lhom Samorkhang and my parents, Nhoo-Aun and Nhoo-Pit Sameenoi.

TABLE OF CONTENTS

CHAPTER 1. DEVELOPMENT OF METHODS FOR ASSESSING OXIDATIVE STRESS CAUSES BY ATMOSTPHERIC AEROSOLS: AN INTRODUCTION

Atmospheric aerosols (airborne particulate matter, PM) are suspensions of liquid or solid particles in the atmosphere with particle diameters in the range of 1 nm – 100 μm.[1] They are emitted from a wide variety of sources including natural and anthropogenic sources.[2] Epidemiological and clinical research has demonstrated strong links between atmospheric aerosols and adverse health effects including premature death,[3] impaired pulmonary function,[4] neurodegenerative disorders,[5] and respiratory and cardiovascular disease. Due to the variety of sources, large particle size range, and varying chemical compositions, the biochemical mechanisms and molecular processes of how aerosol particles cause toxicity are not yet understood.[6-9] To date, one of the most widely proposed and promising hypotheses regarding aerosol toxicity is the generation of oxidative stress, initiated by the formation of reactive oxygen species (ROS) within affected cells.[8,10] Various approaches for measuring the oxidative activity of PM have been developed to study PM-induced oxidative stress to better understand how PM affects human health.[11-14] These approaches rely on chemical composition measurement to estimate the oxidative stress where analysis is based on both biological and chemical assays. Biological assays employ subject exposure to aerosols with analysis of oxidative biomarkers typically carried out *via* enzyme-linked immunosorbant assays (ELISA). However, ELISA typically involves single analyte detection with analysis times of 4-8 h including assay and hands on time. Chemical assays employ a variety of off-line and on-line methods for the detection of chemical compounds associated with the oxidative stress generation in collected aerosols. However, they are limited by aerosol sample collection, handling, storage artifacts, low temporal

resolution, high cost and low portability. To address problems associated with current assays, my research has focused on the developing methods for both biological and chemical assays. A multi-analyte immunoassay for monitoring oxidative stress biomarkers has been developed to overcome the limitations of ELISA in biological assays.[15] For chemical assay development, two microfluidic devices made of poly(dimethylsiloxane) (PDMS) and paper have been developed to measure aerosol oxidative activity. The PDMS device uses electrochemical detection to measure oxidative activity in an on-line format suitable for area-based exposure studies.[16,17] The paper-based microfluidic device uses colorimetric detection to measure PM oxidative activity while requiring 100-fold less PM mass than the existing analysis methods for personal exposure study.

ATMOSPHERIC AEROSOLS: ORIGINS, PARTICLE SIZE, COMPOSITION

Airborne particulate matter (PM) is generated from a wide variety of natural and anthropogenic sources.[2,18] Primary PM is directly released into the atmosphere by combustion (e.g., biomass burning, incomplete combustion of fossil fuels), volcanic eruptions, wind-driven suspension (from road, construction site, sea salt, soil, mineral dust) and biological materials (e.g., pollen, plant fragments, bacteria, microorganisms).[2,19] Secondary PM are formed from photochemical reactions of species in gas-phase, producing less volatile species that form particles in the atmosphere by nucleation and condensation (e.g., ozone, NO_x).[2] Both primary and secondary PM are capable of undergoing further physical and chemical interactions and transformations causing changes in particle size, structure and composition *via* coagulation, restructuring, gas uptake, and/or chemical reaction.[2]

Aerosols can also be classified as indoor and outdoor PM.[20] Indoor aerosols can be generated from cooking and combustion, building materials, air conditioning, consumer

products, smoking, heating as well as biologic agents. Example products released from these activities include primary aerosols (e.g. tobacco, wood smoke, microbial agents and organic dust) and a number of chemicals such as CO, CO_2, volatile organic compounds (e.g., aldehydes, ketones), polycyclic aromatic hydrocarbons (PAHs).[21,22] Outdoor PM is created from outdoor sources including industrial, commercial, mobile engine, urban, regional, agricultural, and natural. Products released from this aerosol type are similar to those from indoor aerosols but appear in different ratios.[23]

Additionally, PM are also characterized according to their aerodynamic diameter into size fractions including coarse particles (size of 2.5-10 μm), fine particles ($PM_{2.5}$, size < 2.5 μm) and ultrafine particles (size < 0.15 μm).[24] These particles are generated from a wide variety of sources and mechanisms. Coarse particles are generated as primary aerosols from various sources including suspension from agitated soil (farming, mining, unpaved roads), construction, plant and animal fragments. They are mainly formed by the mechanical breakdown (crushing, rubbing, grinding of the surfaces) of coating material, minerals and organic waste. $PM_{2.5}$ is primarily generated from power plants, oil refining and metal processing facilities, wildfires, tailpipe and brake emissions from mobile sources, residential fuel combustion. $PM_{2.5}$ is also formed from the process of gas-to-particle conversion by condensation and coagulation. Ultrafine particles are typically produced through fresh emissions from diesel and gasoline combustion and/or tailpipe emissions from mobile sources (motor vehicles, aircrafts, and ships). They are also created as secondary aerosols by the nucleation mode.[25] Residence time in the atmosphere of these PM ranges from minutes to weeks depending on PM properties and meteorological conditions.[19,26]

The composition and concentration of atmospheric PM are also highly variable. Mass concentrations and the total particle number present in the ambient air normally vary in the range of 1–100 $\mu g\, m^{-3}$ and 10^2–10^5 cm^{-3}, respectively.[19,27] The main chemical components of PM are sulfate, nitrate, ammonium, organic compounds, black or elemental carbon and other chemicals from sea salt and mineral dust. These components represent 10-30% of the overall PM mass. Toxic compounds such as PAHs, quinones and transition metals are present as minor components.[28] However, different locations, times, meteorological conditions, and particle size fractions can cause variations of an order of magnitude or more in the relative quantity of different chemical components.[19,29] For example, chemical compositions, total particle numbers and mass concentrations of ultrafine PM measured in urban air (Munich, Germany, 500 m above sea level) and high alpine air (2600 m above sea level) were substantially different.[2] Based on $PM_{2.5}$ analysis, organic compounds, black carbon and elemental carbon were major components (~42%) while sulfate ions were a minor component (~15%) in urban area. In contrast, equal amount of organic compounds as sulfate ions were present in high alpine air (~33% each).[2,19,29-32] Approximate total particle number concentrations were 10^2 cm^{-3} in high alpine air and 10^4 cm^{-3} in urban air. Similarly, particle mass concentrations were 1 $\mu g\ m^{-3}$ and 10 $\mu g\ m^{-3}$ in high alpine air and in urban air, respectively.[2]

HEALTH EFFECTS BY ATMOSPHERIC AEROSOLS: OXIDATIVE STRESS

Numerous epidemiological studies show that atmospheric aerosols are correlated with adverse health effects including enhanced mortality, cardiovascular, respiratory, and allergic diseases.[6,8,9] Due to the high variability of aerosol sources, compositions, properties, and

transformation processes, the actual effects of aerosols on health are still unclear. Some of the possible mechanisms of atmospheric aerosols affect human health are:[6]

1. Atmospheric aerosols- or ozone-induced pulmonary inflammation
2. Free radical production (particularly, reactive oxygen species (ROS)) and oxidative stress generation by transition metals and organic chemical compounds (eg, PAHs, quinones)
3. Covalent modification of key intracellular proteins (eg, enzymes)
4. Biologic compounds, such as endotoxin and glucans, which induce inflammation and innate immune effects
5. Stimulation of nocioreceptor and autonomic nervous system activity, which regulates heart rate variability and airway reactivity
6. Adjuvant effects in the immune system (eg, diesel exhaust particulates and transition metals increasing responses to common environmental allergens)
7. Procoagulant activity by ultrafine particles after access to systemic circulation
8. Suppression of normal defense mechanisms (e.g. suppression of alveolar macrophage functions)

Of these possible mechanisms, oxidative stress caused by the generation of ROS in the affected cells is the most widely proposed and promising hypothesis for adverse health effects in humans.[7,24,33] For example, extensive studies have used diesel exhaust particulates (DEP) as model aerosols to study airway inflammation demonstrating that the pro-inflammatory effects of DEP and concentrated air particles results in enhancing allergic inflammation, acute asthma exacerbation and bronchitis flares which are linked to ROS production.[34-36] Oxidative stress is defined as a serious imbalance between production of reactive oxygen species (ROS) and body's antioxidant defense.[37] ROS originate as a natural byproduct of the normal metabolism of oxygen

and play important roles in cell signaling.[38] However, when present at high levels, they can result in significant damage to cell structures. The presence of these species and their resulting harm to important macromolecules such as DNA, proteins and lipids have been linked with numerous diseases including respiratory, cardiovascular and neurodegenerative disorders.[39-41] Atmospheric PM can generate oxidative stress due to both composition and size. Different PM fractions have substantially different abilities to penetrate cellular targets.[42] Ultrafine PM are believed to be the most hazardous to human health since they are small enough to penetrate the membranes of the respiratory system and get into the blood circulation and transportation through olfactory nerves into the brain.[42-44] Larger sizes of PM ($PM_{2.5}$ and PM_{10}) are also capable of penetrating cellular targets in the lung and systemic circulation.[42] These PM, moreover, arepresent at high concentration in the ambient air and have large surface area per unit mass resulting in enhanced absorption of metals and a large number of organic compounds.[45] These metals such as Fe, V and Cr, even present at very relatively low levels compared to overall PM mass load, can cause the PM to be toxic by participating in Fenton chemistry.[46,47] Organic compounds such as polycyclic aromatic hydrocarbons (PAHs) and quinones can also generate ROS.[48] Because of the chemical complexity of aerosols and the various pathways for oxidation reactions, comprehensive investigations conducted to understand how aerosol particles cause oxidative stress need to consider the size of aerosol particulates as well as their chemical reactivity. Various particles sizes have differences in their chemical compositions as a result of their different sources of origin and modes of generation described above. These differences lead to different oxidative activity and ability to cause mitochondrial damage. Relative composition, oxidative activity and other characteristics of PM fractions are compared in Table 1.1.[17,22,39]

Table 1.1. Contrasting characteristics of ultrafine, fine and coarse particles.

Parameter	**Ultrafine**	**Fine**	**Coarse**
Size (μm)	<0.15	<2.5	2.5-10
Particle number (m^{-3})	***[a]	**	*
Mass (μg m^{-3})	*	**	***
Surface area	***	**	*
Bioavailability of active compounds	***	**	*
Penetrability	***	**	*
Organic carbon content	***	**	*
Elemental carbon content	***	**	*
Metal as % of total element	*	**	***
PAH content	***	**	*
Oxidative activity	***	**	*
Mitochondrial damage	Extensive	Some	None

[a] ***** = high, ** = medium, * = low**

The important finding in which PM caused mitochondrial damage demonstrated that the PM can cause oxidative stress in affected cells.[46] The exact mechanism of PM induced mitochondrial damage, however, is still unknown. Various mechanisms for this damage have been proposed including ability of PM to penetrate cell walls as well as their high surface area to absorb toxic chemicals to generate ROS in cells.[10,49] Again, since the chemical complexity of the PM and various composition and transformation leads to the oxidation reaction caused by the PM, it is necessary to improve the analytical methods capable of measuring oxidative stress as a

result of PM exposure in order to allow for a better understanding of how PM causes adverse health effects in humans.

METHODS FOR ASSESSING OXIDATIVE STRESS CAUSED BY AEROSOLS

Biological Assays

Current methods for assessing aerosol oxidative stress are based on both biological and chemical assays. In biological assays, *in vitro* model systems such as cells in systemic circulation (pulmonary cells, lung epithelial cells and mitochondria or macrophage cell lines, etc.) or whole animal models are exposed to PM and changes in specific markers of oxidative stress analyzed. The exposure system is conducted either *via* a direct inhalation fashion (whole animals)[33,50,51] or the biologically related deposition of PM (*in vitro*)[46,52-54] and the analysis for oxidative stress carried out. Analytical measurements employed for assessing oxidative stress in biological systems are largely based on fluorescence assays[52,55,56], glutathione ratio assays[46,57], lipid peroxidation analysis[50], immunoassays[46]. Principles, advantages, and disadvantages of some of the most widely used biological assays are discussed here.

Fluorescence assays have been widely used for evaluating oxidative stress in biological exposure studies. The assay is based on the addition of an inactivated form of a reduced dye (2′,7′-dichlorodihydrofluorescein diacetate, DCHF-DA). When taken up by the cell cytosol, intracellular esterases cleave the inactive delivery form to the free reduced dye (2′,7′-dichlorodihydrofluorescein, DCHF) which is then oxidized by the ROS produced in the cell to form a strongly fluorescent dye (2′,7′-dichlorofluorescein, DCF) that can be monitored by fluorescence spectroscopy.[52] This assay provides valuable information related to ROS generated

in the cells exposed to the PM; however, stability of the DCF product, due to photobleaching and photo-oxidation results in larger than desired variability.[58,59]

The glutathione ratio assays is a biological assay for assessing oxidative stress.[49] Glutathione (GSH) is known as cell antioxidant. As the cells are exposed to the PM and oxidative stress occurs, GSH with the enzyme glutathione peroxidase reduces the damage of the cells by capturing the ROS and the oxidized glutathione (GSSG) formed. The determination of GSH/GSSG ratio is a useful indicator of oxidative stress in cells or tissues. However, the oxidation of GSH during sample (cells/tissues) preparation is a critical problem for this assay due to an error of measuring GSH/GSSG ratio.[60]

Lipid peroxidation assay is another biological approach for oxidative stress analysis by measuring total amount of product from lipid oxidation reaction in the cells after exposure.[50] After lipid peroxidation reaction, highly reactive and unstable lipid hydroperoxides are formed and decomposed to malondialdehyde (MDA) as a final product. The MDA can be quantified by reacting with thiobarbituric acid and the thiobarbituric acid reactive substances (TBARS) are produced and detected colorimetrically. This is a well-established method for screening and monitoring lipid peroxidation. However, the oxidation of lipid oxidation products during cells/tissue preparation for analysis is the main problem associated with this biological assay.[61]

The immunoassay is the most widely used assay in biological assessment where oxidative stress biomarkers are measured in the cells after exposed to the PM. The most commonly used immunoassay is called Enzyme Linked Immunosorbent Assays (ELISAs), where each biomarker is detected using the natural binding selectivity of its antibody.[62,63] It is normally considered a single-analyte technique. However, there have been attempts to detect multiple analytes using

ELISA.[64] The limitation associated with the different conditions of different enzyme activities including pH and temperature cause problems using multi-analyte ELISA.

While these biological exposure studies provide invaluable information of cellular response to the PM, as mentioned above, their cost and complexity to handle the cell systems and long analysis time are not suitable for extensive operation. Part of this dissertation will discuss extensive improvements of biological exposure analytical measurements that have been carried out with the ultimate goal of fast and inexpensive, multiple oxidative biomarker analysis in single run.

Chemical Assays

Existing chemical assays provide higher spatial and temporal resolution for epidemiological research compared to biological assays. The PM is collected onto filter paper and extraction performed prior the analysis of oxidative capacity.[2,5,65-76] The oldest approach is to analyze specific redox active species in aerosols such as PAHs, quinones and transition metals by, for example, chromatography, electrophoresis, spectroscopy and mass spectrometry.[2] Other methods to evaluate aerosol ROS generation is the use of thiobabituric acid (TBA) assay[65], fluorescence assay[56,57] and dithiothreitol (DTT) assay[5,68-76]. Assay principles, advantages and disadvantages are discussed as follow.

Thiobabituric acid (TBA) assay is used to measure ROS generated by the PM. Deoxyribose is oxidized by the ROS present in the PM. The oxidized deoxyribose is then reacted with thiobabituric acid to form the reactive product of TBA which can be detected colorimetrically. The amount of TBA reactive products is directly related to ROS generated by

the PM. However, high temperature (100°C) is needed to accommodate the reaction to generate the TBA reactive products causing the assay unpractical.[65]

Fluorescence assays used for biological PM exposure studies have been adapted for chemical assay. [66,67] An approach similar to the biological assay is used but without DCHF-DA. ROS-bound PM obtained from the extraction of PM on the filter is reacted directly with the DCHF and the resulting product measured *via* fluorescence. This assay gives a wealth information of ROS-bound PM reactivity; however, as mentioned above, stability of the DCF product, due to photobleaching and photo-oxidation, is a critical problem of the analysis[58,59]

The biochemical dithiotheitol assay (DTT assay) has been the most widely used chemical assay for aerosol oxidative stress assessment. The analysis is based on measurement of oxidative activity of the PM to catalytically oxidize the reduced DTT. After oxidation reaction with the ROS-bound PM for a specific time period, the remaining reduced DTT is developed using Ellman's reagent and detected colorimetically. The rate of DTT consumption by the PM is directly proportional to the oxidative activity of the PM samples.

While these methods offer higher throughput screening and easier sample handling approach than cell-based measurement, they require high PM mass for the analysis to obtain sufficient measurable signal. Long sampling time for filter based sampling method (minimum of 24 h) is required to obtain sufficient mass. In particular to personal exposure study, the PM collection is based the use of light weight low pressure pump. Although long sampling period is used, the PM mass is still not sufficient to be analyzed by fluorescence assay and/or DTT assay. Only highly sensitive instruments are capable of the analysis of specific redox compounds to assess oxidative stress in personal exposure studies. PM extraction procedures normally employing sonication and high amounts of solvent cause reactive species decomposition and

sample dilution. Additionally, the cost of instrument and analysis is relatively expensive. In particular for specific redox chemical species analysis, several instruments are required to obtain sufficient information for chemical analysis including metals (ICP-MS), ions (ion chromatography), organic (LC-MS, GC-MS) and inorganic compounds (X-ray diffraction, scanning electron microscope). These instruments drive the cost analysis analysis up to several hundred dollars per sample. This ultimately limits the number of samples collected and analyzed, leading to a smaller-than-desired data set. More importantly, the analysis is based on laboratory measurement therefore the collected samples must be shipped and stored for several days prior to analysis causing an underestimation of oxidative activity since the short-lived ROS are chemically active and can decompose prior to analysis.

On-line oxidative activity measurement has been invented by the Hopke group to overcome sampling artifacts associated with traditional filter-based collection methods.[66,67,77] Their system uses the Particle Into Liquid Sampler (PILS)[78,79] for aerosol sampling and a fluoresence based assay to determine particle-bound ROS activity. The PILS-fluoresence assay offers the potential for direct PM, real-time measurement of aerosol-bound ROS and represents the first step towards on-line measurement of aerosol oxidative activity. However, stability of the DCHF reagent, due to photobleaching and photo-oxidation, caused a critical problem during analysis, resulting in error of ROS estimation in the PM samples.[58,59] In addition, an internal standard was not used to account for sample dilution by the PILS system resulting in another critical source of error.[59,66,77] Temporal resolution of this system was also limited (>20 min/sample) by the long sampling periods needed for sufficient mass capture and subsequent sample flushing/rinsing periods to ensure proper detector performance.[59]

To date, the lack of appropriate methods providing field test analysis and/or on-line analysis, inexpensive instrumentation, and low sample mass consumption has limited to understand the link between health effects and aerosol particulate matter.

METHOD DEVELOPMENT FOR ASSESSING AEROSOL OXIDATIVE STRESS

To address the problems associated with current methods for assessing oxidative stress caused by atmospheric aerosols, my research has focused on developing methods that provide improvements in the analysis for both biological assay and chemical assay.

For biological assays, a method analogous to immunoassays has been developed called cleavable tag immunoassay (CTI) to overcome problems associated with the most widely used biological assay, called ELISA where only a single analyte is detected per run.[80,81] The CTI coupled with microchip micellar electrokinetic chromatography (MEKC) to measure multi-analyte biomarkers simultaneously based on a sandwich immunoassay format was introduced by Henry research group. The CTI capture chemistry is similar to traditional immunoassays (e.g. ELISA), but changes in the detection step. The analyte signal in CTI is not directly imaged on a surface, but instead a fluorescent tag is cleaved from the detection antibody and analyzed by microchip capillary electrophoresis (MCE). Previously, the CTI was shown for multiple protein markers of cardiac stress in a single run using sandwich immunoassay format.[81] Since the CTI chemistry is an immunoassay analogue, it is not limited to a small class of biomarkers resulting in the application for oxidative stress biomarkers analysis. Oxidative stress biomarkers consist of both small molecules (e.g. 3-nitrotyrosine (3NT), reduced/oxidized glutathione (GSH/GSSG), 8-hydroxydeoxyguanosine (8-OHdG)) and proteins (e.g. C-reactive protein (CRP), superoxide dismutase (SOD), catalase (CAT)). In an attempt to develop the CTI toward the analysis of

oxidative stress biomarkers, CTI was investigated for its ability to measure small molecules and proteins simultaneously. The ultimate goal for this method development is to use the CTI to measure multiple oxidative stress biomarkers in cells/tissues after PM exposure. As a proof-of-concept, multiple small molecules were analyzed using competitive CTI format. Finally, mixed mode CTI including competitive format and sandwich format for detection of a small molecule (3-NT) and a protein (CRP) simultaneously was demonstrated for multiple oxidative stress biomarker measurements. The detailed assay principles as well as procedures toward analysis of such analytes by the developed CTI are discussed in Chapter 2. Again, the developed CTI chemistry is suitable not only for oxidative stress biomarker but different types of disease biomarkers as well.

For chemical assays, my research has focused on developing methods of oxidative stress analysis in both area-based exposure (population exposure) and personal exposure. Area-based exposure studies are designed to investigate how ambient air affects human health in specific region by assuming that every person in the region expose and affect from the PM equally. The influencing factors of this exposure are PM production sources and metrological conditions. Personal exposure, on the other hand, studies the effect of air pollution on an individual in a specific location such as occupational location or daily activity environments. Influencing factors depends on time spent in the location and the PM concentration on the site that an individual passes through.[82]

For area-based exposure study, to address the major problem of sample artifacts associated with the classic filter based sampling method as mentioned above, my research has focused on the development of the on-line monitoring system for analysis oxidative activity caused by atmospheric aerosols. As a first step toward this work, Chapter 3 describes the

development of the microfluidic electrochemical sensor that has robust, inexpensive, high electrochemical response, easily modified properties. The sensor made of polydimethylsiloxane (PDMS) and carbon paste used as the electrode material. The sensor was tested for its ability to provide effective analysis of thiols (DTT, glutathione) and catecholamine (dopamine) in both buffer and biological samples. Then, the microfluidic electrochemical sensor was employed for the detection of aerosol oxidative activity based on the DTT assay, which is described in Chapter 4. Unlike the traditional assay where the remaining DTT is developed and detected colorimetrically, the electrochemical sensor provides the direct determination of remaining DTT after reacted with the PM without the need of developing reagent added to accommodate the detection. The PILS was used for on-line PM sampling and coupled to the microfluidic electrochemical sensor to accommodate a real-time oxidative activity measurement. This prototype of on-line sampling-analysis system demonstrated the highest temporal resolution (3 samples/10 min) reported to date to measure aerosol oxidative activity. The obvious impact of this work is to contribute to the understanding of how PM affected human health during a short time exposure. Furthermore, extensive oxidative stress monitoring caused by PM was conducted and is described in Chapter 5. The microfluidic electrochemical sensor was applied to measure the ability of the PM to generate hydroxyl radicals, highly reactive oxygen species generated primarily from the metals participated to Fenton chemistry resulting in oxidative stress in cells. Salicylic acid trapping method was employed for this study. Salicylic acids react with the hydroxyl radicals created by the PM to form electrochemical active products of dihydroxybenzoic acids (DHBA). In this dissertation, optimization of electrode composition on the sensor, reaction time, and reagent amount was described with the off-line analysis format. Preliminary results for the determination of fly ash samples were demonstrated. The ultimate

goal of this assay is the on-line determination of hydroxyl radicals generated from PM using similar system as demonstrated for oxidative activity measurement using DTT assay described in Chapter 4.

Although the on-line method represents an improvement over the traditional DTT method in terms of sensitivity and speed, it is still limited to area-based exposure assessment since the PILS and associated equipment are too large for personal sampling. In an attempt to develop a method for personal exposure studies that require short sampling durations and provide an analysis that is fast, sensitive, inexpensive, portable and easy to perform, my research employed the microfluidic paper-based analytical device (μPAD) for measuring the oxidative activity of PM collected on personal filter samples. Assay principles, detailed procedures, as well as results of oxidative activity of personal samples collected from various events are described and demonstrated in Chapter 6. The paper based devices successfully showed the ability to measure oxidative activity of samples collected from several events.

Overall, the research described in this dissertation will have impact on the analytical chemistry community by the development of multi-analyte immunoassay for detection of small molecules and proteins simultaneously which is capable of biomarker detection of diseases. The development of a robust microfluidic electrochemical sensor also has the impact on the analytical chemistry field where its application is not limited to only the oxidative activity study but any types of electrochemical relevant application can be applied for. The most significant impact of this dissertation is on the field of environmental public health by providing a means to reach a better understanding of how the atmospheric aerosols cause adverse human health effects by employing the analytical protocols developed here. Further contribution of the aerosol

scientist and the analytical chemist would improve this technology for more fully understanding the impact of atmospheric aerosols on human health.

REFERENCES

(1) Seinfeld, J. H.; Pandis, S. N. *Aerosol Chemistry and Physics*; Wiley: New York, 1998.
(2) Poschl, U. *Angew. Chem-Int. Edit.* **2005**, *44*, 7520.
(3) Hoek, G.; Meliefste, K.; Cyrys, J.; Lewne, M.; Bellander, T.; Brauer, M.; Fischer, P.; Gehring, U.; Heinrich, J.; van Vliet, P.; Brunekreef, B. *Atmos. Environ.* **2002**, *36*, 4077.
(4) de Kok, T. M.; Hogervorst, J. G.; Briede, J. J.; van Herwijnen, M. H.; Maas, L. M.; Moonen, E. J.; Driece, H. A.; Kleinjans, J. C. *Environ. Mol. Mutagen.* **2005**, *46*, 71.
(5) Verma, V.; Pakbin, P.; Cheung, K. L.; Cho, A. K.; Schauer, J. J.; Shafer, M. M.; Kleinman, M. T.; Sioutas, C. *Atmos. Environ.* **2011**, *45*, 1025.
(6) Bernstein, J. A.; Alexis, N.; Barnes, C.; Bernstein, I. L.; Nel, A.; Peden, D.; Diaz-Sanchez, D.; Tarlo, S. M.; Williams, P. B. *J. Allergy Clin. Immunol.* **2004**, *114*, 1116.
(7) Bommel, H.; Haake, M.; Luft, P.; Horejs-Hoeck, J.; Hein, H.; Bartels, J.; Schauer, C.; Poschl, U.; Kracht, M.; Duschl, A. *Int. Immunopharmacol.* **2003**, *3*, 1371.
(8) Donaldson, K.; Stone, V.; Borm, P. J. A.; Jimenez, L. A.; Gilmour, P. S.; Schins, R. P. F.; Knaapen, A. M.; Rahman, I.; Faux, S. P.; Brown, D. M.; MacNee, W. *Free Radic. Biol. Med.* **2003**, *34*, 1369.
(9) Schins, R. P. F.; Lightbody, J. H.; Borm, P. J. A.; Shi, T. M.; Donaldson, K.; Stone, V. *Toxicol. Appl. Pharmacol.* **2004**, *195*, 1.
(10) Sioutas, C.; Delfino, R. J.; Singh, M. *Environ. Health Perspect.* **2005**, *113*, 947.
(11) Kunzli, N.; Mudway, I. S.; Gotschi, T.; Shi, T. M.; Kelly, F. J.; Cook, S.; Burney, P.; Forsberg, B.; Gauderman, J. W.; Hazenkamp, M. E.; Heinrich, J.; Jarvis, D.; Norback, D.; Payo-Losa, F.; Poli, A.; Sunyer, J.; Borm, P. J. A. *Environ. Health Perspect.* **2006**, *114*, 684.
(12) Kovarik, M. L.; Li, M. W.; Martin, R. S. *Electrophoresis* **2005**, *26*, 202.
(13) Jung, H.; Guo, B.; Anastasio, C.; Kennedy, I. M. *Atmos. Environ.* **2006**, *40*, 1043.
(14) Foucaud, L.; Wilson, M. R.; Brown, D. M.; Stone, V. *Toxicol. Lett.* **2007**, *174*, 1.
(15) Sameenoi, Y.; Mensack, M. M.; Murphy, B. M.; Henry, C. S. *Methods* **2012**, *56*, 166.
(16) Sameenoi, Y.; Mensack, M. M.; Boonsong, K.; Ewing, R.; Dungchai, W.; Chailapakul, O.; Cropek, D. M.; Henry, C. S. *Analyst* **2011**, *136*, 3177.
(17) Sameenoi, Y.; Koehler, K.; Shapiro, J.; Boonsong, K.; Sun, Y.; Collett, J.; Volckens, J.; Henry, C. S. *J. Am. Chem. Soc.* **2012**, *134*, 10562.
(18) Prather, K. A.; Hatch, C. D.; Grassian, V. H. *Annu. Rev. Anal. Chem. (Palo Alto Calif)* **2008**, *1*, 485.
(19) Raes, F.; Van Dingenen, R.; Vignati, E.; Wilson, J.; Putaud, J. P.; Seinfeld, J. H.; Adams, P. *Atmos. Environ.* **2000**, *34*, 4215.
(20) Bernstein, J. A.; Alexis, N.; Barnes, C.; Bernstein, I. L.; Nel, A.; Peden, D.; Diaz-Sanchez, D.; Tarlo, S. M.; Williams, P. B. *J Allergy Clin. Immunol.* **2004**, *114*, 1116.
(21) Gorny, R. L.; Dutkiewicz, J. *Ann. Agr. Env. Med.* **2002**, *9*, 17.
(22) Lai, A. C. K. *Indoor Air* **2002**, *12*, 211.
(23) D'Amato, G.; Liccardi, G.; D'Amato, M.; Cazzola, M. *Eur. Respir. J.* **2002**, *20*, 763.
(24) Araujo, J.; Nel, A. *Part. Fibre Toxicol.* **2009**, *6*, 24.
(25) Simkhovich, B. Z.; Kleinman, M. T.; Kloner, R. A. *J. Am. Coll. Cardiol.* **2008**, *52*, 719.
(26) Williams, J.; de Reus, M.; Krejci, R.; Fischer, H.; Strom, J. *Atmos. Chem. Phys.* **2002**, *2*, 133.
(27) Krejci, R.; Strom, J.; de Reus, M.; Williams, J.; Fischer, H.; Andreae, M. O.; Hansson, H. C. *Atmos. Chem. Phys.* **2005**, *5*, 1527.

(28) Li, N.; Hao, M.; Phalen, R. F.; Hinds, W. C.; Nel, A. E. *Clin. Immunol.* **2003**, *109*, 250.
(29) Putaud, J. P.; Raes, F.; Van Dingenen, R.; Bruggemann, E.; Facchini, M. C.; Decesari, S.; Fuzzi, S.; Gehrig, R.; Huglin, C.; Laj, P.; Lorbeer, G.; Maenhaut, W.; Mihalopoulos, N.; Mulller, K.; Querol, X.; Rodriguez, S.; Schneider, J.; Spindler, G.; ten Brink, H.; Torseth, K.; Wiedensohler, A. *Atmos. Environ.* **2004**, *38*, 2579.
(30) Matta, E.; Facchini, M. C.; Decesari, S.; Mircea, M.; Cavalli, F.; Fuzzi, S.; Putaud, J. P.; Dell'Acqua, A. *Atmos. Chem. Phys.* **2003**, *3*, 623.
(31) Putaud, J. P.; Van Dingenen, R.; Dell'Acqua, A.; Raes, F.; Matta, E.; Decesari, S.; Facchini, M. C.; Fuzzi, S. *Atmos. Chem. Phys.* **2004**, *4*, 889.
(32) Ebert, M.; Weinbruch, S.; Hoffmann, P.; Ortner, H. M. *Atmos. Environ.* **2004**, *38*, 6531.
(33) Araujo, J. A.; Barajas, B.; Kleinman, M.; Wang, X. P.; Bennett, B. J.; Gong, K. W.; Navab, M.; Harkema, J.; Sioutas, C.; Lusis, A. J.; Nel, A. E. *Circ. Res.* **2008**, *102*, 589.
(34) Nel, A. E.; Diaz-Sanchez, D.; Li, N. *Curr. Opin. Pulm. Med.* **2001**, *7*, 20.
(35) Frampton, M. W. *Environ. Health Perspect.* **2001**, *109 Suppl 4*, 529.
(36) Utell, M. J.; Frampton, M. W. *J. Aerosol. Med.* **2000**, *13*, 355.
(37) Finkel, T.; Holbrook, N. J. *Nature* **2000**, *408*, 239.
(38) Wolin, M.; Mohazzab-H, K. *Mediation of Signal Transductionby Oxidants, in Oxidative Stress and the Molecular Biology of Antiosidant Defenses*; Cold Spring Harbor Laboratory Press: New York, 1997.
(39) Li, N.; Wang, M.; Bramble, L. A.; Schmitz, D. A.; Schauer, J. J.; Sioutas, C.; Harkema, J. R.; Nel, A. E. *Environ. Health Perspect.* **2009**, *117*, 1116.
(40) Delfino, R. J.; Sioutas, C.; Shaista, M. *Environ. Health Perspect.* **2005**, *113*, 934.
(41) Peters, A.; Veronesi, B.; Calderón-Garcidueñas, L.; Gehr, P.; Chen, L. C.; Geiser, M.; Reed, W.; Rothen-Rutishauser, B.; Schürch, S.; Schulz, H. *Part. Fibre Toxicol.* **2006**, *3:13*.
(42) Nemmar, A.; Hoet, P. H. M.; Vanquickenborne, B.; Dinsdale, D.; Thomeer, M.; Hoylaerts, M. F.; Vanbilloen, H.; Mortelmans, L.; Nemery, B. *Circulation* **2002**, *105*, 411.
(43) Oberdorster, G.; Sharp, Z.; Atudorei, V.; Elder, A.; Gelein, R.; Kreyling, W.; Cox, C. *Inhalation Toxicology* **2004**, *16*, 437.
(44) Oberdorster, G.; Oberdorster, E.; Oberdorster, J. *Environ. Health Perspect.* **2005**, *113*, 823.
(45) Utell, M. J.; Frampton, M. W. *J. Aerosol Med.-Depos. Clear. Eff. Lung* **2000**, *13*, 355.
(46) Li, N.; Sioutas, C.; Cho, A.; Schmitz, D.; Misra, C.; Sempf, J.; Wang, M. Y.; Oberley, T.; Froines, J.; Nel, A. *Environ. Health Perspect.* **2003**, *111*, 455.
(47) Wardman, P.; Candeias, L. P. *Radiat. Res.* **1996**, *145*, 523.
(48) Xia, T.; Korge, P.; Weiss, J. N.; Li, N.; Venkatesen, M. I.; Sioutas, C.; Nel, A. *Environ. Health Perspect.* **2004**, *112*, 1347.
(49) Li, N.; Sioutas, C.; Cho, A.; Schmitz, D.; Misra, C.; Sempf, J.; Wang, M.; Oberley, T.; Froines, J.; Nel, A. *Environ. Health Perspect.* **2003**, *111*, 455.
(50) Ghelfi, E.; Rhoden, R.; Wellenius, G. A.; Lawrence, J.; Gonzalez-Flecha, B. *Toxicol. Sci.* **2008**, *102*, 328.
(51) Tzamkiozis, T.; Stoeger, T.; Cheung, K.; Ntziachristos, L.; Sioutas, C.; Samaras, Z. *Inhal. Toxicol.* **2010**, *22*, 59.
(52) Limbach, L. K.; Wick, P.; Manser, P.; Grass, R. N.; Bruinink, A.; Stark, W. J. *Environ. Sci. Technol.* **2007**, *41*, 4158.
(53) Rahman, I.; MacNee, W. *Am. J. Physiol.-Lung C.* **1999**, *277*, L1067.

(54) Stephanie, V.; Armelle, B. S.; Laurent, M.; Helene, C.; Abderrazak, Y.; Helene, M. *Inhal. Toxicol.* **2011**, *23*, 627.
(55) Wang, H.; Joseph, J. A. *Free Radical Bio. Med.* **1999**, *27*, 612.
(56) Halliwell, B.; Whiteman, M. *Brit. J. Pharmacol.* **2004**, *142*, 231.
(57) Tietze, F. *Anal. Biochem.* **1969**, *27*, 502.
(58) Beer, D.; Weber, J. *Opt. Commun.* **1972**, *5*, 307.
(59) Wang, Y.; Hopke, P. K.; Sun, L.; Chalupa, D. C.; Utell, M. J. *J. Toxicol.* **2011**, *2011*.
(60) Owen, J. B.; Butterfield, D. A. In *Protein Misfolding and Cellular Stress in Disease and Aging: Concepts and Protocols*; Vol. 648, p 269.
(61) Dawn-Linsley, M.; Ekinci, F. J.; Ortiz, D.; Rogers, E.; Shea, T. B. *J. Neurosci. Meth.* **2005**, *141*, 219.
(62) Diamandis, E. P.; Christopoulos, T. K. *Immunoassay*; Academic Press: San Diego, 1996.
(63) Delfino, R. J.; Staimer, N.; Tjoa, T.; Polidori, A.; Arhami, M.; Gillen, D. L.; Kleinman, M. T.; Vaziri, N. D.; Longhurst, J.; Zaldivar, F.; SioutaS, C. *Environ. Health Perspect.* **2008**, *116*, 898.
(64) Wiese, R.; Belosludtsev, Y.; Powdrill, T.; Thompson, P.; Hogan, M. *Clin. Chem.* **2001**, *47*, 1451.
(65) Frampton, M. W.; Ghio, A. J.; Samet, J. M.; Carson, J. L.; Carter, J. D.; Devlin, R. B. *Am. J. Physiol.-Lung C.* **1999**, *277*, L960.
(66) Venkatachari, P.; Hopke, P. K. *J. Aerosol Sci.* **2008**, *39*, 168.
(67) Venkatachari, P.; Hopke, P. K.; Grover, B. D.; Eatough, D. J. *J. Atmos. Chem.* **2005**, *50*, 49.
(68) Chung, M. Y.; Lazaro, R. A.; Lim, D.; Jackson, J.; Lyon, J.; Rendulic, D.; Hasson, A. S. *Environ. Sci. Technol.* **2006**, *40*, 4880.
(69) Hu, S.; Polidori, A.; Arhami, M.; Shafer, M. M.; Schauer, J. J.; Cho, A.; Sioutas, C. *Atmos. Chem. Phys.* **2008**, *8*, 6439.
(70) McWhinney, R. D.; Gao, S. S.; Zhou, S. M.; Abbatt, J. P. D. *Environ. Sci. Technol.* **2011**, *45*, 2131.
(71) Mugica, V.; Ortiz, E.; Molina, L.; De Vizcaya-Ruiz, A.; Nebot, A.; Quintana, R.; Aguilar, J.; Alcantara, E. *Atmos. Environ.* **2009**, *43*, 5068.
(72) Rattanavaraha, W.; Rosen, E.; Zhang, H. F.; Li, Q. F.; Pantong, K.; Kamens, R. M. *Atmos. Environ.* **2011**, *45*, 3848.
(73) Verma, V.; Ning, Z.; Cho, A. K.; Schauer, J. J.; Shafer, M. M.; Sioutas, C. *Atmos. Environ.* **2009**, *43*, 6360.
(74) Verma, V.; Polidori, A.; Schauer, J. J.; Shafer, M. M.; Cassee, F. R.; Sioutas, C. *Environ. Sci. Technol.* **2009**, *43*, 954.
(75) Wang, Y.; Arellanes, C.; Curtis, D. B.; Paulson, S. E. *Environ. Sci. Technol.* **2010**, *44*, 4070.
(76) Cho, A. K.; Sioutas, C.; Miguel, A. H.; Kumagai, Y.; Schmitz, D. A.; Singh, M.; Eiguren-Fernandez, A.; Froines, J. R. *Environ. Res.* **2005**, *99*, 40.
(77) Venkatachari, P.; Hopke, P. K. *Aerosol Sci. Technol.* **2008**, *42*, 629.
(78) Weber, R. J.; Orsini, D.; Daun, Y.; Lee, Y. N.; Klotz, P. J.; Brechtel, F. *Aerosol Sci. Technol.* **2001**, *35*, 718.
(79) Orsini, D. A.; Ma, Y. L.; Sullivan, A.; Sierau, B.; Baumann, K.; Weber, R. J. *Atmos. Environ.* **2003**, *37*, 1243.
(80) Caulum, M. M.; Henry, C. S. *Analyst* **2006**, *131*, 1091.

(81) Caulum, M. M.; Murphy, B. M.; Ramsay, L. M.; Henry, C. S. *Anal. Chem.* **2007**, *79*, 5249.
(82) *Air pollution, the automobile, and public health*; National Academy Press: Washington, D.C., 1988.

CHAPTER 2. MULTIANALYTE IMMUNOASSAY FOR OXIDATIVE STRESS BIOMARKERS

CHAPTER OVERVIEW

The overall goal of the research described in this dissertation is the development of methods including biological assays and chemical assays methods for assessing oxidative stress caused by atmospheric aerosols. This chapter describes the method development for biological assay assessment using a multianalyte immunoassay for detecting multiple oxidative stress biomarkers in a single run as the ultimate goal. As a proof of concept, cleavable tag immunoassay (CTI) chemistry was employed to demonstrate the multianalyte analysis in competitive, non-competitive, and mixed format for the analysis of proteins and small molecule biomarkers. The detailed assay principles as well as procedures toward analysis of such analytes by the developed CTI are discussed below. The method developed here is not only useful for aerosol oxidative stress assessment but also any types of disease biomarkers. This work was published in the journal *Methods,*[1] and most of text and figures are taken from that article. Most of data in this chapter were collected and analyzed by me except for the non-competitive CTI data (Figure 2.5) was collected by Dr. Meghan Mensack. She also worked together with me on data collection and analysis on mixed mode CTI (Figure 2.6).

SYNOPSIS

Immunoassays are one of the most useful diagnostic techniques in disease assessment, drug metabolite analysis and environmental applications due largely in part to the selectivity and sensitivity provided by antibody-antigen interactions. Here, a multiplexed immunoassay termed cleavable tag immunoassay (CTI) was performed in competitive, non-competitive, and mixed formats for the analysis of proteins and small molecule biomarkers of inflammation and tissue damage. Microchip capillary electrophoresis (MCE) with fluorescence detection was employed for the analysis of fluorescently labeled tags corresponding to the analytes of interest cleaved from the detection antibodies. For this work we have selected 3-nitrotyrosine (3-NT) a molecule indicative of reactive nitrogen species (RNS), thyroxine (T4) a molecule used to monitor thyroid gland function and C-reactive protein (CRP) a marker of chronic inflammation as model analytes to demonstrate the assay principles. The simultaneous detection of 3-nitrotyrosine (3-NT) and thyroxine (T4) was carried out as a proof-of-principle for the competitive CTI while non-competitive CTI performance was demonstrated via the analysis of C-reactive protein (CRP). Limit of detections (LOD) and dynamic ranges were investigated. LOD for 3-NT, T4 and CRP were 0.5 μg/mL, 23 nM, and 5 μg/mL, respectively thus demonstrating the ability of the CTI to detect proteins and small molecules within clinical reference ranges. Moreover, this is the first report of the use of mixed format CTI chemistry for the simultaneous detection of proteins (CRP) and small molecules (3-NT) in a single assay. The success of this work demonstrates the ability of CTI to analyze intact proteins and small molecule biomarkers simultaneously.

INTRODUCTION

Immunoassays are one of the most useful diagnostic techniques in disease assessment, drug and drug metabolite analysis and environmental monitoring due largely to the selectivity and sensitivity afforded by antibody-antigen interactions.[2] Since their introduction in 1959, multiple immunoassay formats have been developed, including homogeneous (or solution phase) and heterogeneous (solid supported) formats.[3] Immunoassays have now been developed to allow multi-analyte detection in a single run resulting in reduced analysis times and cost as well as providing the potential for multi-analyte point-of-care screening.[4,5] Heterogeneous immunoassay methods such as Enzyme Linked Immunosorbent Assays (ELISA), however, are based on detecting the signal on or near the surface where the analyte is captured making the measurement subject to background noise associated with non-specific interactions at the surface.[6]

Recently, our group reported a multi-analtye immunoassay based on immunoaffinity capillary electrophoresis[7] called the cleavable tag immunoassay (CTI).[8,9] In CTI, the capture chemistry is similar to traditional immunoassays but the detection step is unique. The analyte signal in CTI is not directly detected on a solid support surface; instead, a fluorescent tag is cleaved from the detection antibody and analyzed via microchip capillary electrophoresis (MCE). This approach allows for the decoupling of the detection and capture steps, eliminating the need for complex imaging systems and reducing noise associated with non-specific adsorption. It also differentiates CTI from traditional CEIA (capillary electrophoresis immunoassays) where the analyte (or antibody-antigen complex) is detected after electrophoresis.[10,11] In CTI, a specific tag with a unique mobility is coded to a specific antibody and therefore each antigen gives a unique peak in the electropherogram where the peak area corresponds to the antigen concentration in the biological sample. Each tag is generated

synthetically and therefore, has a unique and controllable mobility after cleavage and thus a different migration time when analyzed by MCE. We have previously reported the use of CTI for the simultaneous detection of multiple proteins indicative of acute myocardial infarction using a sandwich immunoassay format.[8,9] These results demonstrated the ability to detect cardiac troponin T (cTnT), cardiac troponin I (cTnI), creatine kinase-MB (CK-MB), and myoglobin proteins over a linear range which included the upper reference range for healthy, non-AMI patients.

Many applications such as disease diagnosis[12], drug metabolite analysis[13] and environmental status assessment[14] require detection of small molecules in addition to proteins. Small molecule biomarkers have also been implicated in carcinogenesis, cardiovascular and neurodegenerative disorders.[15] Since these small molecules have a single epitope, the use of competitive immunoassays is required for analysis.[16] Only a few examples of multi-analyte competitive immunoassays have been reported to date[6,17].[5,16] The few existing multianalyte competitive assays allow for fast analysis with low sample consumption, but typically require expensive instrumentation and can be difficult to automate.[6] As an example, a multi-analyte competitive electrophoretic immunoassay with two-color detection was reported for determination insulin and glucagon in islets of Langerhans.[17] While this assay has a large linear range for multiple analytes, further increases in the number of analytes and/or the ability to perform simultaneous sandwich and competitive immunoassays will be challenging because they will require increases in instrumental complexity.

Here, we report the development of competitive CTI for the analysis of small molecules, non-competitive CTI for proteins and a mixed mode competitive/non-competitive CTI for analysis of both small molecules and proteins simultaneously. Very few examples exist of mixed

mode immunoassays.[18] For this work we have selected 3-nitrotyrosine (3-NT) a molecule indicative of cellular damage caused by reactive nitrogen species (RNS), thyroxine (T4) a molecule used to monitor thyroid gland function and CRP a marker of chronic inflammation as model analytes to show the function of CTI for competitive, non-competitive, and mixed format immunoassays.

MATERIALS AND METHODS

Chemicals and Materials

SU-8 2035 photoresist was obtained from MicroChem Corp. (Newton MA). Poly(dimethylsiloxane) (PDMS) and Sylgard 184 elastomer curing agent were purchased from Dow Corning (San Diego CA). Fluorescein-5-isothiocyanate (FITC) was purchased from Molecular Probes, Inc. EZ-LinkTM sulfo-NHS-SS-biotin, EZ-LinkTM sulfo-NHS-biotin, EZ-Link maleimide-PEO solid-phase biotinylation kit, 1-ethyl-3-[3-dimethylaminopropyl]carbodiimide hydrochloride (EDC), Biotin quantification Kit, SuperBlock blocking buffer, Magnabind carboxyl derivatized magnetic beads and Magnetic bead separator were purchased from Thermo Fisher (Rockford, IL). Cystamine dihydrochloride, bovine serum albumin (BSA), sodium cyanoborohydride, ethanolamine and tris (2-carboxyethyl) phosphine (TCEP) were achieved from Sigma Aldrich (St. Louis, MO). 1,4-diaminobutane, 1,6-diaminohexane, methanol and triethylamine (TEA) were purchased from Fisher Scientific (Pittsburgh, PA). Avidin was obtained from EMD biosciences (San Diego, CA). Toyopearl affinity resin (formyl-650M, 40−90 μm diameter) was purchased from Supelco (Bellefonte, PA). F96 MaxiSorp Microtiter Plates was achieved from Nalge Nunc International (Rochester, NY). Antibodies were obtained from Fitzgerald Industries International (Acton, MA). Fluorescence detection was performed on a Photometrics HQ^2 CCD (Roper Scientific, Tuscon, AZ) equipped

with TE2000-U epifluorescence microscope assembly (Nikon, Melville, NY) where a metamorph imaging system software (Molecular Devices, Sunnyvale, CA) was used to collected the data.

Microchip Device Fabrication

A polydimethylsiloxane (PDMS) microfluidic device for MCE was fabricated according previously published methods.[19] The mold master was constructed using SU-8 (MicroChem Corp., Newton MA) photoresist and photolithography. A degassed mixture of Sylgard 184 elastomer and curing agent (Dow Corning, San Diego CA) (10:1) was poured on the mold master as well as a bare silica wafer and allowed to cure at 65 °C for at least 2 h. The cured PDMS was removed from the mold and the reservoirs punched using a standard 6 mm biopsy punch. The surfaces of the two pieces of PDMS were cleaned using methanol and dried in a 65 °C oven for 15 min. The two pieces of PDMS were then placed in an air plasma cleaner and oxidized on high power for 30 s and the two pieces immediately brought together to form an irreversible seal.

Microchip Capillary Electrophoresis

All MCE separations were conducted using PDMS microchips fabricated as described above. The microfluidic channels were 50 μm high by 50 μm wide with a 5 cm long separation channel. The assembled microchip was pre-treated with separation buffer for 1 h prior MCE experiment. The power supply used for electrophoresis was built in-house.[20] For gated injection, a potential of +600 V was applied at both sample and buffer reservoirs. During injection, the potential at buffer waste reservoir was floated causing a sample plug to be generated in the

separation channel. Unless otherwise stated, the separation potential was +75 V/cm and injection time was 1 s. Each well was filled with 50 μL of sample or running buffer. The detection was performed at 4.5 cm from the injection point using an inverted fluorescent microscope.

For pinched injection, a 250 μm double-T injector was used for all experiments giving a 625 pL injection volume. During pinched injection a high potential (+221.25 V/cm) is applied to the sample and buffer, and waste reservoirs while a negative bias (-391 V/cm) is applied to the sample waste in order to draw the sample across the separation channel to the sample waste thereby forming the injection plug in the separation channel. During separation the buffer reservoir is switched to +500 V/cm and the buffer waste reservoir set to ground. A pull-back potential of +190 V/cm is applied to both the sample and sample waste reservoirs to prevent leakage into the separation channel. Detection was carried out at 2.5 cm down the channel from the injection using an inverted fluorescent microscope system.

Cleavable Tag Synthesis

Tags were synthesized according to previously published methods [9]. Cleavable fluorescent tags with an affinity for avidin were selected for the work described here [9]. Shown in Figure 2.1, the tag consists of four functional components: i) detection group: fluorescein (FITC) was used as the detection group for fluorescence detection, ii) spacer group: necessary for generating tags with unique charge-to-mass ratio to provide resolution during separation, iii) a chemically cleavable group: in this case, disulfide bonds were incorporated into the tag using NHS-SS-biotin or cystamine, and iv) conjugation group: avidin-biotin interactions were used to bind the tags to detection antibodies. For the cystamine containing tag sulfo-NHS-biotin was used in place of NHS-SS-biotin. These tags are readily resolved from each other by MCE. In the

case of the competitive assays detailed here, tags were conjugated to the 3-NT and T4 antibodies of the target analytes using avidin-biotin chemistry. For all experiments, FAMB (biotinylated FITC-cystamine) was used for 3-NT and FEB (biotinylated fluorescein thiocarbamyl ethylenediamine) was used for T4. For CRP analysis, FHB (biotinylated thiocarbamyl hexamethylenediamine) was used as a tag.

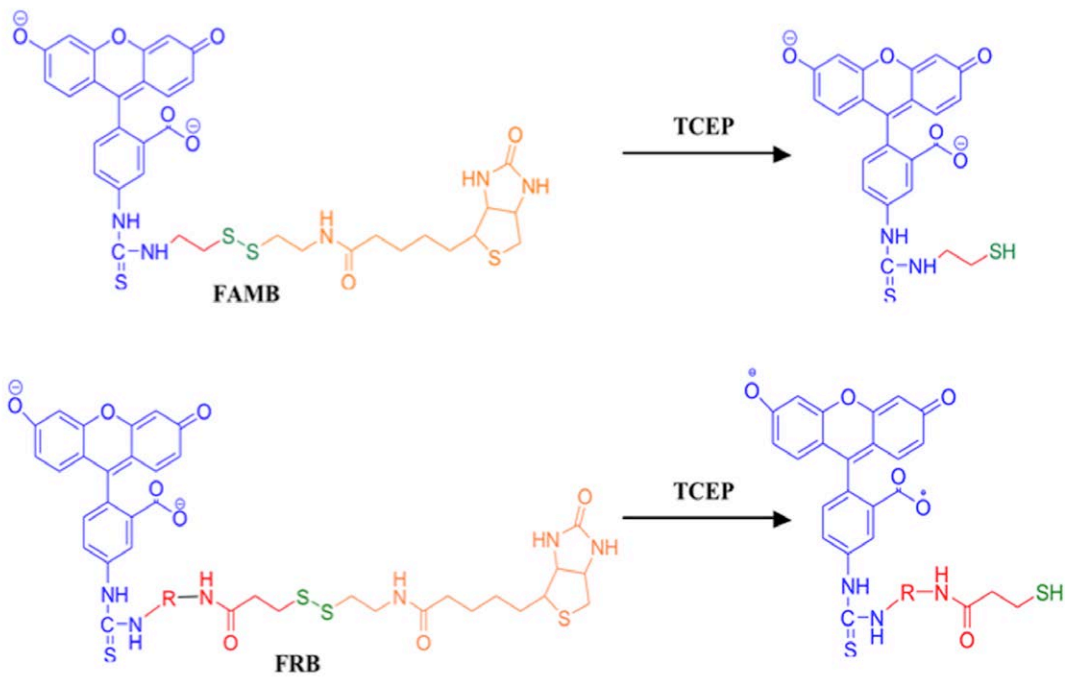

Figure 2.1. CTI tags and their cleavable products used in this work. Each tag consists of four functional elements (i) detection group (-----) (ii) the spacer group (-----) (iii) a chemically cleavable group (-----) (iv) the conjugation group (-----). FRB was synthesized based on homo-bifunctional amine spacer. FAMB was produced using cystamine pathway. TCEP cleaves tags at the disulfide bond.

FAMB Synthesis

Fluorescein isothiocyanate (FITC) (51 mg) was dissolved in methanol (5 mL) containing 0.1% triethylamine (TEA). The solution was added dropwise over 30 min to the solution of cystamine dihydrochloride (180 mg) dissolved in a mixture of methanol (5mL), water (2mL) and TEA (40 μL). The reaction was allowed to proceed overnight at room temperature (22 ± 2 °C) with constant stirring. The solution was evaporated under airflow until the volume was reduced to approximately 5 mL. A 10:1 mixture of acetonitrile/methanol was then added to the solution to precipitate the FITC-cystamine product. The solution was air dried and the product reacted with sulfo-NHS-biotin in a 1:1 molar ratio in phosphate buffer (20 mM, pH 7.4) overnight at 4 °C to create the desired FAMB product. The product was stable for one month when stored dry at 4 °C.

FRB Synthesis

The tags synthesized using this process are generically known as FRB where R represents ethylenediamine (C2) or hexamethylenediamine (C6). The synthesis used to produce the intermediates, fluorescein thiocarbamyl ethylenediamine (FTED) and fluorescein thiocarbamyl hexamethylenediamine (FTHD), has been previously published by our group [8]. FITC (100 mg) was dissolved in a mixture of methanol (5 mL) and TEA (50 μL). C2 (200 mg) or C6 (200 mg) was dissolved in methanol (5 mL) containing 0.1% TEA. The FITC solution was added dropwise to the C2 or C6 solution over 30 min and allowed to react overnight at room temperature with constant stirring. The following day, the product was precipitated using a 10:1 mixture of acetonitrile/methanol and the precipitate dried under constant airflow at room temperature. The dried precipitate was then reacted with sulfo-NHS-SS-biotin in a 1:1 molar ratio in phosphate

buffer (20 mM, pH 7.4) overnight at 4 °C. Purity of the final products can be confirmed using ^{1}H-NMR. The final products, FEB and FHB, were stable for one month when stored dry at 4 °C.

Competitive CTI Assay

Preparation of BSA-Hapten Conjugates

Bovine serum albumin (BSA) was used as a protein carrier for small molecules of interest (haptens) to increase their immunogenicity.[16] Both conjugates of BSA-T4 and BSA-3-NT were prepared using carbodiimide chemistry.[21] In brief, a coupling reagent (EDC, 200 μmol) was added to a 2 mg/mL BSA solution (25 mL, pH 5.5). The small molecule solution (5 mL, 5 mM T4 or 3-NT) was added dropwise to the BSA solution and allowed to react for 10 min at room temperature. After 10 min, an additional 50 μmol of EDC was added. This reaction was carried out in the dark at room temperature (22 ± 2 °C) for 24 h. The product was then dialyzed against deionized water (3.5 kD MWCO dialysis membrane, Thermo Fisher) to remove excess free small molecules and excess EDC. The solution was stored up to 1 year at -20 °C.

Detection Antibody Preparation

The detection antibody was biotinylated using maleimide chemistry in order to better control the number of biotins bound to the antibody. Typically, 2-4 biotins per antibody can be expected using this chemistry (quantifiable using a HABA biotin quantification kit). This solid phase biotinylation kit also takes advantage of the propensity of antibodies to bind to metal chelate supports. Binding to the nickel chelate support occurs primarily through the histidine rich Fc region of IgG molecules allowing for the reduction of the disulfides within the Fab regions of the antibody, site-directed biotinylation and removal of excess reagents while the antibody is

bound to the support. Following antibody biotinylation, avidin was added (1:1 biotin bound/avidin) and allowed to react at room temperature for 2 h. Finally, the biotin-terminated tag was added in three-fold excess (3:1 tag/avidin) to the solution and reacted for 2 h at room temperature.[39] Excess tag was removed using a 3 kD MWCO Nanosep centrifugal concentrator (Pall Corporation). This process results in 2-8 fluorescent tags per antibody.

Assay Procedure

The steps for competitive CTI are shown in Figure 2.2A. As in our previous work, MCE with fluorescence detection was used for analysis of cleaved tag fragments [8,9]. Here, two model analytes, 3-NT and T4 demonstrate proof-of-principle for the multi-analyte competitive CTI chemistry. Conjugates of bovine serum albumin (BSA) and the analyte of interest (BSA-T4, BSA-3-NT) were immobilized onto a microtiter plate surface overnight at room temperature. The solution was removed and the well surface rinsed 2 times with 1X PBS followed by a single rinse with SuperBlock blocking buffer. Detection antibody (100 µL of 100 µg/mL) and a given amount (10 µL of each concentration/sample) of the corresponding analytes (T4 or 3-NT) were added to the well to run the competitive immunoassay. The reaction was allowed to proceed for 2 h at room temperature. The wells were then rinsed 3 times with PBS and 3 times with TAPS buffer (10 mM, pH 9). TCEP (50 µL, 1 mM in 10 mM TAPS, pH 9) was added and allowed to react for 1 h at room temperature. Finally, the solution containing cleavable product was analyzed using MCE with fluorescence detection. The run buffer for MCE was 10 mM TAPS, 5 mM SDS, 0.05% Triton-X 100 pH 9.

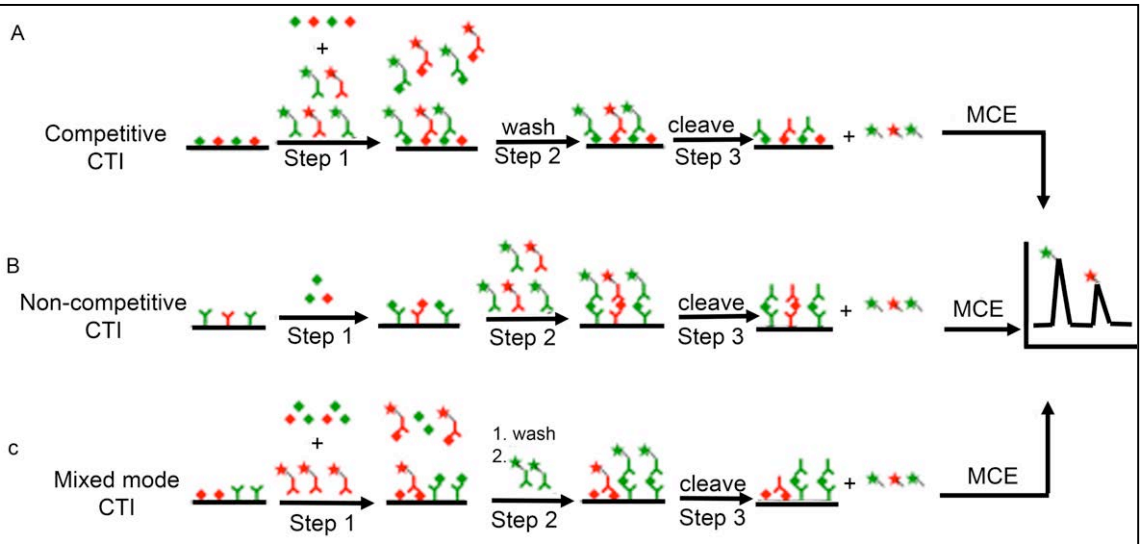

Figure 2.2. Steps to perform (A) multi-analyte competitive, (B) non-competitive, and (C) mixed competitive/non-competitive mode CTI. Surface to perform both assays can be either bead particles or microtiter plate. The different colors represent different biomarkers. Antibodies and tags have been colored to correspond to the biomarkers.

Non-Competitive CTI

Antibody preparation

Capture antibodies for the non-competitive CTI were immobilized on aldehyde functionalized Toyopearl affinity resin (formyl-650M, 40−90 µm diameter) at a concentration 10-fold greater than the upper reference limit for CRP. The particles (800 µL) were washed three times with 1 mL of K_2HPO_4 (100 mM, pH 7.5) to remove the azide used to preserve the particles prior to antibody immobilization. The K_2HPO_4 was removed and the antibody solution (2 mL) added to the vial. Sodium cyanoborohydride (10 mg) was added to facilitate reductive amination during the antibody attachment and allowed to react with gentle mixing for 2 h at room temperature. After 2 h, the resin was washed three times with K_2HPO_4 (100 mM, pH 7.5), and 2 mL of ethanolamine (1 M, pH 8) was added to each vial of particles and allowed to react for 2 h at room temperature to block all remaining aldehyde groups. Sodium cyanoborohydride (10 mg)

was again added to facilitate the coupling reaction. The particles were then washed three times with K_2HPO_4 (100 mM, pH 7.5). An additional three rinses with SuperBlock blocking buffer were carried out to reduce the amount of nonspecific binding in the remaining steps of the CTI. Particles can be stored in K_2HPO_4 (100 mM, pH 7.5) at 4 °C for up to 1 month. Detection antibodies were prepared according to procedures described in section 2.5.2 above.

Assay procedure

Capture beads (150 µL), prepared as described in section 2.6.1 were rinsed 3 times with KH_2PO_4 (100 mM, pH 7.5) and the rinse solution discarded. The antigen solution (250 µL) was then added to the beads and allowed to react for 2 h at room temperature. After 2 h, the beads were centrifuged and the liquid discarded. The particles were then rinsed 3 times with NaCl (1 M) containing 0.05% Tween 20 followed by 3 rinses with KH_2PO_4 (100 mM, pH 7.5). To reduce the amount of nonspecific binding, the beads were rinsed three times with SuperBlock blocking buffer. Finally, the detection antibody (500 µL, 500 µg/mL) was added to the beads and allowed to react for 2 h at room temperature. To remove any non-specifically bound detection antibodies, the beads were rinsed five times with NaCl (1 M) followed by three times with KH_2PO_4 (100 mM, pH 7.5). Cleavage was carried out using TCEP (500 µM, 75 µL) for 30 min at room temperature. Finally, the solution containing the fluorescent fragment was removed from the beads and analyzed using microchip MEKC. The run buffer for MEKC was 10 mM tetraborate, 50 mM SDS, 10 mM DDAPS (N-dodecyl-N,N-dimethyl-3-ammonio-1- propanesulfonate). The steps for non-competitive CTI are shown in Fig. 2B.

Mixed Mode Competitive/Non-Competitive CTI

Antibody Preparation

The original non-competitive CTI was carried out on polymer beads. Since the ultimate goal of the CTI is to perform the entire assay, including sample processing, within a microfluidic device, we chose to move to magnetic beads for the mixed non-competitive/competitive CTI. Capture antibodies/BSA-small molecules were immobilized on carboxyl derivatized magnetic beads using carbodiimide coupling chemistry. The functionalized magnetic beads (15 µL for CRP, 30 µL for BSA-3-NT) were first washed 3 times with 1X PBS. Capture antibody (1 mL, 70 µg/mL) or the BSA-hapten (1 mL, 67 µg/mL) was added along with EDC (100 µL, 10 mg/mL) and allowed to react overnight at room temperature. The EDC was added to facilitate coupling of the protein to the magnetic beads. All dilutions were made in the conjugation buffer (0.1 M MES, 0.9% NaCl, pH 4.7). The solution was then aspirated and the beads washed 3 times with 1X PBS. The capture beads for either CRP or BSA-3-NT were resuspended in 1 mL 1X PBS and stored at 4 °C for up to 1 month. Coupling efficiency was determined by measuring the absorbance (λ = 280 nm) of the protein solution before and after the coupling reaction. The difference in absorbance and the corresponding molar extinction coefficient (IgG = 210,000 $M^{-1}cm^{-1}$, BSA = 43,824 $M^{-1}cm^{-1}$) were used to calculate the amount of protein bound to the particles based on the Beer-Lambert law. Detection antibodies were prepared according to procedures described in section 2.5.2 above.

Assay procedure

CRP capture beads (300 µL) and BSA-3-NT functionalized beads (200 µL) were combined in a single microcentrifuge tube. The antigen solution (75 µL) containing CRP, 3-NT

and the 3-NT detection antibody (30 µg/mL) was added to the beads and allowed to react for 2 h at room temperature. After 2 h, the beads were separated from the liquid using a stationary magnet and the liquid discarded. The particles were then rinsed 3 times with NaCl (1 M) containing 0.05% Tween 20 followed by 3 rinses with 1X PBS. To reduce the amount of nonspecific binding, the beads were rinsed three times with SuperBlock blocking buffer. Finally, the detection antibody for CRP (75 µL, 30 µg/mL) was added to the beads and allowed to react for 30 min at room temperature. To remove any non-specifically bound detection antibodies, the beads were rinsed three times with NaCl (1 M) followed by three times with 1X PBS. Cleavage was carried out using TCEP (500 µM, 70 µL) for 20 min at room temperature. Finally, the solution containing the fluorescent fragment was removed from the beads and analyzed using microchip micellar electrokinetic chromatography (MEKC). The run buffer for MEKC was 10 mM tetraborate, 50 mM SDS, 10 mM DDAPS (N-dodecyl-N,N-dimethyl-3-ammonio-1-propanesulfonate). The steps for mixed competitive/non-competitive CTI are shown in Figure 2.2C.

Generation of Calibration Curves

Calibration curves for all analytes were constructed for concentrations which spanned the reference ranges (Table 1). The curves were fit using a standard 4-parameter logistic model described by the following equation [16]:

$$y = A_2 + \frac{(A_1 - A_2)}{\left(1 + \left(\frac{x}{x_0}\right)^p\right)} \qquad (1)$$

where y is the response signal, A_2 is the response at infinite analyte concentration (antibody saturation), A_1 is the response at zero analyte concentration, x is the analyte concentration, x_0 is

the inflection point on the curve (IC_{50}, center of the curve), and *p* is the slope factor. The logistic equation fit was also used to determine the limit of detection (LOD), defined as the analyte signal that corresponded to three times the standard deviation of the zero analyte signal, and the limit of quantification (LOQ), defined as the analyte signal that corresponded to ten times the standard deviation of the zero analyte signal.[22]

RESULTS

Competitive CTI

In a competitive immunoassays, as the analyte concentration increases, the concentration of the captured tagged antibody decreases, and hence the detectable signal decreases.[16] Assays for T4 and 3-NT were first carried out individually to demonstrate competitive CTI. Sample electropherograms for the detection of varying concentrations of T4 using competitive CTI are shown in Figure 2.3A. Similar results were obtained when 3-NT was used as the model analyte (data not shown). These results show the characteristic competitive behavior. The inconsistent migration times from run-to-run are the result of low electroosmotic flow stability from the polydimethylsiloxane surface used in these experiments.[23] A sample competitive CTI calibration curve for T4 is shown in Figure 2.3B. Fitting the T4 standard curve using the 4-parameter logistic model described in section 2.8 above gave a correlation coefficient (R^2) of 0.997, a calculated LOD of 23 nM and LOQ of 77 nM while the fit using the 4-parameter logistic model for 3-NT gave an R^2 of 0.981, an of 0.5 μg/mL and an LOQ of 1.7 μg/mL. Differences in units here reflect the differences in reported clinical units. The upper reference level for T4 analytes was marked on curves indicating that our method provided the analysis of the markers in the normal range. This method also gave an acceptable reproducibility with the average relative

standard deviation for each analyte concentration of 6.37% and 7.69% for T4 and 3-NT, respectively. All errors were calculated as a standard deviation of the signals from three MCE runs.

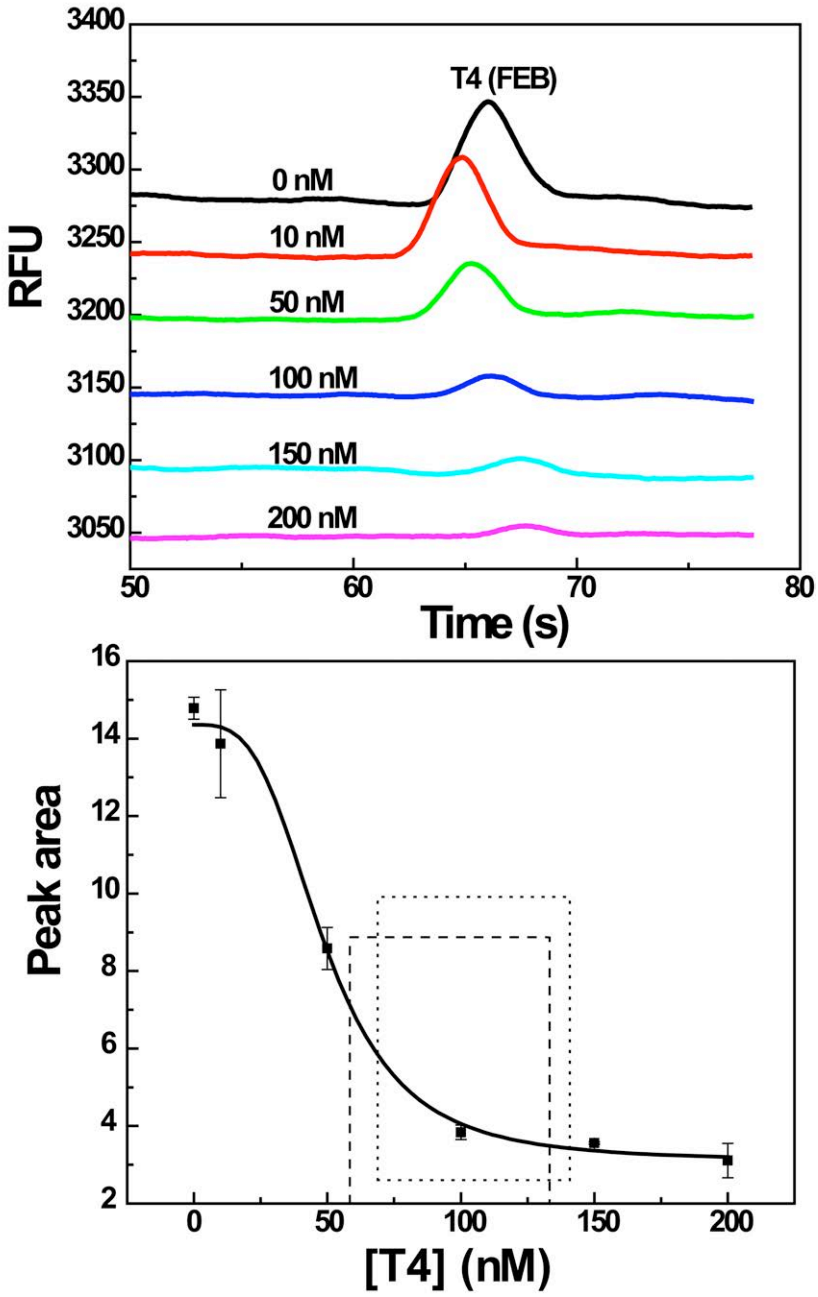

Figure 2.3. (A) Example electropherograms for competitive CTI of T4. (B) Typical competitive CTI calibration curve for T4. The reference range of T4 is marked on the curve for male (dashed line) and female (dotted line). T4 detection antibody tagged by FEB. Separation conditions are reported in the text. Fluorescence detection was performed using an inverted fluorescent microscope. RFU is relative fluorescence units.

After demonstrating the proof-of-concept for competitive CTI for a single analyte, a multi-analyte assay was performed using 3-NT and T4. The BSA-3-NT and BSA-T4 conjugates were co-immobilized onto a well surface. In this case, the 3-NT concentration was varied while the T4 concentration was held constant. The data presented in Figure 2.4A demonstrate the detection of these two analytes from a single sample. The cleaved tags are well resolved using the separation conditions described in Figure 2.3. The dose response curve for 3-NT in the presence of 50 nM T4 is shown in Figure 2.4B as a function of 3-NT concentration. A decrease in signal is observed for the 3-NT as the concentration is increased in the sample while no change in the peak area is observed for T4 thus illustrating the selectivity of the system. In addition, these results demonstrate the possibility of multi-analyte biomarker detection in complex biological samples with no need for complicated sample preparation.

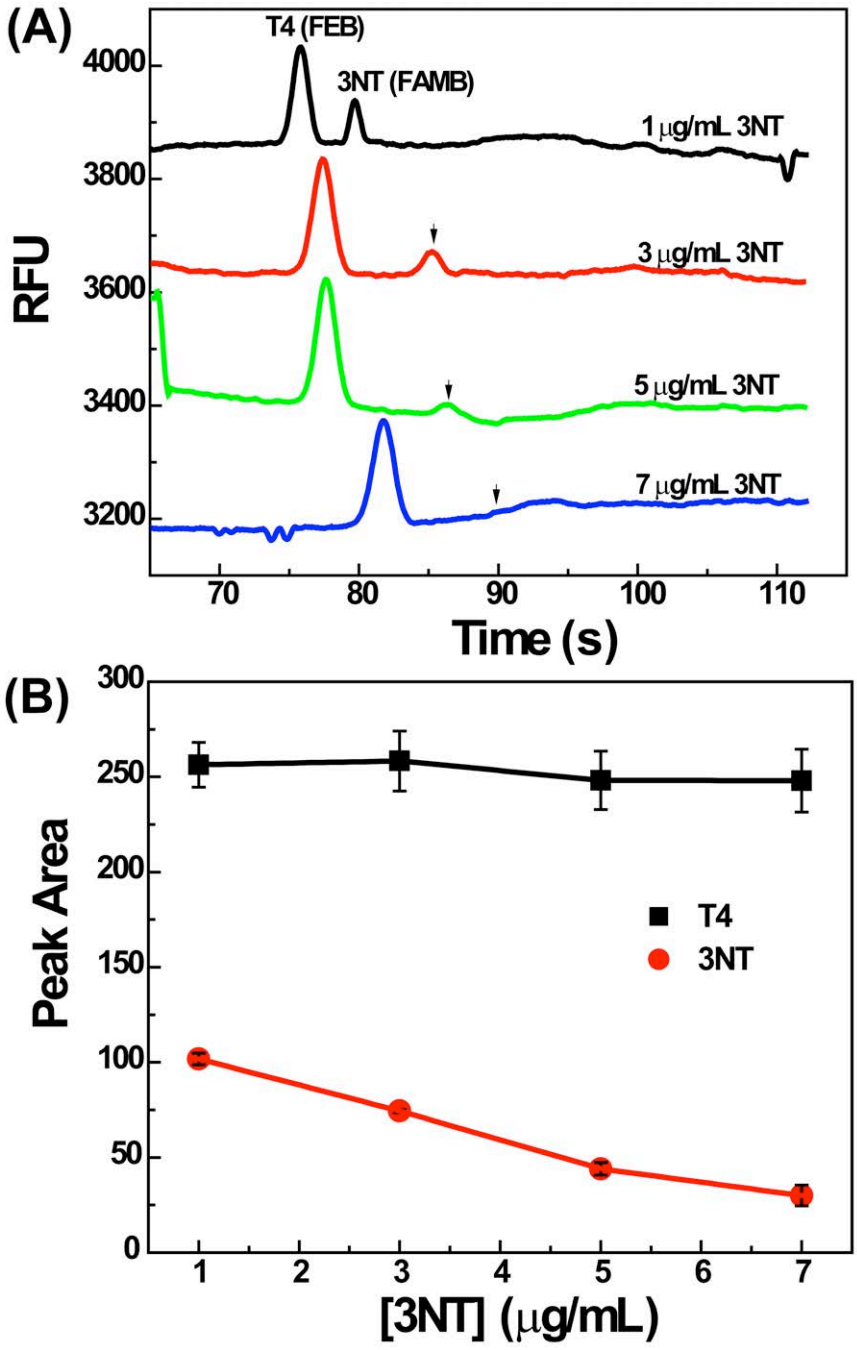

Figure 2.4. Electropherograms of multi-analyte competitive CTI. (A) Electropherograms showing the multi-analyte competitive CTI of 3-NT and T4, variable concentration of 3-NT (1-7 μg/mL) and constant concentration of T4 (50 nM) were added to run competitive CTI. (B) Resulting dose-response curve for 3-NT (●) and T4 (■). Error bars for 3-NT are contained within the points. Separation conditions are the same as those given in Figure 3

Non-competitive CTI

Bead-based immunoassays are dependent on both bead volume (solid-phase) and amount of cleavage agent added. By adjusting these parameters, the sensitivity can be shifted to the desired concentration range for the analyte of interest. In this case, assay parameters were adjusted to ensure that the sensitive portion of the curve for CRP bracketed the reference interval. The reference interval is generally defined as the level below which 95% of the normal population falls. As is typical for immunoassays, the data is shown in semi-log format (Figure 2.5). The reference interval is marked on the calibration curve in order to illustrate the ability of non-competitive CTI to distinguish between normal and elevated CRP levels. The linear range, and LOD, and LOQ for CRP are also given in Table 2.1 along with the reference interval. The limit of detection is defined here as a signal greater than three times the baseline noise. Furthermore, when a healthy control serum sample was run, no signal was seen for CRP demonstrating the selectivity of this assay in the presence of serum proteins.

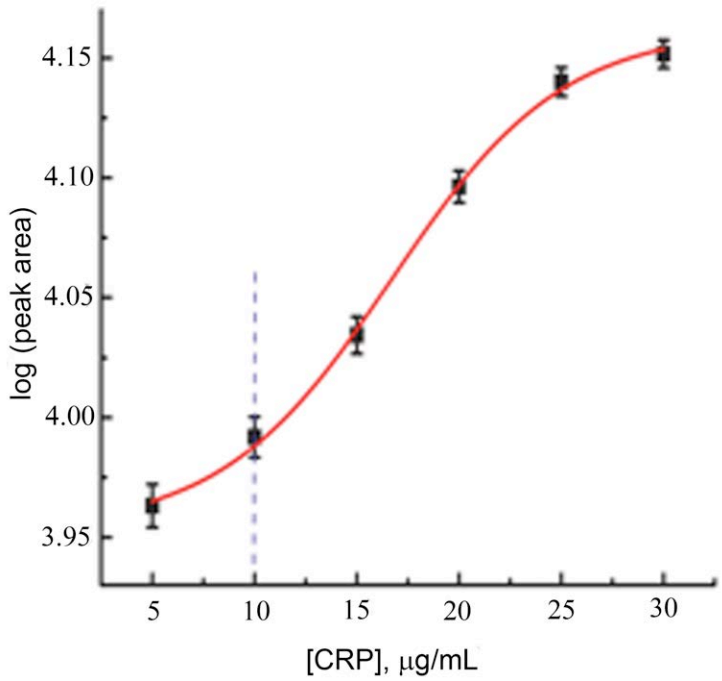

Figure 2.5. Calibration curve for CRP detected via non-competitive CTI. Concentrations span both normal and elevated levels. The upper reference limit is marked on the curve. CRP was diluted in 1X PBS. Detection antibody for CRP tagged with FHB. Separation conditions are reported in the text. Fluorescence detection was performed using an inverted fluorescent microscope.

Table 2.1. Linear range, LOD, and LOQ for CRP, T4, and 3-NT.

Biomarker	Reference Interval	LOD	LOQ	Linear Range
C-reactive protein (CRP)	< 10 µg/mL[24]	5 µg/mL	17 µg/mL	10-25 µg/mL
Thyroxine (T4)	Male: 59-135 nM[24] Female: 71-142 nM[24]	23 nM	77 nM	10-100 nM
3-nitrotyrosine (3-NT)	< 1.2 µg/mL[25]	0.5 µg/mL	1.7 µg/mL	0.5-7 µg/mL

Mixed format CTI

After showing viability of non-competitive and competitive CTI individually, a mixed format CTI was carried out with 3-NT (competitive) and CRP (non-competitive) as the molecules of interest. In this two component assay, FAMB was used for 3-NT and FHB was used for CRP. The data presented in Figure 2.6 demonstrates the detection of these two entities from a single sample. Two separate samples with differing known amounts of 3-NT and CRP were used for the mixed format CTI. In Figure 2.6A the concentrations were 5 μg/mL and 10 μg/mL for 3-NT and CRP, respectively and in Figure 2.6B the concentrations were 3 μg/mL and 30 μg/mL for 3-NT and CRP. In the resulting electropherograms, the peak height for CRP increased by a factor of 2.8 while the 3-NT peak height decreased by a factor of 0.17. These changes are in line with the stated concentration changes from the samples. Furthermore these changes bracket the clinical reference values for both 3-NT and CRP. This represents the first example of a mixed format immunoassay done using CTI. It should be noted that these calculations were based on the peak height and not peak area as a result of the shoulder on the 3-NT peak. The identity of the shoulder is not known at this time but is currently under investigation.

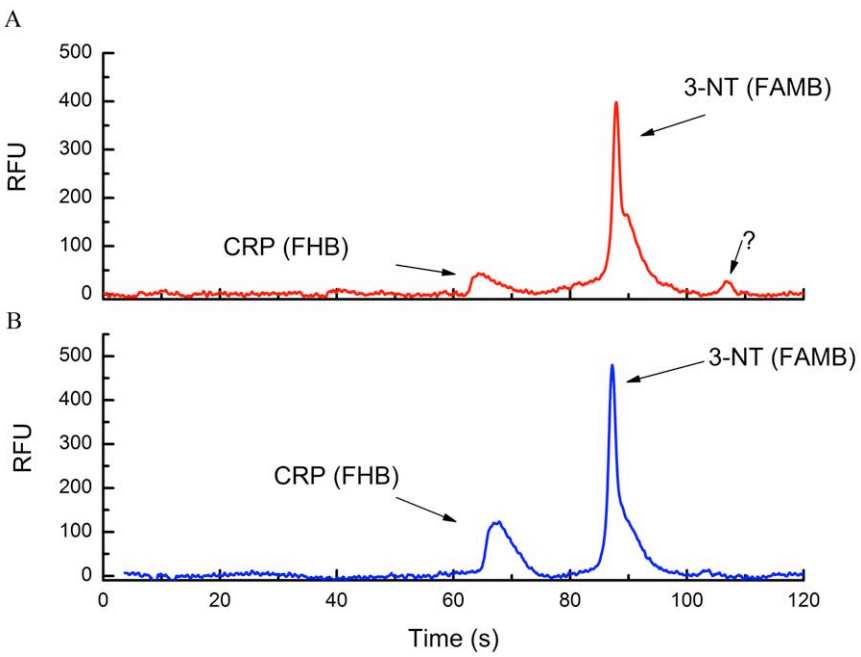

Figure 2.6. Electropherograms of mixed non-competitive/competitive CTI. (A) 5 μg/mL 3-NT and 10 μg/mL CRP in PBS (B) 3 μg/mL 3-NT and 23 μg/mL CRP in PBS. Separation conditions are reported in the text. Fluorescence detection was performed using an inverted fluorescent microscope. RFU is relative fluorescence units.

DISCUSSION

Chronic diseases typically cause changes in both circulating proteins and metabolites; however, currently available assays are generally capable of screening for one or the other but not both of these classes of biomarkers. CTI chemistry is able, with small modifications, to measure both small molecule metabolites and proteins in a single run using a mixed format approach to immunoassays. We have successfully shown that the CTI can be used to separately quantify small molecules (metabolites) in competitive format and proteins in the non-competitive format. Furthermore, we successfully demonstrate the ability to use non-competitive and competitive CTI simultaneously in a single assay for the detection of markers related to inflammation, namely 3-NT (competitive CTI) and CRP (non-competitive CTI). To our

knowledge this is the first report of a mixed competitive/non-competitive CTI. The concentrations studied fall at or above the reference intervals for both 3-NT and CRP indicating the ability to discern between normal and elevated levels of small molecules and proteins. The results shown here were collected from 3-NT and CRP standards diluted in PBS; however, given that we have not seen any interference from complex samples such as serum when performing non-competitive or competitive CTI separately, we do not anticipate any issues when transitioning to real samples.

We were able to detect 3-NT, T4, and CRP at both normal and elevated levels with LODs in the low μg/mL range. One reason for this is that the final step in the CTI, the cleavage step, not only serves to cleave the tags from the detection antibodies but also as a pre-concentration step as the volume of solution in which the detectable product is present has been reduced by 5-50 % compared to the original sample volume. It is important to note that the incubation times currently employed in the off-chip CTI are quite long (30 min. to 2 h). In our future work, the incubation time will be significantly shortened due to reduced diffusion distances when the entire assay is performed within a microfluidic device and magnetic beads will be used as a solid support in on-chip immunoassay as they can be held within the chip by the external magnetic field.[26]

While the use of a microtiter plate instead of polymer beads for the competitive CTI simplifies the rinse steps compared to the non-competitive CTI, the use of well surfaces as a solid support causes lower sensitivity than bead-base materials due to lower surface area.[16]

This is the first report of the use of magnetic particles in the CTI. Magnetic particles are known to provide better volume control, ease of sample manipulation and an increase in the solid support surface area compared to polymer microparticles or microtiter plates. For these reasons

we chose to use carboxyl derivatized magnetic particles for the mixed mode competitive/non competitive CTI. Furthermore, the use of magnetic particles will facilitate the transition to performing the entire CTI assay, including sample processing, within a microfluidic device.

CONCLUSIONS

Here we successfully demonstrated the ability to perform CTI in competitive, non-competitive and mixed competitive/non-competitive formats for the detection of inflammation biomarkers. As model analytes, T4 and 3-NT were selected to show the proof-of-principle for multi-analyte competitive CTI. CRP was successfully analyzed by non-competitive CTI. LOD, LOQ and working range were determined and encompass the upper reference levels for the three molecules studied. Finally, CRP and 3-NT were selected to demonstrate that the mixed competitive/non-competitive CTI can be conducted with successful results indicating that using CTI proteins and small molecules can be determined simultaneously. This assay gives a promising method for screening small molecule and protein biomarkers, and offers an alternative for to clinical applications requiring a multi-analyte point-of-care screening system. This novel assay provides much lower analysis time, sample consumption as well as cost of analysis compared to the traditional analytical methods.

REFERENCES

(1) Sameenoi, Y.; Mensack, M. M.; Murphy, B. M.; Henry, C. S. *Methods* **2012**, *56*, 166.
(2) Wu, A. H. B. *Clin. Chim. Acta* **2006**, *369*, 119.
(3) Yalow, R. S.; Berson, S. A. *Nature* **1959**, *184*, 1648.
(4) MacBeath, G. *Nature Genet.* **2002**, *32*, 526.
(5) Ekins, R.; Chu, F. *Clin. Chem.* **1993**, *39*, 369.
(6) Seidel, M.; Niessner, R. *Anal. Bioanal.Chem.* **2008**, *391*, 1521.
(7) Guzman, N. A. *Anal. Bioanal. Chem.* **2004**, *378*, 37.
(8) Caulum, M. M.; Henry, C. S. *Analyst* **2006**, *131*, 1091.
(9) Caulum, M. M.; Murphy, B. M.; Ramsay, L. M.; Henry, C. S. *Anal. Chem.* **2007**, *79*, 5249.
(10) Guzman, N. A.; Blanc, T.; Phillips, T. M. *Electrophoresis* **2008**, *29*, 3259.
(11) Amundsen, L. K.; Siren, H. *Electrophoresis* **2007**, *28*, 99.
(12) Gowda, G. A. N.; Zhang, S. C.; Gu, H. W.; Asiago, V.; Shanaiah, N.; Raftery, D. *Expert Rev. Mol. Diagn.* **2008**, *8*, 617.
(13) Debbage, P. *Curr. Pharm. Design* **2009**, *15*, 153.
(14) McKinney, J. D.; Waller, C. L. *J. Toxicol. Env. Health-Pt b-Crit. Rev.* **1998**, *1*, 27.
(15) Giustarini, D.; Dalle-Donne, I.; Tsikas, D.; Rossi, R. *Crit. Rev. Clin. Lab. Sci.* **2009**, *46*, 241.
(16) Eleftherios P. Diamandis, T. K. C. *Immunoassay*; Academic Press: San Diego, CA, 1996.
(17) Guillo, C.; Roper, M. G. *Electrophoresis* **2008**, *29*, 410.
(18) Murphy, B. M.; Dandy, D. S.; Henry, C. S. *Anal. Chim. Acta* **2009**, *640*, 1.
(19) Liu, Y.; Fanguy, J. C.; Bledsoe, J. M.; Henry, C. S. *Anal. Chem.* **2000**, *72*, 5939.
(20) Garcia, C. D.; Liu, Y.; Anderson, P.; Henry, C. S. *Lab Chip* **2003**, *3*, 324.
(21) Englebienne, P. *Immune and receptor assays in theory and practice*; CRC Press: Boca Raton, 2000.
(22) Taylor, J.; Picelli, G.; Harrison, D. J. *Electrophoresis* **2001**, *22*, 3699.
(23) Garcia, A. L.; Ista, L. K.; Petsev, D. N.; O'Brien, M. J.; Bisong, P.; Mammoli, A. A.; Brueck, S. R. J.; Lopez, G. P. *Lab Chip* **2005**, *5*, 1271.
(24) Tietz, N. W. *Clinical Guide to Laboratory Tests*; 3rd ed.; W.B. Saunders: Philadelphia, Pennsylvania, 1995.
(25) Ryberg, H.; Caidahl, K. *J. Chromatogr. B* **2007**, *851*, 160.
(26) Gijs, M. A. M. *Microfluid. Nanofluid.* **2004**, *1*, 22.

CHAPTER 3. DEVELOPMENT OF A ROBUST MICROFLUIDIC ELECTROCHEMICAL SENSOR: A TOOL FOR AEROSOL OXIDATIVE ACTIVITY MESUREMENT

CHAPTER OVERVIEW

A second goal of my research was to create an on-line monitoring system to assess oxidative stress caused by atmospheric aerosols. In this chapter, as the first step toward this goal, a robust microfluidic electrochemical sensor was created using a novel fabrication method. New carbon paste materials employing a mixture of poly(dimethylsiloxane) (PDMS) and mineral oil as the binder and graphite powder as electrode materials were used to create a robust electrode. The device was fabricated using a screen printing analogue where the paste was filled on the channel of the PDMS slab. The sensor created in this work has been extensively used for chemical assay oxidative stress assessment *via* oxidative activity generated by atmospheric aerosol described in Chapter 4 (dithiothreitol (DTT) assay) and Chapter 5 (salicylic acid trapping assay). In particular, the cobalt phthalocyanine modified carbon paste used as electrode material on the sensor was tested for DTT analysis and demonstrated the improvement detection compared to unmodified electrodes. The analysis of DTT shown in this work demonstrated the ability to detect the remaining DTT in the DTT assay for measuring oxidative activity. This work was published in the journal *Analyst,*[1] and the text and figures in this Chapter were obtained from that article. This work was contributed by Dr.Meghan Mensack and Rebecca Ewing on data collection and analysis on Figure 3.3, 3.4, 3.8 and 3.9 and the rest of the work was performed by me.

SYNOPSIS

Recently, the development of electrochemical biosensors as part of microfluidic devices has garnered a great deal of attention because of the small instrument size and portability afforded by the integration of electrochemistry in microfluidic systems. Electrode fabrication, however, has proven to be a major obstacle in the field. Here, an alternative method to create integrated, low cost, robust, patternable carbon paste electrodes (CPEs) for microfluidic devices is presented. The new CPEs are composed of graphite powder and a binder consisting of a mixture of poly(dimethylsiloxane) (PDMS) and mineral oil. The electrodes are made by filling channels molded in previously cross-linked PDMS using a method analogous to screen printing. The optimal binder composition was investigated to obtain electrodes that were physically robust and performed well electrochemically. After studying the basic electrochemistry, the PDMS-oil CPEs were modified with multi-walled carbon nanotubes (MWCNT) and cobalt phthalocyanine (CoPC) for the detection of catecholamines and thiols, respectively, to demonstrate the ease of electrode chemical modification. Significant improvement of analyte signal detection was observed from both types of modified CPEs. A nearly 2-fold improvement in the electrochemical signal for 100 μM dithiothreitol (DTT) was observed when using a CoPC modified electrode (4.0 ± 0.2 nA (n=3) versus 2.5 ± 0.2 nA (n=3)). The improvement in signal was even more pronounced when looking at catecholamines, namely dopamine, using MWCNT modified CPEs. In this case, an order of magnitude improvement in limit of detection was observed for dopamine when using the MWCNT modified CPEs (50 nM versus 500 nM). CoPC modified CPEs were successfully used to detect thiols in red blood cell lysate while MWCNT modified CPEs were used to monitor temporal changes in catecholamine release from PC12 cells following stimulation with potassium.

INTRODUCTION

The integration of electrochemical biosensors as part of microfluidic devices is attractive because of the size and volume compatibility between electrochemistry and microfluidics. One of the major challenges in this field, however, has been electrode fabrication. Traditional thin-film fabrication methods are limited to the use of either noble metals or reactive metals such as Cu. Noble metal electrodes are easily modified through self-assembled monolayers and exhibit fast electron transfer kinetics but readily foul in biological media.[2,3] One solution is the use of carbon-based electrode materials.[4] Carbon-based electrodes are attractive for electrochemical sensing due to their ability to withstand fouling and they possess a larger potential range compared to metal electrodes.[5-7] Common forms of carbon electrodes used in the development of biosensors include glassy carbon,[8,9] pyrolyzed carbon,[10] carbon pastes,[11,12] micromolded carbon ink,[13] carbon doped photoresist,[14] and carbon nanotubes (CNTs).[6,15-17] Each of these forms of carbon has unique advantages and disadvantages with regards to fabrication and use. For example, pyrolyzed carbon electrodes can be made in a wide range of sizes and shapes but require a substrate that can withstand the high temperatures necessary for photoresist pyrolysis.[10] Carbon doped photoresist electrodes overcome the need for high temperatures by making the photoresist conductive. Unfortunately, the large graphite particles cause light scattering during photopatterning, making it difficult to create small electrodes.[14] Finally, all of these methods generate raised electrode structures that disrupt the sealing of device layers and cause leakage around the electrodes. Of these materials, carbon pastes are one of the most attractive because they are easily fabricated and can be readily modified to enhance selectivity.[5-7,18,19] Unfortunately, they are generally unstable in flow based analysis devices such as those used in

microfluidics. Here, a new method is reported for fabricated carbon paste electrodes in poly(dimethylsiloxane) (PDMS) microfluidic devices that addresses these limitations.

Carbon paste electrodes (CPE) are amenable to miniaturization and have shown utility in a broad range of applications.[20,21] The mixture of graphite carbon and a binder (mineral oil, etc.) allows for ease of fabrication of CPEs; furthermore, CPEs can be modified with dopants, are size adjustable and can be easily integrated with various systems.[22] Recently, CPEs have shown promise as electrochemical sensors in microfluidic devices.[18,19] Various methods have been used for the integration of CPEs as sensors within microfluidic devices including filling tube sleeves with carbon paste[19,23] and screen printing of carbon paste on PDMS substrates.[18] Tube sleeve electrodes are not readily amenable to on-chip production because of their large size (on the order of several mm in diameter) which can lead to sealing issues. In contrast, screen-printed electrodes can be directly fabricated on-chip with the electrode size and shape controlled by the screens used for patterning on the microfluidic devices.[18] Screen printing also allows for simple, rapid, inexpensive mass-production of disposable electrochemical sensors.[24,25] Carbon paste for screen-printed electrodes can be classified as soft or rigid composites. This distinction is based largely upon their mechanical properties.[26] Soft composites are obtained by mixing graphite powder with mineral oils resulting in a chemically inert, electroinactive, pliable electrode material with moderate viscosity, low volatility and minimal solubility in aqueous solution.[22] Soft composites can be physically unstable, which becomes an issue in a microfluidic device where the solution flow can cause the soft paste to flow between electrodes. In contrast, rigid composites utilize mixtures of graphite powder and non-conducting polymeric binders to create rigid features resulting in a more robust electrode.[26]

Poly(dimethylsiloxane) (PDMS) is widely used as a microchip material due to its ease in fabrication and low cost. In this report, the use of PDMS as a binder to facilitate sealing of CPEs to microfluidic devices was investigated. The PDMS composition of both the CPE and the microfluidic substrate allows for better adhesion between the two materials. Another advantage to the use of carbon-PDMS electrodes is the reduction in capacitive current compared to bulk glassy carbon and other patternable electrodes.[27] The low capacitive current of these electrodes, however, also comes at the cost of reduced analyte signal. To overcome this, a large amount of graphite must be incorporated into the paste, which in turn results in mixing issues and electrode surface heterogeneity. Recently, PDMS was successfully used as a binder to create low-cost, patternable carbon-PDMS electrodes for chip-based electrochemical detection[27] and demonstrated compatibility within a PDMS microfluidic environment; however, since PDMS was the only binder used, the resulting electrodes exhibited slow electron transfer kinetics.

Here, we report the use of a mixed binder to create on-chip CPEs in microfluidic devices. The binder mix is a combination of a rigid composite (PDMS) and a soft composite (mineral oil) providing an improvement in physical stability and electrochemistry of the CPE compared to using PDMS or mineral oil alone. Optimal compositions of the binder mixture were investigated to obtain robust electrodes with low capacitive currents. Moreover, a new on-chip method for CPE fabrication is reported that is based on screen printing. Our method uses molded PDMS containing electrode channels filled with carbon paste where the channels provide well-defined electrodes for integration into microfluidic systems. Electrode performance was investigated by cyclic voltammetry in static solutions and amperometry with flow injection analysis. CPEs made using our methods can also be readily modified to improve selectivity. Mixed PDMS-mineral oil CPEs were modified with cobalt phthalocyanine (CoPC) and multi-walled carbon nanotubes

(MWCNT) for the detection of thiols and catecholamines, respectively. The utility of the modified electrodes is shown with the detection of thiols in erythrocyte lysate and catecholamine release from PC12 cells.

MATERIALS AND METHODS

Chemicals and Materials

All chemicals used were of analytical grade. The following materials and chemicals were used as received: poly(dimethylsiloxane) (PDMS) Sylgard 184 elastomer kit (Dow Corning, Midland, MI), Hydrochloric acid (Thermo Fisher), potassium chloride (Thermo Fisher), mineral oil (Thermo Fisher), sodium chloride (Thermo Fisher), graphite powder (Sigma Aldrich), nitric acid (Thermo Fisher) and silver conductive paint (SPI supplies, West Chester, PA). Copper wire was obtained from NTE Electronics (Bloomfield, NJ). A stock solution of dopamine hydrochloride (100 mM, Sigma Aldrich) was prepared in 0.01 M HCl and 0.1M NaCl which was subsequently diluted to 1 mM using the background electrolyte prior to analysis.

Electrode Fabrication

Electrode fabrication was achieved using a method analogous to screen printing. Channels were created in PDMS using soft lithography techniques.[28] Carbon paste (a mixture of electrocatalyst reagent, graphite powder, mineral oil and PDMS) was spread on the PDMS containing the electrode channels using a plastic artist's pottery scraper or screen printing squeegee. Prior to applying the carbon paste, Scotch Magic Tape™ was applied around the electrode channels to act as a border for the carbon paste for an easy cleaning purpose. Excess paste was removed by wiping the scraper over the electrode channel and any remaining paste

removed by application and removal of a piece of tape over the paste until all excess carbon paste around the electrode area was removed, leaving the patterned electrodes. For the flow injection analysis, a second piece of PDMS containing a flow channel was plasma sealed to the piece of PDMS containing the electrodes in an orthogonal orientation. A 1 mm diameter hole was punched in one end of the flow channel as the inlet hole for connection to the off-chip injection valve and syringe pump (PHD 4400, Harvard Apparatus, Holliston, MA) and an 8 mm waste reservoir was punched at the opposite end of the channel. Finally, copper electrode leads were attached to the ends of the carbon electrodes using silver epoxy. The schematic diagram for the electrode fabrication process and the resulting electrode design are shown in Figure 3.1. For cyclic voltammetry (CV) data collection, 8 mm PDMS fluidic reservoirs were plasma sealed over the electrodes leaving an 8 mm × 0.25 mm working electrode area within the well. For the flow system, the surface area of the working electrode was approximately 0.0625 mm^2. Electrodes were cleaned using air plasma (20 min, 150 W, 0.8 torr) prior to chip assembly.

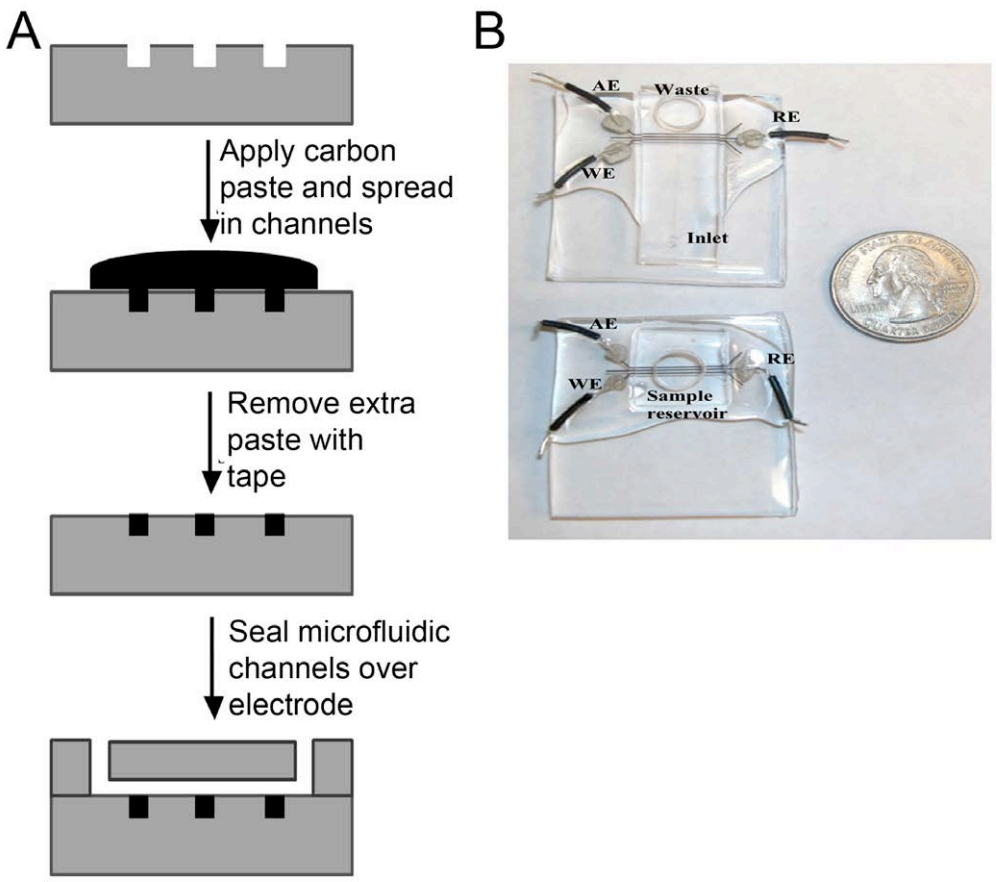

Figure 3.1. Flow-based microfluidic system using CPEs. (A) Schematic for electrode fabrication process (side view) (B) Actual picture of electrode alignment in a microfluidic device for the flow injection system with amperometric detection (top) and for cyclic voltammetry study (bottom). Size of electrodes: 250 µm wide and 50 µm deep. Electrode spacing (center-to-center), 300 µm. Microfluidic channel dimension: 250 µm wide, 50 µm deep and 2.5 cm long.

Electrochemical Detection System

Commercially available potentiostats (CHI660b, CH Instruments and EA164 Quadstat, eDAQ) were used for amperometry and cyclic voltammetry experiments. Cyclic voltammograms were carried out at scan rates of 0.05, 0.1, 0.2, 0.25, 0.4 and 0.5 V/s from -0.2 V to 1.2 V with the initial potential set at 0.0 V. An average of three repetitions was done for each potential sweep rate. Amperometry was run at +0.6 V, +0.2 V, and +0.8V for dopamine, dithiothreitol

(DTT), and glutathione (GSH), respectively. All experiments were conducted using a three-electrode system consisting of a screen printed carbon electrode as a working electrode and either a Ag/AgCl (3 M KCl) reference electrode and a platinum counter electrode in the waste reservoir or a set of integrated unmodified carbon paste electrodes. Noise was determined by measuring peak-to-peak current at 35 random points along the baseline.

Thiol Analysis System

For thiol detection, graphite electrodes were modified with cobalt phthalocyanine (CoPC). CoPC was added to graphite powder (12% w/w) and the mixture added to diethyl ether in a ratio of 1:10 (w/v). The solution was mixed for 2 h to ensure a homogeneous mixture of CoPC and graphite powder. Diethyl ether was evaporated prior to electrode fabrication. CoPC modified graphite powder was then mixed with oil and PDMS in a ratio of 5:3:2 (w:w:w) of graphite powder: mineral oil: PDMS. This mixture was used to fabricate electrodes as described above. For DTT detection, a Ag/AgCl (3 M KCl) reference electrode and a platinum counter electrode were placed in the waste reservoir. For GSH analysis, on-chip unmodified carbon paste electrodes were used as the reference and auxiliary electrodes.

Dopamine Analysis System

Electrodes were also modified with multiwall carbon nanotubes (MWCNT) to improve electrode performance in the detection of dopamine. In this case, MWCNT were mixed with the graphite powder at 10% (w/w) prior to electrode fabrication. A 1:1 mixture of binder and graphite/MWCNT were combined to produce the carbon paste. Electrodes were fabricated as described above.

Sample Preparation

Red blood cell (RBC) lysate for GSH analysis was prepared according to the literature.[29,30] In brief, freshly collected human whole blood (5 mL) was centrifuged 1000 × g for 15 min at 4 °C to separate plasma and erythrocytes. The plasma was then discarded and the erythrocytes rinsed three times with phosphate buffer saline (PBS, pH 7.4). Portions of the erythrocytes were hemolysed in 1 mM Na_2H_2EDTA solution (1:1 v/v) with 10% (w/v) of 5-sulfosalicylic acid. The mixed solution was centrifuged at 1000 × g for 15 min at 4 °C. The supernatant containing RBC lysate was collected for GSH analysis. Dilutions of RBC lysate were carried out using PBS.

PC12 cells were obtained from American Type Culture Collection (ATCC, Manassas, VA) and maintained in F-12K medium supplemented with 10% fetal bovine serum. The cells were grown on poly-D-lysine-coated T-25 culture flasks (VWR International, Radnor, PA). Cell medium was replaced every 3 d and subcultured as needed. Cells were trypsinized at 37 °C for 10 min to release adherent cells from culture flask surface. Trypsin was neutralized by the addition of an equal amount of F-12K medium. The cells were centrifuged and the supernatant aspirated from the pellet. The pellet was resuspended in 4 mL PBS. Cells (20 μL) were diluted 1:1 with 0.4% trypan blue for counting. Cells were washed 3x with PBS (pH 7.4) to remove any residual media prior to analysis.

Stimulation of the PC12 cells was carried out by exposing the cells to 80 mM K+ (KCl) in 1X PBS (pH 7.4) at room temperature. For the time course study, approximately 6.15 x 10^4 cells (300 μL) were placed in 1.5 mL microcentrifuge tubes and the high potassium buffer added (300 μL) to each tube at 1 min increments for 10 min total. The cells were centrifuged at 1000X

g for 5 min and 500 μL of supernatant removed and placed in a fresh tube for later analysis. Samples were kept on ice until analysis to prevent dopamine degradation.

RESULTS AND DISCUSSION

Optimization of binder composition

The long-term goal of this project is to create low-cost biosensors that can be used repeatedly for weeks to months. To meet this objective, carbon paste electrodes containing mineral oil as the binder were integrated into microfluidic devices. Initial attempts at creating stable biosensors in flow-based analytical devices were unsuccessful, however, due to leakage of carbon between electrodes after just 2 h in a flow injection device as shown in Figure 3.2A. To increase the electrode's physical stability, PDMS was tested as an additive to the mineral oil binder expecting that the PDMS would cross-link with the existing PDMS of the channel resulting in physically stable electrodes. This approach proved successful with electrodes remaining intact for extended periods in flowing systems as shown in the photomicrographs of Figure 3.2B.

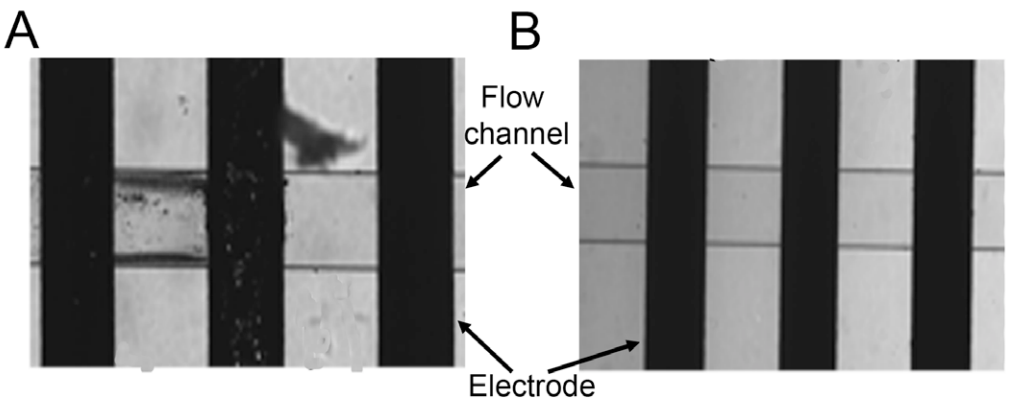

Figure 3.2. Electrode photomicrographs within flow-based analytical devices after flow injection experiment for 2 hours at a flow rate of 60 μL min^{-1}. (A) Electrodes made with mineral oil binder. (B) Electrodes made with 2:3 PDMS:mineral oil binder. Size of electrodes and dimension of microfluidic channels are the same as described in Figure 1.

Once a method for physically stabilizing the electrodes was demonstrated, the effect of binder composition on peak current (i_p) was studied for varying PDMS:mineral oil ratios. Traditionally, CPEs are used as prepared, however, our group has recently shown that use of an oxygen plasma increases peak current density, shifts the ratio of cathodic to anodic current closer to unity, and decreases peak-to-peak separation for carbon electrodes.[14] The benefits are the result of exposure of additional graphite surfaces during the plasma treatment process. As a result of these findings, all CPE electrodes were treated with air plasma prior to use to expose additional graphite from the solid binder. A series of studies were conducted to determine the optimal ratio of PDMS:mineral oil in the electrode binder material. The ratios studied were 1:0, 3:2, 1:1, and 2:3 (PDMS:mineral oil). In all cases, the ratio of graphite to binder was held constant at 1:1 (w:w). The difference between cathodic and anodic peaks (ΔE), capacitive current, and the effect of scan rate on peak current density were used to determine the best ratio of PDMS to mineral oil. Three separate electrodes on different chips were tested for each ratio. Table 1 shows the values for anodic peak current (I_{pa}), ΔE, and capacitive current for all binder

ratios tested at 100 $mV*s^{-1}$ scan rate. Cyclic voltammograms at 100 $mV*s^{-1}$ for background electrolyte (0.01M HCl, 0.1M NaCl) and 1 mM dopamine using 1:0, 3:2, 1:1, and 2:3 PDMS:mineral oil ratios are shown in Figure 3.3A, while Figure 3.3B shows a scan rate study for the 1:1 ratio electrode. ΔE values at 100 $mV*s^{-1}$ scan rate for electrodes at the different ratios are 564.0 ± 55.7 mV, 221.6 ± 45.9 mV, 298.7 ± 71.8 mV, and 186.7 ± 43.0 mV (n=3) for 1:0, 3:2, 1:1 and 2:3 (PDMS:mineral oil), respectively.

Table 3.1. Electrode characterization. Values are reported for 100 mV/s scan rate. BGE: 10 mM HCl, 100 mM NaCl.

	ΔE (mV)	Capacitive Current ($\mu A/cm^2$)	I_{pa} (μA)
All PDMS	564.0 ± 55.7	3.0 ± 1.3	1.7 ± 0.2
3:2	221.6 ± 45.9	29.2 ± 10.7	2.1 ± 0.3
1:1	298.7 ± 71.8	19.6 ± 7.5	2.4 ± 1.0
2:3	186.7 ± 43.0	22.6 ± 12.0	2.8 ± 0.8

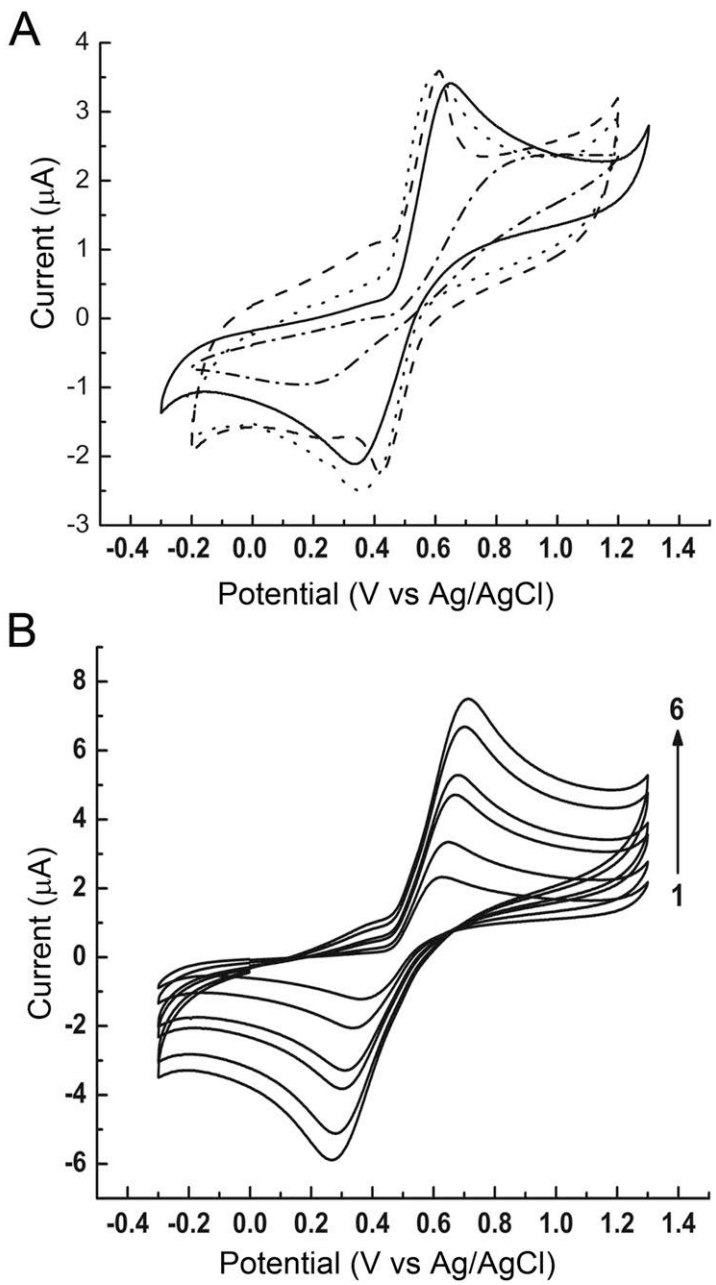

Figure 3.3. Comparison of electrode performance for the detection of dopamine at unmodified carbon paste electrodes. A) Cyclic voltammograms of 1 mM dopamine at four different binder composition electrodes: 1:0 (- · -), 3:2 (- -), 1:1 (**–),** and 2:3 (· · ·) (PDMS:mineral oil). Conditions: scan rate of 0.1 V/s between -0.2 and 1.2 V for 1:0, 3:2, and 2:3 binder composition and between -0.3 and 1.3 V for 1:1 binder composition in 10 mM HCl, 100 mM NaCl. B) Cyclic voltammograms of 1 mM dopamine in 10 mM HCl, 100 mM NaCl at varying scan rates (1-6) of 100, 200, 250, 400, 500, and 1000 mV/s.

All of the electrodes exhibit a linear relationship between the current density and the square root of the scan rate as predicted by the Randles-Sevcik equation indicating a diffusion limited reversible reaction [31] as shown in Figure 3.4. It is interesting to note that as the amount of PDMS in the binder is increased, the electrode sensitivity decreases as indicated by a decrease in slope of current density versus square root of the scan rate plot. The experimentally obtained peak oxidation current densities for dopamine (1 mM) are slightly less than expected for all ratios of chips tested based on the Randles-Sevcik equation given a diffusion coefficient of 4.2×10^{-6} cm^2 s^{-1}, scan rate of 100 mV s^{-1} and a measured geometric electrode area of 0.02 cm^2. Based on these conditions, the expected peak oxidation current density for dopamine (1 mM) should be 3.47 μA cm^{-2}, while the measured current density was 2.41 μA cm^{-2}. The deviation is likely due to the fact that the Randles-Sevcik equation assumes a uniform electrode surface. The carbon paste electrodes are a porous surface and contain a mixture of conducting graphite particles and non-conducting binder. From this study, it can also be noted that the CPEs deviate slightly from ideal electrode behavior. In a completely reversible reaction, one would expect the slope of current density versus scan rate$^{1/2}$ for oxidation and reduction to be equal and opposite; however, only the slopes for the oxidation and reduction reactions for the 1:1 binder composition were near equal and opposite with a ratio of 0.9. In contrast, the CPE made with all PDMS exhibited a ratio of just 0.6.

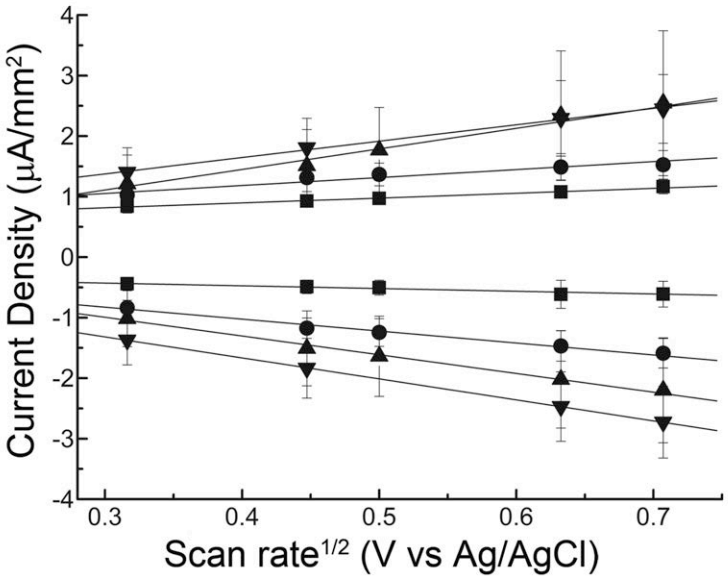

Figure 3.4. Current density-scan rate study for 1 mM dopamine in 10 mM HCl, 100 mM NaCl at four different binder composition electrodes: 1:0 (■), 3:2 (●), 1:1 (▲), 2:3 (▼) (PDMS:mineral oil). All show a linear dependence of the current density as a function of the square root of the scan rate. All electrodes were run in triplicate at each scan rate.

The capacitive current was also determined for each binder composition. Capacitive current is an important measure of surface area and also contributes to background noise for CV-based measurements. For the electrodes with all PDMS binder, the capacitive current was measured to be 3.0 ± 1.3 (n=3) μA cm^{-2} which was statistically lower than the other three binder compositions containing mineral oil measured at 29.2 ± 10.7 μA cm^{-2}, 19.6 ± 7.5 μA cm^{-2}, and 22.6 ± 12.0 μA cm^{-2} for the 3:2, 1:1, and 2:3 ratios, respectively (unpaired t-test, $p < 0.05$). None of the three mixed binder systems, however, were statistically different.

CoPC modified carbon paste electrodes

Thiol compounds play an important role in numerous biological functions.[32,33] Cysteine is an important structural element in many proteins while glutathione (GSH) plays a major role in intracellular oxidative stress defense as it reacts readily with free radicals and reactive oxygen species.[34] Fluorescence, UV and electrochemical detection have been employed previously for total thiol analysis.[35,36] Both fluorescence and UV detection generally require derivatization prior to detection to obtain selectivity.[36] Electrochemical detection, on the other hand, can be used to directly detect thiols without derivatization owing to the moderate oxidation potential of thiols.[35,37] Unmodified electrode materials such as gold and platinum can be used to detect thiols but require high applied potential (> +1.0 V) and often lead to electrode fouling after just a few runs.[38,39] Carbon electrodes can also be used to detect thiols but suffer from low peak currents due to less than ideal interactions between the carbon and the thiols. To overcome these problems, an electrocatalytic reagent is often added to decrease the detection potential and increase peak current. Cobalt phthalocyanine (CoPC) has been widely used as a redox mediator that lowers the overpotential for thiols.[39-41] Carbon paste has been used as an electrode material with CoPC.[30,39,40] Here, CoPC was doped into the PDMS:mineral oil CPEs to demonstrate the compatibility of the new fabrication method with chemical modification.

DTT was used as a model analyte to demonstrate the utility of CoPC modified carbon paste electrodes for thiol detection. The performance of bare CPEs and CoPC modified CPEs was compared using cyclic voltammetry and amperometry. Figure 3.5A shows cyclic voltammograms of CoPC modified CPE (solid line) and unmodified CPE (dashed line) of 1 mM DTT in MES buffer (30 mM, pH 7). With the conditions used for these experiments, DTT was not detected using unmodified CPEs whereas the oxidation peak of DTT was observed using

CoPC modified CPE as expected.[42] The two-step electrocatalytic process begins with the electrochemical oxidation of Co(II)phthalocyanine followed by the chemical oxidation of DTT as it regenerates the Co(II)phthalocyanine.[40] The optimal amount of CoPC added to the CPE was also investigated, and it was found that a CPE consisting of a 12% mixture of CoPC in graphite (w/w) provided the best performance for DTT detection (data not shown). The composition of the binder to create the paste was also investigated and found that the ratio of 2:3 (PDMS:mineral oil) provided the best electrode composition in terms of robustness and electrochemical performance. Finally, flow injection analysis using amperometric detection was employed to study electrode performance and provide continuous analysis of DTT. At +0.2 V (vs. Ag/AgCl (3 M KCl)), a higher signal was obtained for 100 μM DTT using CoPC modified CPEs (4.0 ± 0.2 nA, n=3) as compared to bare CPEs (2.5 ± 0.2 nA, n=3) (Figure 3.5B). Limit of detection (LOD, defined as the concentration that gives a signal 3x larger than the baseline noise) for DTT using CoPC modified CPE and unmodified CPE systems were 2.5 ± 0.2 μM (n=5) and 16.8 ± 1.3 μM (n=5), respectively.

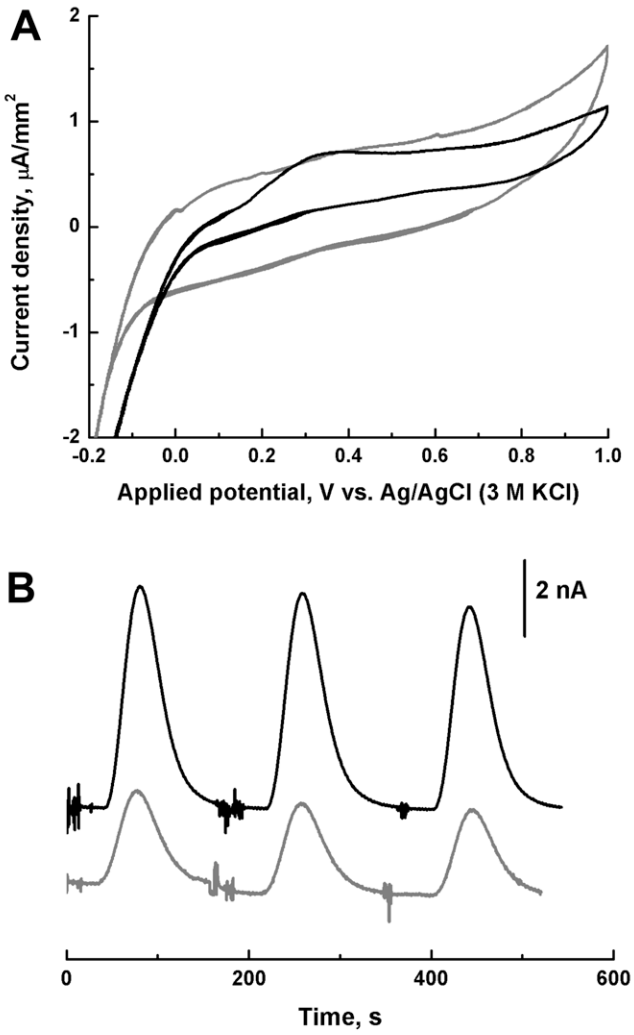

Figure 3.5. Comparison of working electrode performance for DTT detection between CoPC modified CPE (black line) and unmodified CPE (gray line). (A) Cyclic voltammograms of 1 mM DTT in 30 mM MES buffer, pH 7. (B) Flow injection analysis with amperometric detection of 100 μM DTT using 30 mM MES, pH 7, as a running buffer. Paste composition ratio is 5:3:2 (graphite:oil:PDMS). Off-chip reference and auxiliary electrodes were used. Applied potential: 0.2 V (vs. Ag/AgCl (3 M KCl)) for both types of working electrodes with Pt wire as an auxiliary electrode. Flow rate: 60 μL min^{-1}.

Amperometric sensing for glutathione in RBC lysate

To further evaluate the performance of CoPC modified CPEs, the detection of a second thiol compound, GSH, in a biological matrix, RBC lysate, was performed. One of the most important functions of glutathione in human body is its antioxidant property to protect cells from free radicals and reactive oxygen species while maintaining an appropriate intracellular redox status.[34] RBC lysate solution was prepared in 1X PBS for the GSH study. The solution containing GSH was injected to the microfluidic device via an off-chip injection valve and PBS as the running buffer. As shown in Figure 3.6A, duplicate injections of 0.5% RBC lysate with various amounts of added H_2O_2 are monitored amperometrically. H_2O_2 oxidizes GSH to glutathione resulting in a decrease of GSH in the sample, observed as a decrease in the GSH signal. Figure 6B shows the dose response curve for this experiment and demonstrates a good linear relationship between the amount of added H_2O_2 and the thiol signal in the RBC lysate ($y = -0.0023x + 0.6157$, $R^2 = 0.9874$). This microfluidic device with an on-chip three electrode system can be used over several injections of RBC lysate with no electrode fouling and a very reproducible signal (%RSD = 1.61%, n = 10) (Figure 3.7).

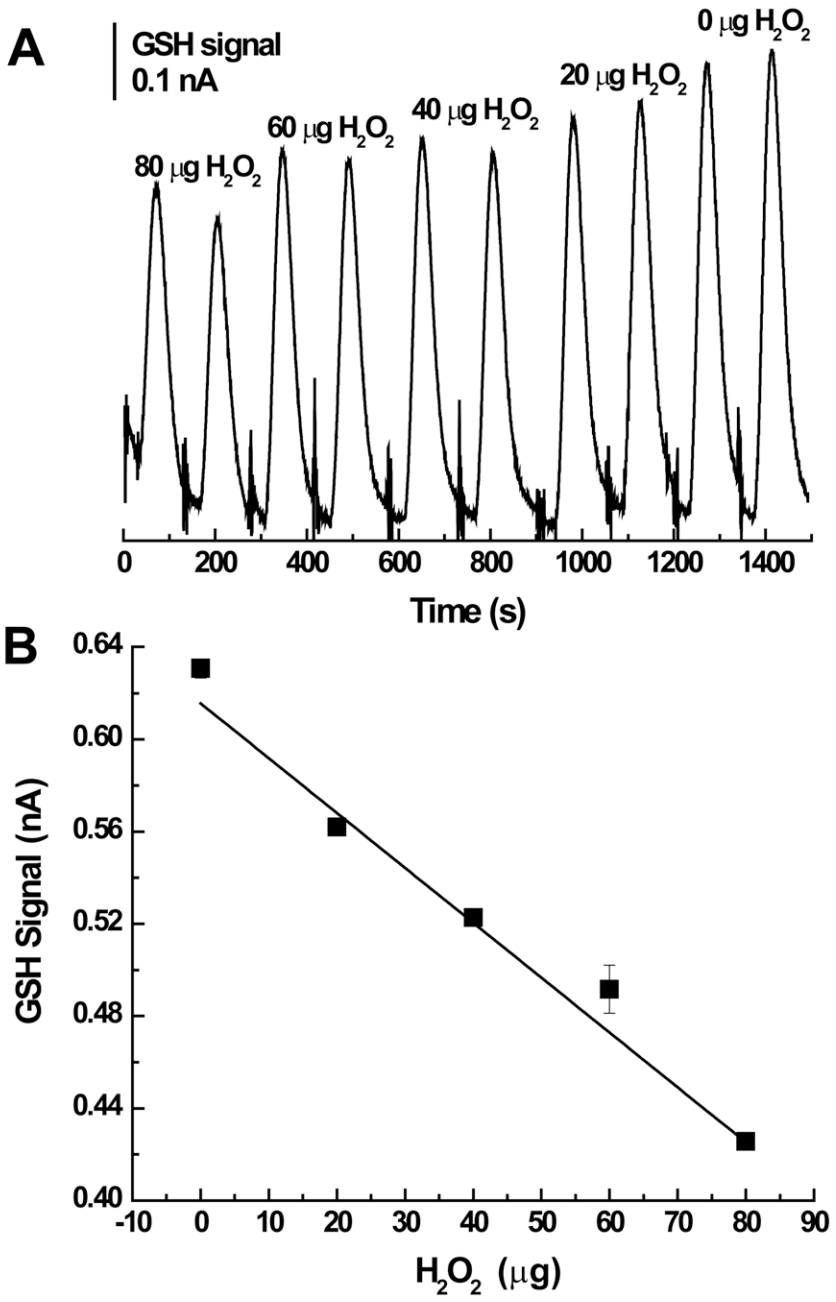

Figure 3.6. (A) Flow injection signal of GSH in 0.5% RBC lysate in PBS with different added amount of H_2O_2. (B) Dose response curve of GSH as a function of added H_2O_2. Experimental condition: Working electrode: 12% CoPC modified CPE, Applied potential: 0.8 V vs. CPE, Auxiliary electrode: CPE, Running buffer: Phosphate buffered saline (pH 7.4), flow rate: 60 μL min^{-1}.

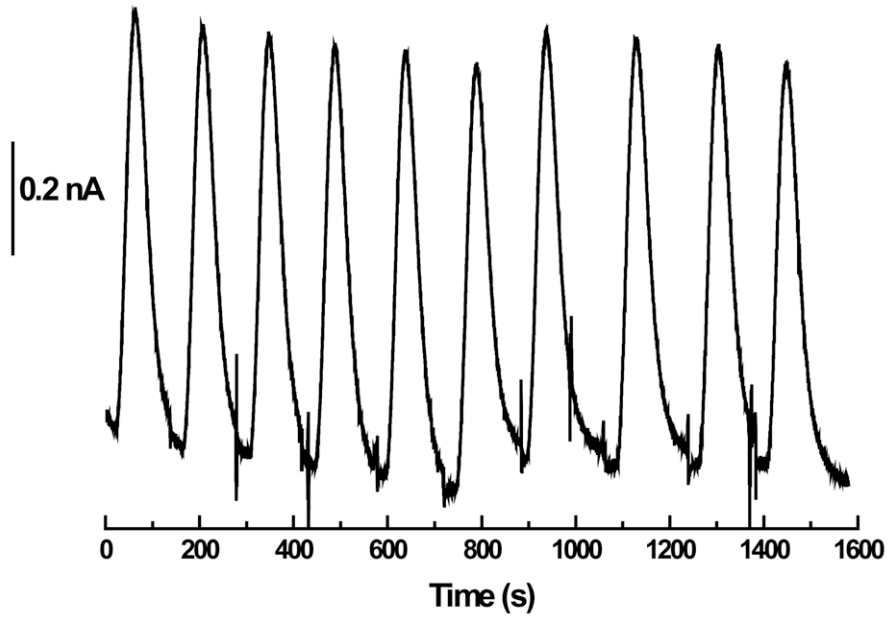

Figure 3.7. Showing the reproducibility test for analysis of GSH in 5% RBC lysate in PBS. All experimental conditions same as described in Figure 6.

Multi-walled carbon nanotube modified carbon paste electrodes for detection of dopamine

The ability to quantitatively detect catecholamines such as dopamine is important because of their known role in the progression of Parkinson's and Alzheimer's diseases.[43,44] To demonstrate the further utility of the electrode fabrication method, multi-walled carbon nanotube (MWCNT) modified electrodes were fabricated for the measurement of catecholamine release from cultured PC12 cells. MWCNTs act to improve mass transfer, and thus, sensitivity of the CPEs.[45-48] Figure 3.8 shows flow injection analysis data for the detection of 10 μM dopamine at both an unmodified and a MWCNT modified CPEs. The lowest detectable concentration of dopamine for the MWCNT modified CPEs was 50 nM with a signal to noise ratio (S/N) of 27 while the lowest concentration detectable for unmodified CPE was 500 nM (S/N = 4.6). Injections of dopamine below 50 nM did not result in measurable peaks, and the mechanism for

this rapid drop-off in signal was not investigated further here. This order of magnitude improvement in the lowest detectable dopamine concentration when adding the MWCNT is likely caused by an increase in surface area of the electrode and thus the peak currents obtained for the electrode. The collection efficiencies for 500 nM dopamine at the two electrode types are nearly equal at 0.54% for unmodified CPEs and 0.53% for MWCNT modified CPEs. The experimentally determined peak area for 500 nM dopamine was compared to the theoretical charge to determine the collection efficiency of the CPEs. The theoretical charge was determined using the relation of $N = Q/nF$, where N is the number of moles, F is Faraday's constant, n is the number of electrons transferred (for catecholamines such as dopamine, n=2), and Q is the charge of the peak in nC. Both of these collection efficiencies are quite low. This is likely due to the fact that the surface area of the electrode is very small (0.0625 mm^2) compared to the diffusional distances in the fluidic channel. By increasing the surface area of the electrode in the channel and decreasing the channel height, we would expect to see marked improvements in the collection efficiency of these electrodes.

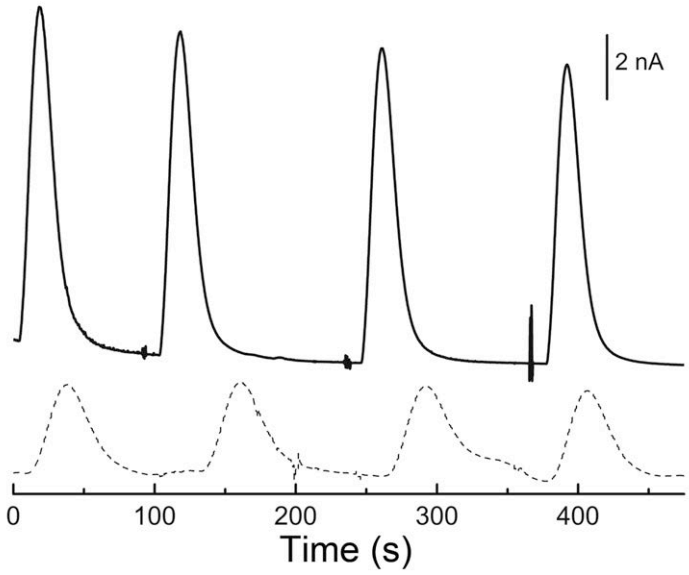

Figure 3.8. Flow injection analysis of dopamine. Comparison of unmodified CPE (dashed line) and CNT modified CPE (solid line). Sequential injections of 10 μM dopamine. Off-chip reference and auxiliary electrodes were used. Applied potential: 0.6 V (vs. Ag/AgCl (3 M KCl)) with Pt wire as an auxiliary electrode. Flow rate: 60 μL min^{-1}.

Amperometric sensing for release of catecholamines from PC12 cells

A plot of peak area versus time following cellular exposure to high concentrations of potassium is shown in Figure 3.9. In this study, 6 x 10^4 cells were used at each time point. The data shows that the majority of catecholamines appear to be released 3 min after cellular stimulation. The calculated concentration of catecholamines released at 3 min using the flow injection analysis system with MWCNT modified CPEs was estimated to be 3.6 μM (58.3 pM/cell). Previous publications indicate that PC12 cell vesicles contain an average catecholamine concentration of 110 μM and release just 0.06% of this concentration, or 67 μM, during exocytotic events.[49,50] Another report by Martin's group showed that 1.3 x 10^4 cells released a catecholamine concentration of 20-160 μM dopamine following calcium stimulation.[51]

The amount of catecholamines detected in our system is lower than numbers published previously, an effect that can be attributed to the very low collection efficiency of this non-optimized CPE design. Also of note is the sharp decrease in catecholamine signal following the high level of catecholamine secretion at 3 min. These results support the common theory that catecholamine re-uptake occurs in neuronal cells such as PC12 cells.

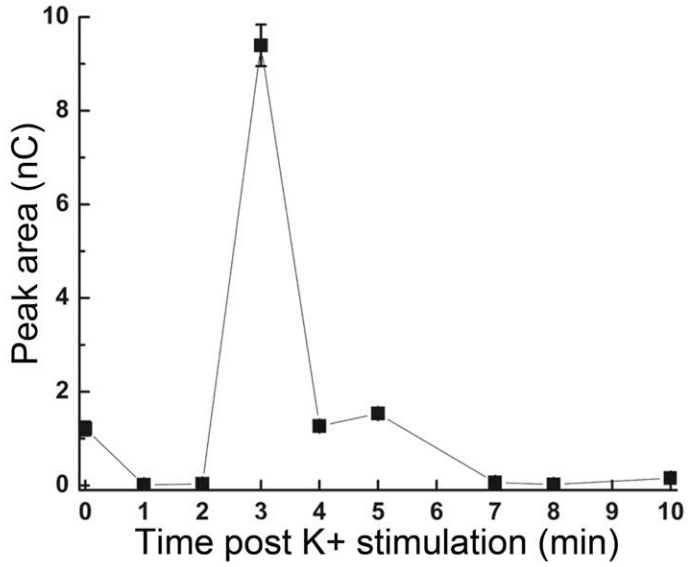

Figure 3.9. Effect of potassium on catecholamine release from PC12 cells. 6.15 x 10^4 cells were stimulated at each time point. Supernatant was removed and stored on ice until analysis. All experimental conditions same as in Figure 7.

CONCLUSION

We have demonstrated the use of a mixed PDMS-mineral oil binder to create a low cost, patternable, highly robust, carbon paste electrodes. Microfluidic electrochemical sensors were created using an on-chip fabrication method based largely on screen printing techniques. The robustness of the electrode was obtained from the cross-linking of PDMS components between the electrode and microfluidic substrate. A decrease in sensitivity (decrease in slope of current

density versus square root of the scan rate) was observed as the amount of PDMS was increased in the electrode binder material. A binder composition of equal amounts of PDMS and mineral oil showed nearly ideal behavior based on the Randles-Sevcik equation. Although an increase in capacitive current was observed when mineral oil was added to the binder, ΔE was lower and the anodic peak current was higher in the CPEs made with hybrid binder compositions when compared to the CPEs made with all PDMS binder indicating improved electrode performance. The same CPEs were modified with dopants to demonstrate the ease with which CPEs can be tailored for detection of specific analytes. In this case, these electrodes were designed for the detection of thiols and catecholamines by modification with CoPC or MWCNTs, respectively. These modified electrodes exhibited a higher response to these classes of analytes at low detection potentials compared to unmodified CPE. Furthermore, the mixed binder CPEs did not exhibit electrode fouling when performing analysis in complex biological matrices including RBC lysate (thiol detection) and PC12 cell supernatant (detection of catecholamine release). Our proposed method is readily adaptable, can be applied to various electrode materials and is amenable to chemical modification.

REFERENCES

(1) Sameenoi, Y.; Mensack, M. M.; Boonsong, K.; Ewing, R.; Dungchai, W.; Chailapakul, O.; Cropek, D. M.; Henry, C. S. *Analyst* **2011**, *136*, 3177.
(2) Sassa, F.; Morimoto, K.; Satoh, W.; Suzuki, H. *Electrophoresis* **2008**, *29*, 1787.
(3) Wang, J. *Talanta* **2002**, *56*, 223.
(4) Dumitrescu, I.; Unwin, P. R.; Macpherson, J. V. *Chem. Commun. (Camb)* **2009**, 6886.
(5) Shiddiky, M. J. A.; Won, M. S.; Shim, Y. B. *Electrophoresis* **2006**, *27*, 4545.
(6) Pumera, M.; Merkoci, A.; Alegret, S. *Electrophoresis* **2007**, *28*, 1274.
(7) Tang, D. Y.; Xia, B. Y. *Microchim. Acta* **2008**, *163*, 41.
(8) Chailapakul, O.; Wonsawat, W.; Siangproh, W.; Grudpan, K.; Zhao, Y. F.; Zhu, Z. W. *Food. Chem.* **2008**, *109*, 876.
(9) Blasco, A. J.; Barrigas, I.; Gonzalez, M. C.; Escarpa, A. *Electrophoresis* **2005**, *26*, 4664.
(10) Fischer, D. J.; Vandaveer, W. R.; Grigsby, R. J.; Lunte, S. M. *Electroanalysis* **2005**, *17*, 1153.
(11) Xu, L. J.; Du, J. J.; Deng, V.; He, N. Y. *Electrochem. Commun.* **2010**, *12*, 1329.
(12) Qi, H.; Li, X. X.; Chen, P.; Zhang, C. X. *Talanta* **2007**, *72*, 1030.
(13) Kovarik, M. L.; Torrence, N. J.; Spence, D. M.; Martin, R. S. *Analyst* **2004**, *129*, 400.
(14) Gonzalez, C. F.; Cropek, D. M.; Henry, C. S. *Electroanalysis* **2009**, *21*, 2171.
(15) Yao, X.; Xu, X. J.; Yang, P. Y.; Chen, G. *Electrophoresis* **2006**, *27*, 3233.
(16) Crevillen, A. G.; Pumera, M.; Gonzalez, M. C.; Escarpa, A. *Electrophoresis* **2008**, *29*, 2997.
(17) Chen, Z.; Zhang, L. Y.; Chen, G. *Electrophoresis* **2009**, *30*, 3419.
(18) Martin, R. S.; Gawron, A. J.; Fogarty, B. A.; Regan, F. B.; Dempsey, E.; Lunte, S. M. *Analyst* **2001**, *126*, 277.
(19) Siangproh, W.; Chailapakul, O.; Laocharoensuk, R.; Wang, J. *Talanta* **2005**, *67*, 903.
(20) Morrin, A.; Killard, A. J.; Smyth, M. R. *Anal. Lett.* **2003**, *36*, 2021.
(21) Wang, J.; Pedrero, M.; Sakslund, H.; Hammerich, O.; Pingarron, J. *Analyst* **1996**, *121*, 345.
(22) Svancara, I.; Vytras, K.; Kalcher, K.; Walcarius, A.; Wang, J. *Electroanalysis* **2009**, *21*, 7.
(23) Noh, H. B.; Lee, K. S.; Lim, B. S.; Kim, S. J.; Shim, Y. B. *Electrophoresis* **2010**, *31*, 3053.
(24) Martinez, N. A.; Messina, G. A.; Bertolino, F. A.; Salinas, E.; Raba, J. *Sensor Actuat. B-Chem.* **2008**, *133*, 256.
(25) Ledru, S.; Ruille, N.; Boujtita, M. *Biosens. Bioelectron.* **2006**, *21*, 1591.
(26) Pividori, M. I.; Alegret, S. *Anal. Lett.* **2005**, *38*, 2541.
(27) Brun, M.; Chateaux, J.-F.; Deman, A.-L.; Pittet, P.; Ferrigno, R. *Electroanalysis* **2011**, *23*, 321.
(28) Liu, Y.; Fanguy, J. C.; Bledsoe, J. M.; Henry, C. S. *Anal. Chem.* **2000**, *72*, 5939.
(29) Luz, R.; Maroneze, C.; Tanaka, A.; Kubota, L.; Gushikem, Y.; Damos, F. *Microchim. Acta* **2010**, *171*, 169.
(30) Raoof, J.-B.; Ojani, R.; Baghayeri, M. *Sensor Actuat. B-Chem.* **2009**, *143*, 261.
(31) Strobel, H. A., Heineman, W.R. *Chemical Instrumentation: A Systematic Approach, 3rd ed.*; Wiley-Interscience: New York, 1989.
(32) Bayle, C.; Causse, E.; Couderc, F. *Electrophoresis* **2004**, *25*, 1457.

(33) Pastore, A.; Federici, G.; Bertini, E.; Piemonte, F. *Clinica. Chimica. Acta* **2003**, *333*, 19.
(34) Griffith, O. W. *Free Radic. Biol. Med.* **1999**, *27*, 922.
(35) Kruusma, J.; Benham, A. M.; Williams, J. A. G.; Kataky, R. *Analyst* **2006**, *131*, 459.
(36) Toyo'oka, T. *J. Chromatogr. B* **2009**, *877*, 3318.
(37) White, P. C.; Lawrence, N. S.; Davis, J.; Compton, R. G. *Electroanalysis* **2002**, *14*, 89.
(38) Jackson, D. J.; Naber, J. F.; Roussel, T. J.; Crain, M. M.; Walsh, K. M.; Keynton, R. S.; Baldwin, R. P. *Anal. Chem.* **2003**, *75*, 3643.
(39) Korfhage, K. M.; Ravichandran, K.; Baldwin, R. P. *Anal. Chem.* **1984**, *56*, 1514.
(40) Halbert, M. K.; Baldwin, R. P. *Anal. Chem.* **1985**, *57*, 591.
(41) Pereira-Rodrigues, N.; Cofre, R.; Zagal, J. H.; Bedioui, F. *Bioelectrochemistry* **2007**, *70*, 147.
(42) Kuhnline, C. D.; Gangel, M. G.; Hulvey, M. K.; Martin, R. S. *Analyst* **2006**, *131*, 202.
(43) Du, M.; Flanigan, V.; Ma, Y. F. *Electrophoresis* **2004**, *25*, 1496.
(44) Westerink, R. H. *Neurotoxicology* **2004**, *25*, 461.
(45) Agui, L.; Yanez-Sedeno, P.; Pingarron, J. M. *Anal. Chim. Acta* **2008**, *622*, 11.
(46) Rivas, G. A.; Rubianes, M. D.; Rodriguez, M. C.; Ferreyra, N. F.; Luque, G. L.; Pedano, M. L.; Miscoria, S. A.; Parrado, C. *Talanta* **2007**, *74*, 291.
(47) Sinha, N.; Ma, J.; Yeow, J. T. *J Nanosci. Nanotechnol.* **2006**, *6*, 573.
(48) Balasubramanian, K.; Burghard, M. *Anal. Bioanal. Chem.* **2006**, *385*, 452.
(49) Chen, T. K.; Luo, G.; Ewing, A. G. *Anal. Chem.* **1994**, *66*, 3031.
(50) Kozminski, K. D.; Gutman, D. A.; Davila, V.; Sulzer, D.; Ewing, A. G. *Anal. Chem.* **1998**, *70*, 3123.
(51) Li, M. W.; Spence, D. M.; Martin, R. S. *Electroanalysis* **2005**, *17*, 1171.

CHAPTER 4. MICROFLUIDIC ELECTROCHEMICAL SENSOR FOR ON-LINE MONITORING OF AEROSOL OXIDATIVE ACTIVITY

CHAPTER OVERVIEW

This chapter discusses the development and testing of on-line monitoring system for aerosol oxidative activity employing microfluidic electrochemical sensor discussed in Chapter 3 coupled with a particle into liquid sampler (PILS). This was the first on-line system for aerosol oxidative activity measurement. The system creates the analysis with the measurement of 3 min temporal resolution which is fastest time information on the aerosol oxidative activity available. This work was published in the *Journal of the American Chemical Society*,[1] and most of the text and figures are taken from that article. Most of data in this chapter were collected and analyzed by me. Dr. Kirsten Koehler and Jeff Shapiro created aerosols in the chamber for the on-line system and collected aerosol concentration and size distribution data. Dr. Kirsten Koehler also helped correlate the data between aerosol concentration and DTT consumption rate. Dr. Yele Sun worked on PM extraction process which was used for method validation study.

SYNOPSIS

Particulate matter (PM) air pollution has a significant impact on human morbidity and mortality; however, the mechanisms of PM-induced toxicity are poorly defined. A leading hypothesis states that airborne PM induces harm by generating reactive oxygen species (ROS) in and around human tissues, leading to oxidative stress. We report here, a system employing a microfluidic electrochemical sensor coupled directly to a Particle-into-Liquid-Sampler (PILS) system to measure aerosol oxidative activity in an on-line format. The oxidative activity measurement is based on the dithiothreitol assay (DTT assay) where after oxidized by PM, the remaining reduced DTT was analyzed by the microfluidic sensor. The sensor consists of an array of working, reference, and auxiliary electrodes fabricated in a poly(dimethylsiloxane) (PDMS)-based microfluidic device. Cobalt (II) phthalocyanine (CoPC)-modified carbon paste was used as the working electrode material allowing selective detection of reduced DTT. The electrochemical sensor was validated off-line against the traditional DTT assay using filter samples taken from urban environments and biomass burning events. After off-line characterization, the sensor was coupled to a PILS to enable on-line sampling/analysis of aerosol oxidative activity. Urban dust and industrial incinerator ash samples were aerosolized in an aerosol chamber and analyzed for their oxidative activity. The on-line sensor reported DTT consumption rates (oxidative activity) in good correlation with aerosol concentration (R^2 from 0.86-0.97) with a time-resolution of approximately 3 minutes.

INTRODUCTION

Airborne particulate matter (PM) is a prime candidate for the generation of biological oxidative stress.[2,3] Epidemiological and clinical research has demonstrated strong links between atmospheric aerosols and adverse health effects, including premature deaths,[4] impaired pulmonary function,[5] neurodegenerative disorders,[6] and respiratory and cardiovascular diseases.[7] Chemical compounds in ambient PM, including aromatic compounds and transition metals such as Fe, V, Cr, Mn, Co, Ni, Cu, Zn, and Ti, may contribute to these effects through the generation of reactive oxygen species (ROS).[5,8,9] The exact mechanism by which PM causes oxidative stress is not completely understood; however, PM-associated ROS can cause damage to lipids, proteins, and DNA and these species have been implicated in pro-inflammatory effects in living tissues.[5,6,8-13] In normal biological systems, generation of ROS as a result of natural aerobic metabolism is balanced by endogenous antioxidants.[14] When ROS levels exceed cellular antioxidant capacity, the redox status of the cell and its surrounding environment changes, thereby triggering a cascade of events associated with inflammation and, at higher concentrations, significant cellular damage.[15,16]

Various approaches for measuring the oxidative activity of PM have been developed to study PM-induced oxidative stress.[17-20] Chemical assays offer the best potential for analysis of effective ROS dose in a format that can support epidemiological research[2,21] and many different types of chemical assays have been developed for assessing PM oxidative activity.[2,17-19,21-23] The oldest of these assays focused on measuring redox-specific chemicals such as transition metals and polyaromatic hydrocarbons (PAH).[23] Other methods have been proposed that make use of chromatography,[19,24] electron paramagnetic resonance (EPR),[25] and fluorescence.[26,27] The dithiothreitol (DTT)-based chemical activity assay is currently the most widely reported

technique used to assess the capacity of PM to catalyze ROS generation.[28,29] In this assay, reduced DTT is oxidized to its disulfide in the presence of ROS generated by PM. After the reaction, the remaining reduced DTT is reacted with Ellman's reagent (5,5′-dithiobis-(2-nitrobenzoic acid or DTNB) to produce a chromophore that absorbs light at 412 nm (Scheme 1). Thus, the rate of DTT consumption is proportional to the oxidative activity of the PM sample.[3] Using this assay, redox-active quinones have been shown to catalyze the transfer of electrons from DTT to oxygen, generating superoxide.[28,30] Furthermore, levels of PM oxidative activity measured by this assay have been correlated with increased levels of biological oxidative stress *in vitro*.[29] The traditional assay, however, requires the use of both quenching and developing agents, which results in sample dilution and a higher detection limit. Another major limitation of all current assays for PM oxidative activity is that they rely on classic filter-based collection of PM. These methods require long (up to 110 hrs) aerosol sampling durations to capture sufficient mass for detection.[31] The long sampling times not only reduce the temporal resolution of the measurement but also increase the potential for collected species to react and change composition prior to analysis.[20,22] These methods also require analysis using laboratory-based instrumentation that is not readily integrated into portable, field measurement systems.

To overcome problems with filter collection and off-line laboratory analysis, an on-line analysis system was developed by the Hopke group.[26,27,32] Their system uses the Particle Into Liquid Sampler (PILS)[33,34] for aerosol sampling and a dichlorofluorescein (DCHF) based assay to determine particle-bound ROS activity. The PILS offers the potential for direct, real-time measurement of aerosol-bound ROS and represents the first step towards on-line measurement of aerosol oxidative activity. However, stability of the DCHF reagent, due to photobleaching and photo-oxidation, proved problematic during analysis, resulting in larger than desired

variability.[35,36] In addition, an internal standard was not used to account for sample dilution by the PILS system.[26,32,36] Temporal resolution of this system was also limited (>20 min/sample) by the long sampling periods needed for sufficient mass capture and subsequent sample flushing/rinsing periods to ensure proper detector performance.[36]

Here we present a microfluidic electrochemical sensor for on-line monitoring of aerosol oxidative activity that is smaller, less expensive, and more portable than previously reported systems. Microfluidic devices can handle small sample volumes efficiently and thus, they are attractive for field-based measurements.[37,38] They can also be multiplexed to carry out multiple types of chemistry at the same time.[39-41] Electrochemical sensing is also well-suited for microfluidics because of the ease of integration and low cost.[42,43] By the choice of detection potential and/or electrode modification, electrochemistry also provides high sensitivity and high selectivity even when working with low analyte masses.[44-46] The sensor reported here is based on the existing DTT assay, with several simplifying modifications. A schematic of the procedure for both the traditional and new DTT assays is shown in Scheme 4.1. Following the reaction of DTT with PM, the remaining DTT is analyzed directly by the sensor, eliminating the need for quenching and developing reagents associated with UV-Vis detection. The electrochemical sensor is highly sensitive and capable of detecting small changes in the DTT electrochemical signal following reaction with a small amount of PM. Reducing the required sample mass also increases temporal resolution of the instrument, as less mass is needed for each individual measurement. Reducing the number and quantity of reagents also simplifies the system, making it more portable.

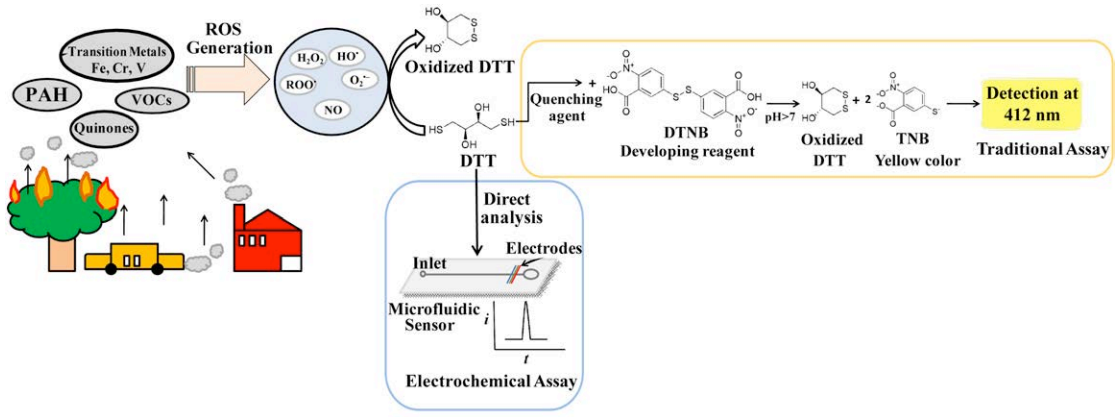

Scheme 4.1. The analysis of aerosol oxidative activity using the DTT assay with traditional (yellow box) and microfluidic electrochemical detection (blue box) methods.

To create an electrochemical sensing device for DTT detection, cobalt (II) phthalocyanine (CoPC)-modified carbon paste electrode (CPE) was used as an electrode material. CoPC-CPE has shown good selectivity for the catalytic oxidation of thiol compounds like DTT, is stable for long periods of time, and can be fabricated in a microfluidic device.[47,48] The electrode design and fabrication is based on our prior work and utilizes PDMS-containing binder to generate a CPE with high physical stability and good electron transfer properties. Electrode composition and system operating parameters were optimized using cyclic voltammetry. System performance was then characterized off-line using flow injection analysis and amperometric detection to establish the linear range, detection limit, and sensitivity of the electrode towards DTT. Then to characterize DTT assay, the working range and sensitivity of the assay chemistry were then determined using a model oxidant, 1,4-naphthoquinone (1,4-NQ). Reactions of DTT and 1,4-NQ were performed off-line and the remaining DTT was directly measured by the sensor. The sensor performance was found to depend on the starting concentration of DTT, with lower concentrations giving higher sensitivity but a lower working

range. As a final off-line validation step, 14 extracted filtered samples of ambient urban PM and biomass burning aerosols were analyzed. Results showed no significant difference in the oxidative activity measured by the sensor versus the traditional method. Finally, to demonstrate that the sensor can be applied for the measurement of aerosol oxidative activity in-situ, we connected the sensor to an on-line aerosol sampling system (Scheme 4.2). PM collected by the PILS reacted with DTT in sample transfer lines and the remaining reduced DTT was analyzed directly. Lithium fluoride was used as an internal standard to account for aerosol dilution by the PILS. A strong linear correlation between aerosol concentration and the measured oxidative activity (DTT consumption rate) was observed at concentrations similar to those found in polluted air (4 –120 μg m^{-3}). High temporal resolution was obtained; at least 3 aerosol samples were analyzed every 10 min. To the best of our knowledge, the system gives the fastest time information on the aerosol oxidative activity available, which can greatly contribute to the future understanding of how aerosols affect human health during short-term exposure events.

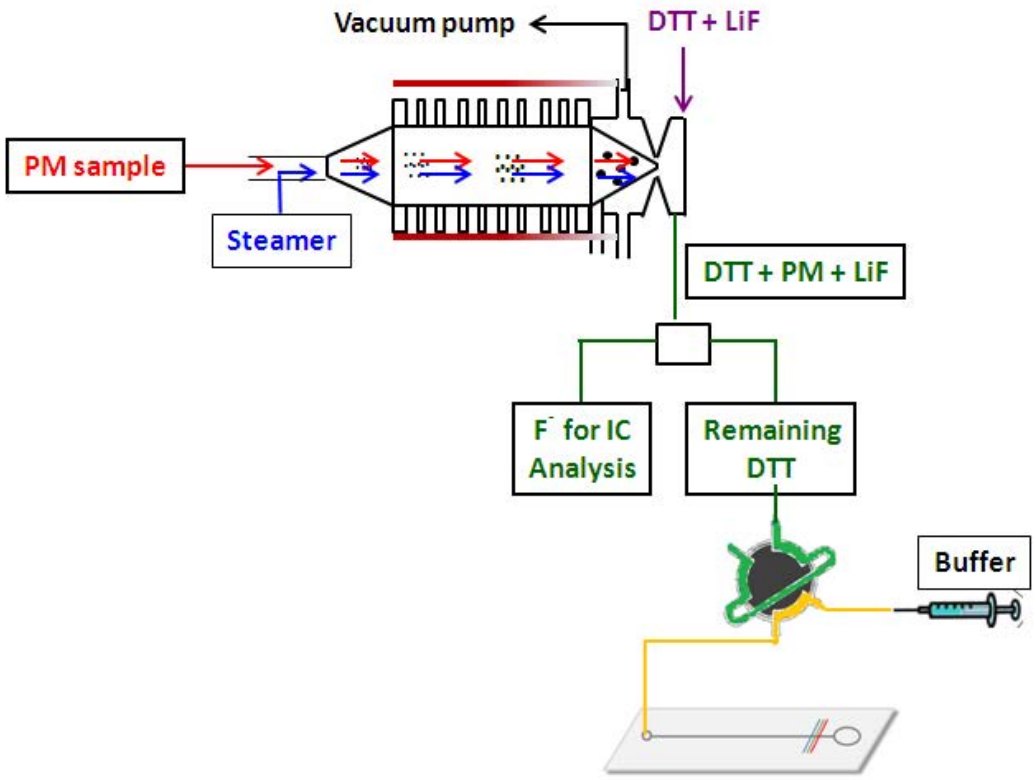

Scheme 4.2. An automated sampling-analysis system for aerosol oxidative activity. Aerosol was collected by the PILS and mixed with DTT reagent and Lithium Fluoride (internal standard LiF). Following reaction within the sample line, the remaining DTT was analyzed directly by a microfluidic electrochemical sensor.

MATERIALS AND METHODS

Chemicals and Materials

Unless otherwise stated, all chemicals were purchased from Sigma-Aldrich (St. Louis, MO, USA). Mineral oil was obtained from Fisher Scientific (Fair Lawn, NJ, USA). Poly(dimethyl siloxane) (PDMS) Sylgard 184 elastomer kit was purchased from Dow Corning (Midland, MI, USA). Silver paint was purchased from SPI supplies (West Chester, PA, USA). Copper wire was obtained from NTE Electronics (Bloomfield, NJ, USA). All electrochemical

measurements were conducted using a commercially available potentiostat (CHI660b, and CHI812, CH Instruments, Austin, TX, USA).

Microfluidic Electrochemical Sensor Fabrication and Operation

Construction of microfluidic devices with integrated electrochemical detection were performed as described previously.[45] A schematic diagram of the electrode fabrication process and the resulting microfluidic electrode design is shown in Figure 3.1 chapter 3.[45] On-chip three electrode systems were created to allow for a fully portable device in which a CoPC-modified carbon paste was used as the working electrode and unmodified carbon paste was used as pseudo-reference and auxiliary electrodes. For both off-line and on-line systems, an off-chip injection valve (6-port, fitted with a 10 μL injection loop) and syringe pump (PHD 4400, Harvard Apparatus, Holliston, MA, USA) were connected to the inlet of the microfluidic device with the pump flow rate set to 60 μL min^{-1}.

Off-line Measurement of Aerosol Oxidative Activity

Aerosol Sampling and Preparation

Eight $PM_{2.5}$ samples were collected on quartz filters over separate, integrated three-day sampling periods in Cleveland, OH during the Summer of 2007 and the Winter of 2008 using a Thermo Anderson Hi-Volume Air Sampler (Windsor, NJ, USA). The quartz filters were pre-baked in an oven at 550 °C for 12 h and wrapped in aluminum foil before use. After sampling, the filters were stored at -20 °C. Blank filter samples were prepared and handled in the same way, except that they were placed in the sampler for 2 min and no air was passed though them. Six biomass-burning $PM_{2.5}$ aerosol samples from the combustion of commonly-burned

vegetation from North American wildfires were also collected with a Hi-volume filter sampler at the USDA Forest Service's Fire Science Laboratory in Missoula, Montana as part of the third Fire Lab at Missoula Experiment study.[49] The selection of urban winter, urban summer, and fresh biomass burning aerosol samples was made to test system performance on a range of aerosol types.

Filtered aerosol samples were prepared as described previously.[50] Briefly, two 25 mm diameter punches from each filter sample were extracted in 5 mL of deionized water in a Nalgene Amber High Density Polyethylene (HDPE) bottle using sonication with heat (70 ± 5 °C) for 75 min. The aerosol extracts were syringe filtered (0.2 μm PTFE membrane, Millipore, Billerica, MA, USA) to remove insoluble materials. The filtered samples were kept in the dark at 4 °C until analysis.

DTT Assay Procedure

Sample preparation and DTT assay chemistry were conducted similarly to previous reports.[28,51] One milliliter of 0.1 M phosphate buffer (pH 7.3) was used as the reaction buffer. Fifty microliters of 0.5 mM DTT were added to the buffer followed by the addition of 15 μL of filtered aqueous aerosol extract (or 1,4-NQ external standard, 0-10 μg mL^{-1}). After mixing, the solution was incubated at 37 °C for 20 min. The remaining DTT in each reaction mixture was measured electrochemically and using the traditional absorbance method. For electrochemical detection, the solution was placed into an ice bath (2 ± 1 °C) until analysis to quench the reaction between DTT and oxidants. This step precluded the need for a quenching reagent (10% trichloroacetic acid) as called for in the traditional DTT assay.[28,30] To verify the approach, 1,4-NQ was mixed with DTT at 2°C, allowed to react, and then the amount of remaining DTT was

measured. Addition of 1,4-NQ to the DTT solution at 2°C resulted in no decrease in the amount of reduced DTT, confirming that the reaction is effectively halted at this temperature during the time course of these experiments (Figure 4.1). The electrochemical analysis was performed by injecting the temperature-quenched reaction mixture into a 10 μL injection loop within the FIA system and then quantifying the amount of reduced DTT remaining. Amperometric detection was set at detection potential of +0.2 V. For the traditional assay, 100 μL 100 mM of 5,5′-dithiobis-(2-nitrobenzoic acid) (DTNB) was added to the reaction mixture to consume the remaining reduced DTT, forming a yellow colored solution of 2-nitro-5-thiobenzoate (TNB). Levels of TNB were then quantified by absorption at 412 nm using a Gensys UV10 spectrometer.

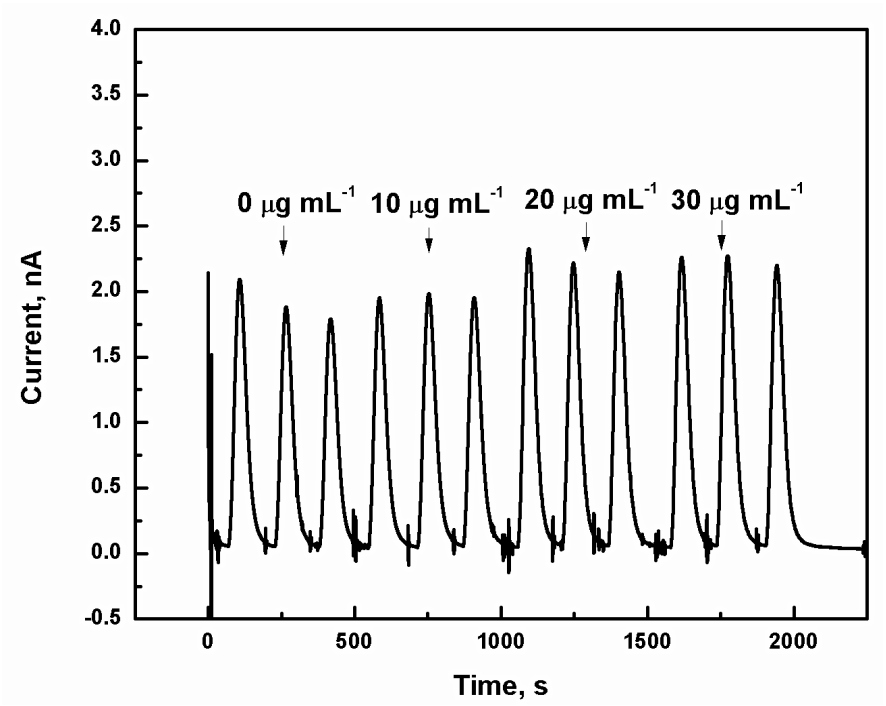

Figure 4.1. DTT signal obtained from the reaction of DTT (constant concentrations) and various amount of 1,4-NQ (0-30 μg mL^{-1}) in the DTT assay to study the effect of low temperature (2 °C) on the assay reaction.

In the off-line system, aerosol oxidative activity is reported in terms of oxidative equivalent relative to an external standard. Thus, readings from the two methods were expressed as a 1,4-NQ equivalent as follows[28]:

$$1,4-NQ\ Equivalent = \frac{1,4-NQ\ mass\ (ng_{NQ})}{PM\ mass\ (\mu g_{PM})} \qquad (1)$$

where 1,4-NQ mass (ng_{NQ}) is the amount of 1,4-NQ that yields the same DTT consumption as the aerosol sample and PM mass (μg_{PM}) is the amount of PM in the filter extract used to conduct the assay.

On-line Measurement of Aerosol Oxidative Activity

The on-line measurement set up consists of two major parts: the aerosol sampling system using the Particle Into Liquid Sampler (PILS) and the aerosol oxidative activity analysis system using the microfluidic electrochemical sensor. First, aerosol PM was pulled through a high temperature and humidity region at 12.5 L min^{-1}. The particle-laden, humidified airstream was subsequently cooled causing the particles to grow by water condensation in the supersaturated region to form supermicron droplets within the PILS. The droplets then impacted on a collection plate within the PILS forming a PM solution. A DTT solution containing a LiF internal standard (50 μM DTT, 1 mM LiF in 100 mM phosphate buffer pH 7.4) was added to the PILS above the impaction plate through an existing internal standard line. The mixture of the PM solution and DTT solution reacted immediately and was pulled by a peristaltic pump through a sampling line yielding a reaction time of 20 min. This reaction time is consistent with that we have investigated off-line. Solution temperature in the sample line dropped during the 20 min reaction time from

~37 ºC at the impaction plate to ~28 ºC at the injection loop. The sample line was connected via the injection loop to the FIA system described in off-line system. DTT consumption rate was used to express aerosol oxidative activity. The reacted solution was also collected at 500 s intervals through a second sample line and analyzed by Ion Chromatography (IC) off-line to determine the amount of water vapor collected by the PM in the PILS via the dilution of the LiF internal standard.

Two liquid pumps were used to control the liquid flows in this on-line system, an 8-channel peristaltic pump (Ismatec IPC 8 high precision multichannel pump, Glattbrugg, Switzerland) and a syringe pump (PHD 4400, Harvard Apparatus, Holliston, MA, USA). The peristaltic pump (30 rpm rotor speed) was used to feed water to the PILS humid region (1.40 mL min^{-1}) and DTT containing LiF to the impaction plate (120 μL min^{-1}). The reaction mixture containing DTT and PM was delivered by the pump (70 μL min^{-1}) to the sensor and was also collected for IC analysis. This pump was also used to deliver the liquid waste from the PILS (1.07 mL min^{-1}). The syringe pump was used to control the flow rate of phosphate buffer to the electrochemical sensor for remaining DTT analysis.

To demonstrate system performance on-line, the aerosol of interest was created in a 0.8 m^3 aerosol chamber. Urban Dust (Standard reference material 1649b Urban Dust, National Institute of Standards & Technology, Gaithersburg, MD) and Fly Ash (Industrial Incinerator Ash CRM012-100, Resource Technology Corporation, Laramie, WY) were suspended in ultrapure water at a concentration of 0.1% (w/v). The suspensions were sonicated to break up agglomerates and then aerosolized with a Collison Nebulizer. The aerosol concentration in the chamber was monitored with a Dust Trak aerosol photometer (TSI, Inc.) and a Sequential Mobility Particle Sizer (Grimm SMPS+C, Inc.). The size distribution of the aerosol was

approximately lognormal with a mean of 0.039 μm and 0.056 μm and geometric standard deviation of 1.46 and 1.41 for the Urban Dust and Fly Ash samples, respectively.

Blank aerosol oxidative activity for the negative control of on-line DTT assay was performed by directing PTFE filtered room air into to the PILS. The sensor measured DTT concentration, which was highest at this point because there was very little DTT consumption. The LiF concentration, measured off-line, was also typically the highest concentration at this point since there was negligible dilution by the PILS (low aerosol concentration). The other negative control for this system was performed by directing the PM to the PILS without DTT delivered. No signal for this control was observed.

Ion chromatography (881 Compact IC Pro coupled with 863 Compact Autosampler, Metrohm, Riverview, FL) was employed to determine the concentration of the LiF internal standard collected from the PILS system at a time resolution of 500 second for on-line aerosol oxidative activity analysis. Anion exchange column Metrosep A Supp 7-250/4.0 (Metrohm, Riverview, FL) was used to analyze F^-. Na_2CO_3 solution (3.6 mM) was used as an eluent and ultra pure water and 50 mM H_2SO_4 used as column suppressors. Collected samples were diluted 1500 times prior to the IC analysis with 1 mL injection loop.

RESULTS AND DISCUSSION

Electrode Composition and System Optimization

Carbon paste electrodes, a mixture of graphite and binders (mineral oils, non-conducting polymers, etc.), have shown potential as electrochemical sensors in microchip devices[52,53] because of their ease of fabrication and the ability to the modify the electrode with a range of chemically-selective dopants.[54] Various methods have been reported for carbon paste electrode

fabrication on microfluidic devices including the insertion of tube sleeves into the device and screen printing.[53,55] Of these methods, screen printing is particularly attractive because it can be performed directly on-chip with electrode dimensions controlled by screens or channels on the device itself. In this work, an electrode fabrication method analogous to screen-printing was used to produce on-chip electrodes using carbon paste with a custom designed binder (detail for electrode fabrication provided in CHAPTER 2 and our previously published work).[45] We found that these electrode systems provided robustness and well electrochemical properties. The electrochemical sensor can be re-used over a month by rising with de-ionized water daily. They were also characterized with catecholamines that have limited fouling potential. DTT requires the addition of a catalyst, however, to reduce the oxidation potential and reduce fouling.[55,56] Cobalt phthalocyanine (CoPC) is one of the more common electrocatalytic agents used and acts as a redox mediator that lowers the overpotential for thiols.[56-58] The two-step electrocatalytic mechanism starts with the electrochemical oxidation of Co(II)phthalocyanine to Co(III)phthalocyanine, followed by the chemical oxidation of DTT and regeneration of the Co(II)phthalocyanine.[56] Since both solution pH and CoPC composition impact DTT detection, the signal for 1 mM DTT as a function of %CoPC and solution pH was studied using cyclic voltammetry.[56,59-61] A two-variable experimental design was used for this optimization study.[62] Result shown in Figure 4.2 is a plot of detection current of DTT as a function of CoPC amount in carbon paste electrode and pH of running buffer. The condition that gives the highest peak current is demonstrated in the light green area (Figure 4.2A) where %CoPC is between 11-15 and pH of DTT solution is between 6-8. From this result, it can be hypothesized that, at lower concentration of CoPC, there is not enough electrocatalyst for DTT oxidation, leading to lower sensitivity. However, too much CoPC results in a lower amount of graphite for electron

transport to the circuit. At low pH, CoPC has poor electrocatalytic activity because of insufficient thiol dissociation.[63] In addition, at high pH, oxidized DTT can be easily formed due to air oxidation, resulting in a low amount of reduced DTT to give an electrochemical signal.[64] To get an optimal value, more detailed conditions were then studied by observing 1% intervals of CoPC in range of 11-15, and pH of DTT solution in the range of 6-8 (Figure 4.2B). Optimal values giving the highest signal of anodic current (scan range -0.1 to 1 V vs. unmodified CPE) were obtained at a CoPC concentration of 12% (w/w) and a solution pH of 7. Therefore, this composition of CoPC was used for CPE modification and a solution pH of 7 was used as the running buffer for all subsequent experiments.

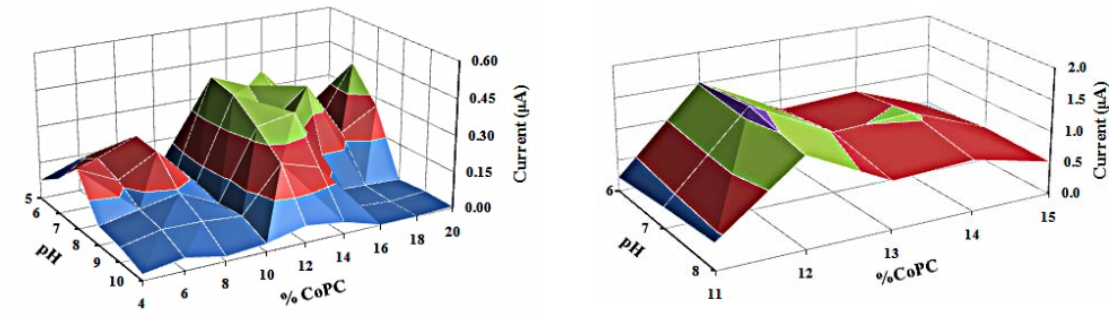

(A) **(B)**

Figure 4.2. Two-variable optimization for electrode composition and experimental system: CoPC amount in carbon paste electrode and pH of running buffer. (A) 4-20 % (w/w) CoPC with 2% interval study and pH of 5-10 (B) detailed study of 11-15 % (w/w) CoPC with 1% interval and pH of 6-8. Anodic current is obtained from cyclic voltammetry at each condition (scan rate: 0.1 V/s, scan range: -0.1 to 1 V (vs unmodified CPE)). Running solution: 1 mM DTT in 30 mM MES buffer at pH of interest.

As a first step to test the performance of the sensor, a flow injection analysis system was designed for off-line measurements of aerosol oxidative activity. The voltammetric behavior of the systems was established first (Figure 4.3A). The voltammogram shape is different from most

hydrodynamic voltammograms where the current plateaus at higher potentials because of mass transport. The unusual behavior shown here can be attributed to many factors such as additional oxidation and decomposition of the phthalocyanine ring at higher potentials and irreversible complexation of the Co(III) center.[61,65,66] While the highest signal-to-noise ratio (S/N) was observed at +0.5 V, we selected a potential of +0.2 V for selective DTT detection to avoid potential interference (i.e., oxidation signal) from other redox-active species typically present in ambient aerosols. These species include metals such as Fe, Cr, V, Ni and a broad spectrum of organic compounds such as PAHs (for example, pyrene, fluoranthene, chrysene), redox cycling agents (hydroquinones), olefins, aldehydes, ketones, nitro-compounds.[67,68] Although some chemicals can be oxidized at 0.2 V (according to standard reduction potentials), our electrochemical sensor is chemically modified as discussed above for selective detection of DTT.[69] For each measurement, we also injected an aerosol sample extract in the absence of DTT (i.e., as a negative control) to ensure the sample did not contribute to the electrochemical signal. Since aerosol composition is highly variable, fourteen different filter samples were employed to test for interferences. These samples included biomass burning aerosol, and urban aerosols collected during both summer and winter seasons. All samples showed negligible inferences at the DTT detection potential (data not shown). Example results (Figure 4.3B) show a high signal for DTT (20 μM) and no signal for the extracted aerosol sample.

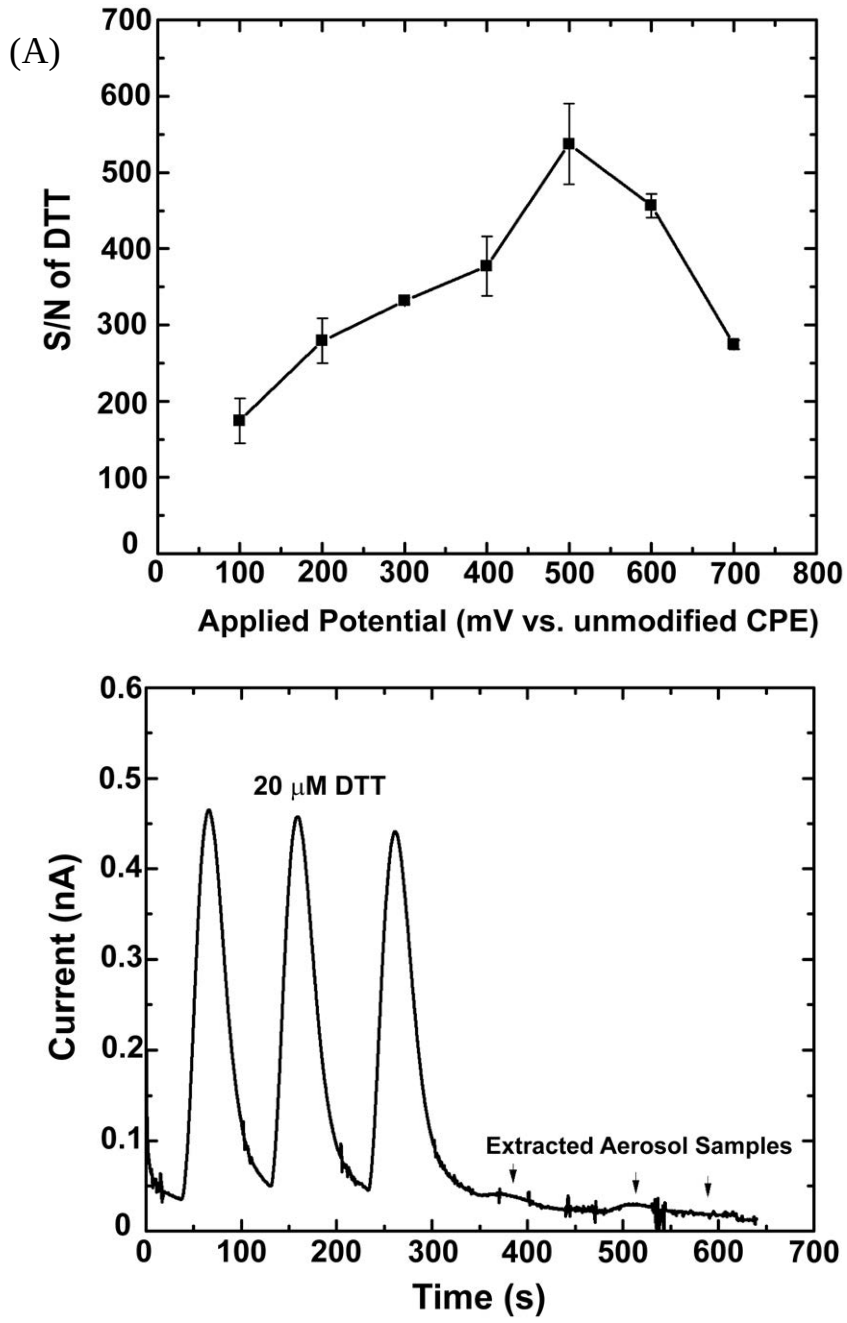

Figure 4.3. Selectivity of the microfluidic electrochemical sensor for DTT. (A) Hydrodynamic voltammogram plotted as signal-to-noise ratio as a function of applied potential from 100 μM DTT injection (n=3) (B) Flow profiles from injections of DTT and extracted aerosol samples.

Analytical Figures of Merit

After determining the optimal electrochemical conditions, the figures of merit for DTT were determined to ensure that the experimental conditions provide effective analysis for the remaining reduced DTT using flow injection analysis for DTT concentrations of 10-100 μM. A plot of average peak current (nA) (n=3) as a function of DTT concentration (μM) gave a linear calibration curve from 10 to 100 μM ($y = 0.037x - 0.43$, $R^2 = 0.997$) (Figure 4.4A). The relative standard deviation from ten consecutive injections of 500 μM DTT was 7.0 % and electrode fouling was not observed (Figure 4.4B). The limit of detection for DTT defined as the concentration that gives a signal 3x larger than the baseline noise was 2.49 ± 0.20 μM (n=5) (equivalent to 24.9 pmol for 10 μL injection), which is comparable to similar microfluidic electrochemical sensors.[61,70]

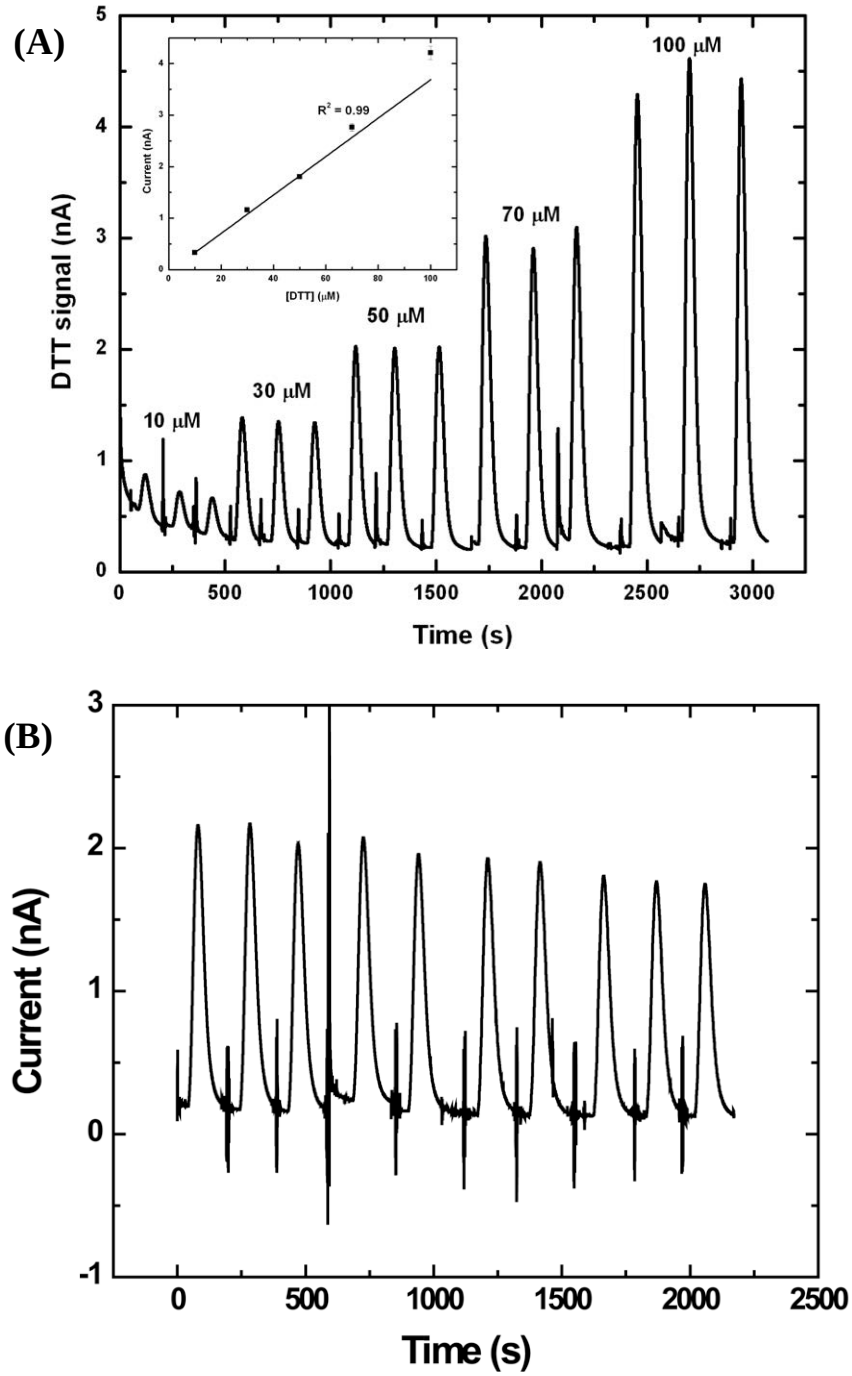

Figure 4.4. (A) Flow injection analysis profiles of DTT in the concentration range of 0-100 μM. (B) Ten consecutive injections of 50 μM DTT for reproducibility study

Sensor Performance Study

Following calibration, the sensor was used to measure PM oxidative activity. The effect of DTT starting concentration on the assay dose response curve using 1,4-NQ as a model oxidant was studied for sensitivity and working range. Results shown in Figure 4.5 demonstrate that at low starting DTT (25 nmol), the signal dropped quickly with increasing 1,4-NQ concentration, providing the highest sensitivity of all three conditions tested (sensitivity of -1.50, -0.75, -0.50 %DTT remaining/ng 1,4-NQ, for 25, 50 and 75 nmol, respectively). The decrease in signal at higher starting DTT levels (75 nmol) is more gradual but provides a larger assay working range. These results indicated that the assay sensitivity and working range can be tuned according to the levels of DTT present in solution. In all remaining off-line assays, 25 nmol (50 μL 0.5 mM) DTT was used to provide high sensitivity at the low oxidative activity of our PM samples.

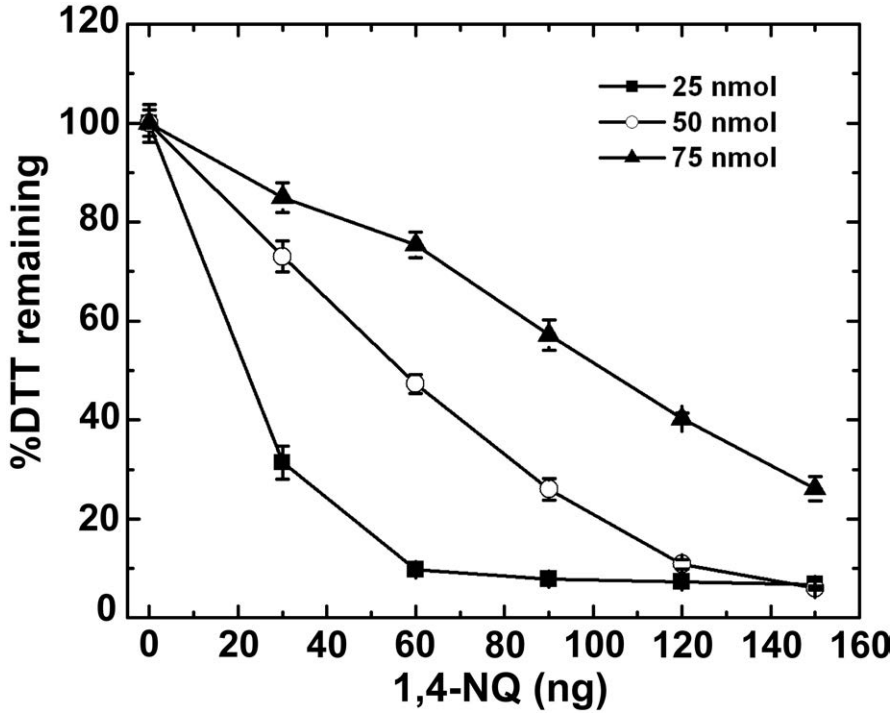

Figure 4.5. The impact of initial DTT amount on assay dose-response (n=3).

Finally, the new sensor was compared to the traditional DTT assay for aerosol oxidative activity using 14 representative aerosol filter samples (Supporting Information Table S-1). The 1,4-NQ equivalent values obtained by the two methods were compared using a paired t-test and plotted for correlation (Figure 4.6). There was no significant difference ($t_{observed}$ = 1.621, $t_{critical}$ = 2.179, p = 0.05) in the 1,4-NQ equivalent values obtained using the electrochemical DTT sensor and the traditional DTT assay. For the regression test, a good correlation with no significant difference for the 1,4-NQ equivalent values based on 95% confidence inderval determined by the two methods was observed where the intercept and slope are not significantly different from 0 and 1, respectively (y = 1.12 (±0.25) x - 0.10 (±0.57), R^2 = 0.98). The equivalence between the two methods demonstrates that the new electrochemical DTT assay is suitable for the measurement of oxidative activity from PM samples collected on filters. Moreover the electrochemical assay for filter samples requires 100 times less sample for detection when compared to the traditional assay (10 μL vs. 1000 μL).[28-30,51] This reduction allows for a commensurate reduction in field sampling duration, representing a significant advantage over the traditional DTT assay. The inclusion of several aerosol types (biomass burning smokes, urban winter aerosols, urban summer aerosols) indicates that this finding is not restricted to a small class of aerosol types.

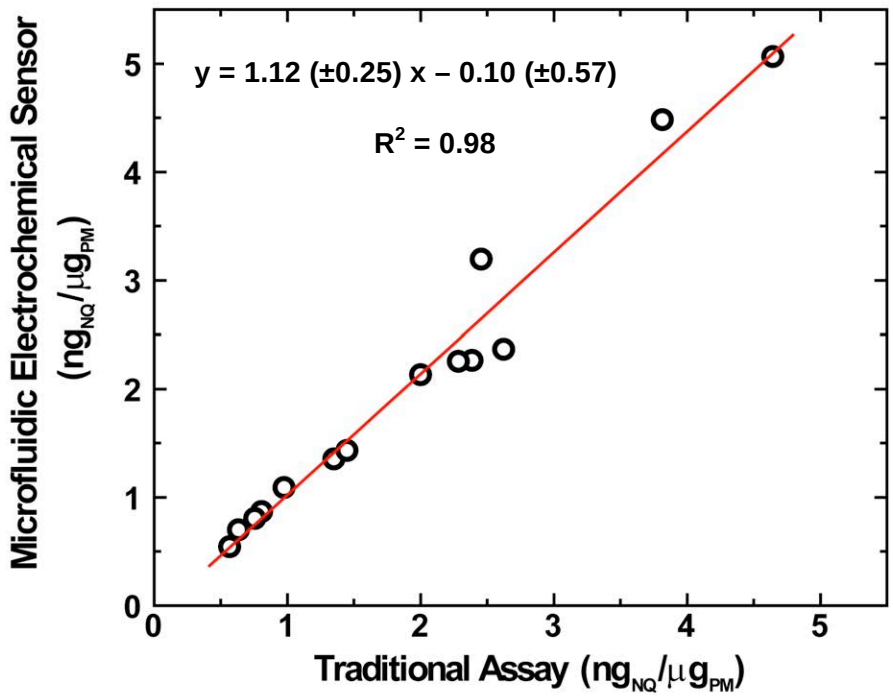

Figure 4.6. Comparison of PM oxidative activity (1,4-NQ equivalent unit, $ng_{NQ}/\mu g_{PM}$) between the traditional DTT assay and the microfluidic electrochemical sensor (off-line). Data represent aqueous extracts of 14 different aerosol samples.

On-Line Aerosol Oxidative Activity Measurement

After the electrochemical microfluidic sensor was validated for measurement of DTT consumption by PM from filters, the sensor was connected to a PILS to create an on-line aerosol oxidative activity analysis system (Scheme 4.2).

As a first step, the system was tested to show the ability to detect reduced DTT in the presence of non-oxidizing aerosols. Sodium chloride (NaCl) aerosol, which has no oxidative activity, was created in the chamber at various concentrations and the DTT signal measured. Results shown in Figure 4.7 demonstrated a decreasing DTT signal for increasing NaCl aerosol concentration (and thus increased water) delivered to the PILS impaction plate, which is indicative of sample dilution. The internal standard was used to account for this dilution effect and to correct the measurement of aerosol oxidative activity. A decrease in measured fluoride

concentration determined by ion chromatography (off-line), proportional to the salt aerosol concentration, is also shown in Figure 4.7 and demonstrates our ability to account for this phenomenon. Typical ion chromatogram for fluoride analysis is shown in Figure 4.8.

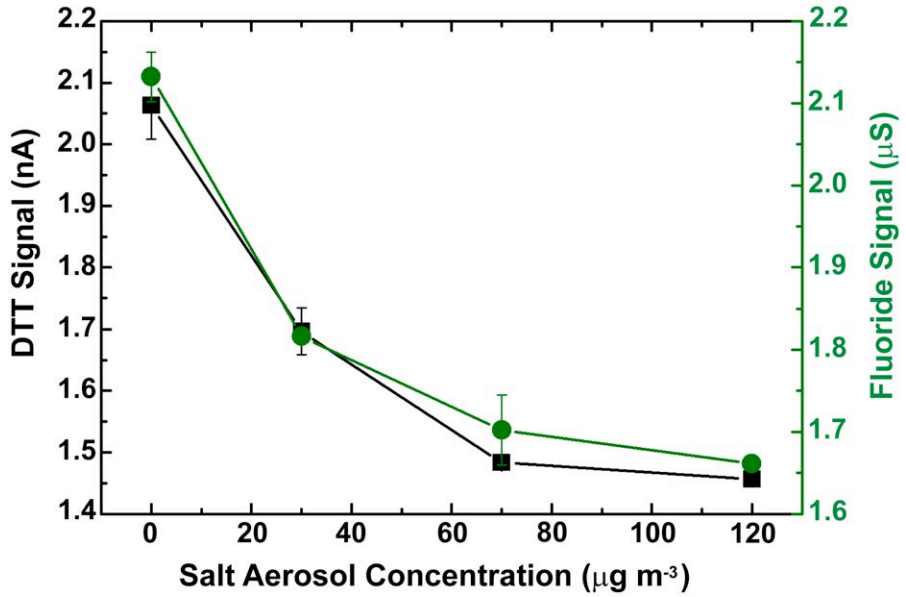

Figure 4.7. DTT (black) and fluoride (green) response curve as a function of salt aerosol concentration without oxidative activity. DTT levels were measured using the electrochemical sensor. F^- levels were measured using ion-chromatography.

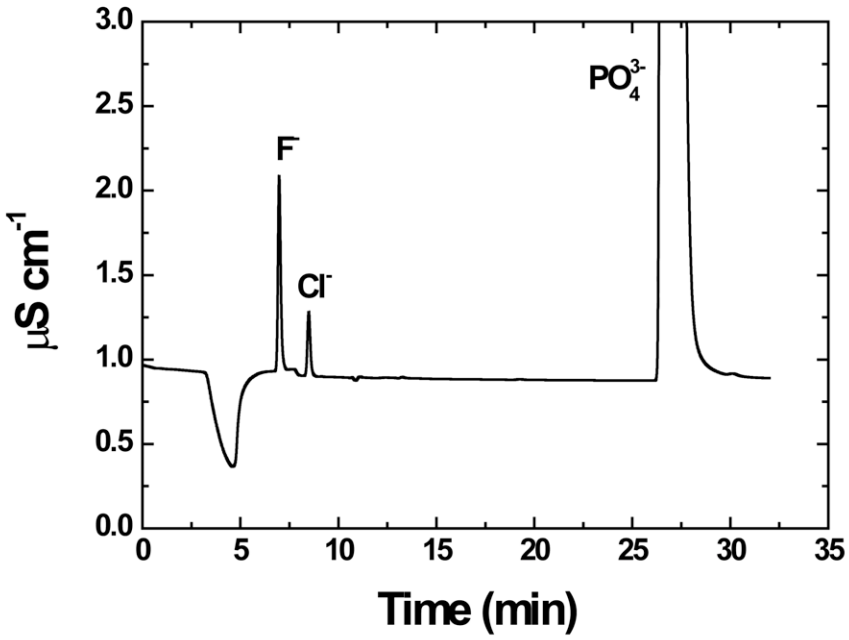

Figure 4.8. Typical ion chromatogram for fluoride analysis.

In the on-line system, various experimental conditions were different from our validated off-line assay, including temperature (~37 ºC to ~28 ºC) and the chemical mixing environment. The on-line DTT assay was therefore tested using 1,4-NQ as a model oxidant. For this test the PILS was allowed to sample only filtered, particle-free air. To simulate exposure to an oxidant under the conditions of the PILS, 1,4-NQ was injected through a T-valve at the entrance to the PILS which is above the impaction plate. Decreasing DTT signal for higher concentrations of 1,4-NQ demonstrated DTT consumption by a standard oxidant under on-line operation (Figure 4.9). The amount of 1,4-NQ used was equivalent to what was used in the off-line system, and the DTT consumption of the standard oxidant was of the same magnitude observed in the off-line system indicating that the viability of the on-line DTT assay.

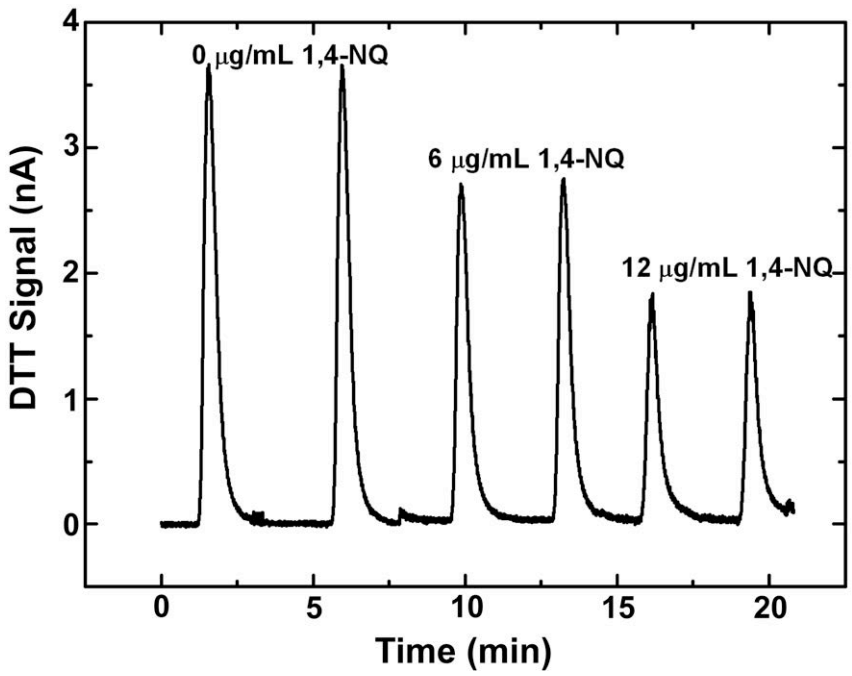

Figure 4.9. DTT signal response as standard oxidant (1,4-NQ) added to react on-line without aerosol delivered.

To demonstrate on-line performance more fully, standard reference samples of urban dust and fly ash (industrial incinerator ash) were aerosolized, sampled, and analyzed for their oxidative activity directly. These aerosols were selected because of their varying chemical composition and because they represent typical toxicants found in outdoor air. For each sample, aerosol concentrations generated in the chamber were in the range of those found in urban atmosphere (4-120 μg m^{-3}). Results shown in the top panel of Figure 4.10 show DTT consumption corresponding to urban dust aerosol concentrations. As aerosol concentration increased, DTT consumption rate increased. Furthermore, the system provided high temporal resolution, reporting an independent measurement approximately once every three minutes. To the best of our knowledge, this is the highest temporal resolution for an aerosol oxidative activity measurement system that has been reported.[26,27,32] Higher temporal resolution could ultimately be obtained by reducing the volume of the injection loop and increasing buffer flow rate through

the system. In terms of aerosol mass, the on-line system required between 7 and 214 ng of particle mass per injection to observe quantifiable DTT consumption. This range was calculated using the PILS air sampling rate (12.5 L min^{-1}), aerosol concentrations measured in the chamber (4-120 μgm^{-3}) and a 10 μL injection loop. This mass range is approximately three orders of magnitude lower than amount required for the traditional DTT assay (5-40 μg).[28-30,51] A correlation plot between DTT consumption rate and aerosol concentration was constructed and a strong linear correlation coefficient was obtained (R^2 = 0.97) (Figure 4.10, bottom panel). Performance of the system was further confirmed with a fly ash test aerosol. In this example, the fly ash aerosol concentration was varied faster and DTT consumption rate was analyzed (Figure 4.11, top panel) continuously. The on-line system was able to measure DTT consumption rates that were strongly correlated with aerosol concentration (R^2 = 0.86, Figure 4.11, bottom panel) even during periods of rapid concentration change. The oxidative activity of the urban dust and fly ash samples were comparable. The oxidative activity of the fly ash aerosol is believed to result from the transition metal content of the sample.[71,72] ROS generated from urban dust aerosol might be attributed to PAHs and nitro-PAHs which are major components of such sample.[73]

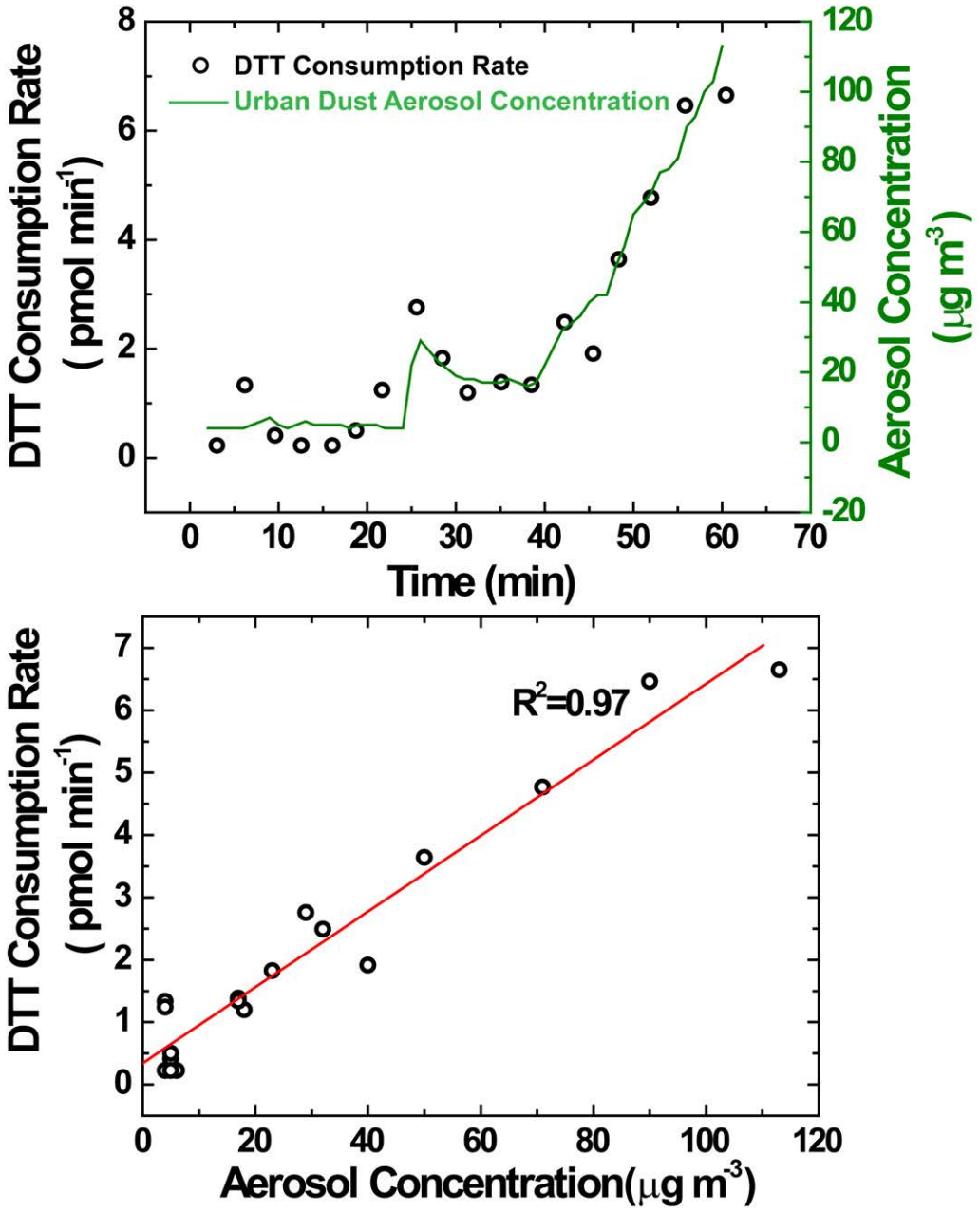

Figure 4.10. Correlation of DTT consumption rate with aerosol concentration for standard reference material urban dust. The top panels show DTT consumption rate (black y axis) and aerosol concentration (green y axis) as a function of experiment time. The bottom panels plot DTT consumption rate as a function of aerosol concentration and show the resultant correlation coefficient.

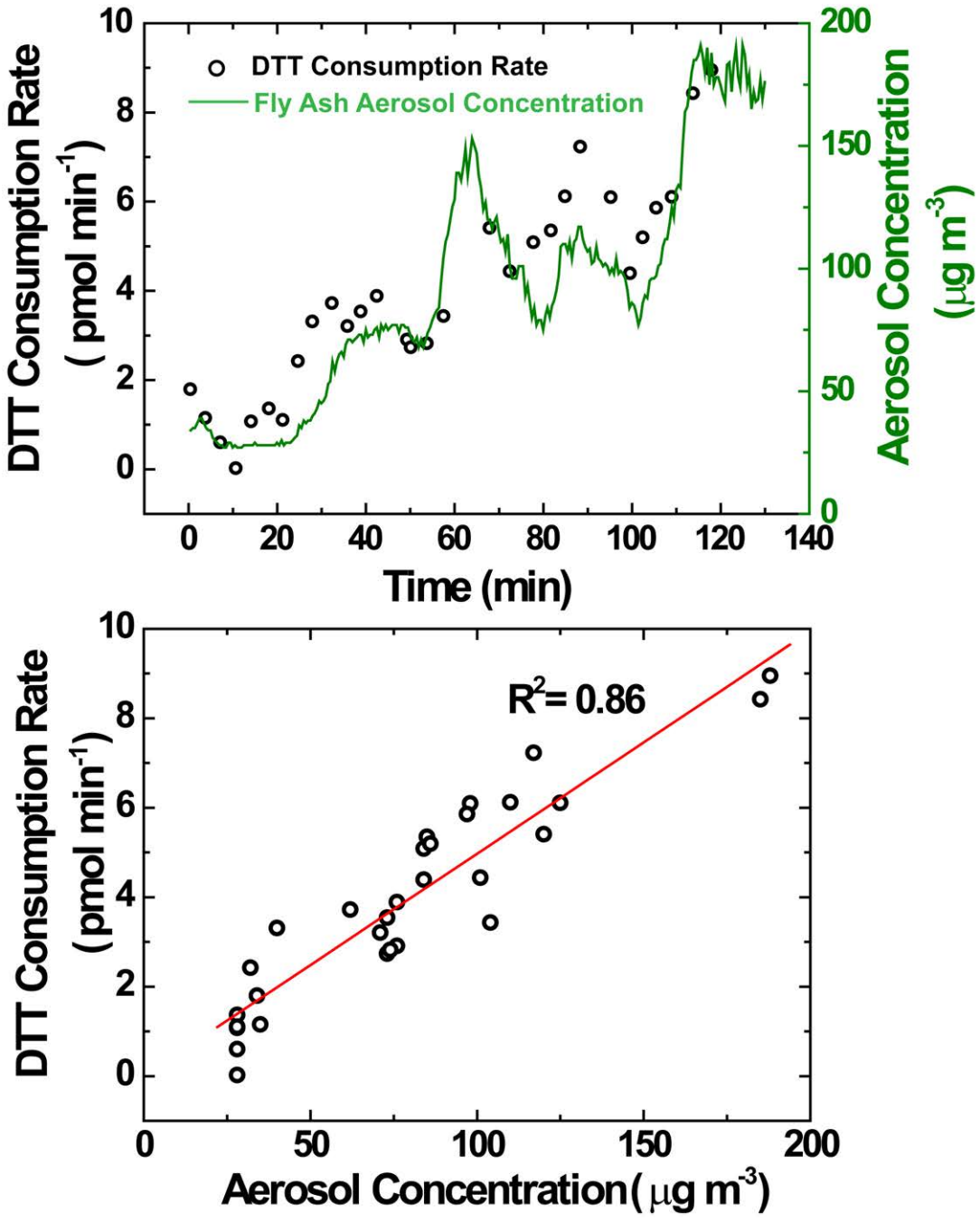

Figure 4.11. Correlation of DTT consumption rate with aerosol concentration for standard reference fly ash. The top panels show DTT consumption rate (black y axis) and aerosol concentration (green y axis) as a function of experiment time. The bottom panels plot DTT consumption rate as a function of aerosol concentration and show the resultant correlation coefficient.

CONCLUSIONS

We present here for the first time a high temporal resolution on-line sampling/analysis system for aerosol oxidative activity using a microfluidic electrochemical sensor coupled with an on-line aerosol collection system. The determination of aerosol oxidative activity was based on the widely-reported DTT assay but used electrochemical detection instead of photometric detection. The sensor was validated off-line for its performance in aerosol oxidative activity measurement. No significant differences for the aerosol oxidative activity expressed as the 1,4-NQ equivalent was observed between the traditional assay and the sensor for 14 extracted ambient aerosol and biomass burning smoke filter samples. Using on-line monitoring of aerosol oxidative activity, high correlations between aerosol concentration and DTT consumption rate were observed for two representative test aerosols. The on-line system developed here shows promise as an eventual tool for field studies of aerosol oxidative activity. Such studies may lead to a better understanding of how PM can affect human and environmental health.

REFERENCES

(1) Sameenoi, Y.; Koehler, K.; Shapiro, J.; Boonsong, K.; Sun, Y.; Collett, J.; Volckens, J.; Henry, C. S. *J. Am. Chem. Soc.* **2012**, *134*, 10562.

(2) Ichoku, C.; Andreae, M. O.; Andreae, T. W.; Meixner, F. X.; Schebeske, G.; Formenti, P.; Maenhaut, W.; Cafmeyer, J.; Ptasinski, J.; Karnieli, A.; Orlovsky, L. *J. Geophys. Res-Atmos.* **1999**, *104*, 24371.

(3) Ghelfi, E.; Rhoden, R.; Wellenius, G. A.; Lawrence, J.; Gonzalez-Flecha, B. *Toxicol. Sci.* **2008**, *102*, 328.

(4) Hoek, G.; Meliefste, K.; Cyrys, J.; Lewne, M.; Bellander, T.; Brauer, M.; Fischer, P.; Gehring, U.; Heinrich, J.; van Vliet, P.; Brunekreef, B. *Atmos. Environ.* **2002**, *36*, 4077.

(5) de Kok, T. M.; Hogervorst, J. G.; Briede, J. J.; van Herwijnen, M. H.; Maas, L. M.; Moonen, E. J.; Driece, H. A.; Kleinjans, J. C. *Environ.Mol. Mutagen.* **2005**, *46*, 71.

(6) Verma, V.; Pakbin, P.; Cheung, K. L.; Cho, A. K.; Schauer, J. J.; Shafer, M. M.; Kleinman, M. T.; Sioutas, C. *Atmos. Environ.* **2011**, *45*, 1025.

(7) Gauderman, W. J.; Vora, H.; McConnell, R.; Berhane, K.; Gilliland, F.; Thomas, D.; Lurmann, F.; Avol, E.; Kunzli, N.; Jerrett, M.; Peters, J. *Lancet* **2007**, *369*, 571.

(8) Prahalad, A. K.; Soukup, J. M.; Inmon, J.; Willis, R.; Ghio, A. J.; Becker, S.; Gallagher, J. E. *Toxicol. Appl. Pharmacol.* **1999**, *158*, 81.

(9) Clarke, R. W.; Catalano, P.; Coull, B.; Koutrakis, P.; Murthy, G. G. K.; Rice, T.; Godleski, J. J. *Inhal. Toxicol.* **2000**, *12*, 73.

(10) Ghelfi, E.; Rhoden, C. R.; Wellenius, G. A.; Lawrence, J.; Gonzalez-Flecha, B. *Toxicol. Sci.* **2008**, *102*, 328.

(11) Cho, A. K.; Sioutas, C.; Miguel, A. H.; Kumagai, Y.; Schmitz, D. A.; Singh, M.; Eiguren-Fernandez, A.; Froines, J. R. *Environ. Res.* **2005**, *99*, 40.

(12) Beck-Speier, I.; Dayal, N.; Karg, E.; Maier, K. L.; Schumann, G.; Schulz, H.; Semmler, M.; Takenaka, S.; Stettmaier, K.; Bors, W.; Ghio, A.; Samet, J. M.; Heyder, J. *Free Radic. Biol. Med.* **2005**, *38*, 1080.

(13) Kreyling, W. G.; Semmler, M.; Moller, W. *J. Aerosol Med.* **2004**, *17*, 140.

(14) Hatzis, C.; Godleski, J. J.; Gonzalez-Flecha, B.; Wolfson, J. M.; Koutrakis, P. *Environ. Sci. Technol.* **2006**, *40*, 2805.

(15) Xiao, G. G.; Wang, M. Y.; Li, N.; Loo, J. A.; Nel, A. E. *J. Biol. Chem.* **2003**, *278*, 50781.

(16) Li, N.; Kim, S.; Wang, M.; Froines, J.; Sioutas, C.; Nel, A. *Inhal. Toxicol.* **2002**, *14*, 459.

(17) Kunzli, N.; Mudway, I. S.; Gotschi, T.; Shi, T. M.; Kelly, F. J.; Cook, S.; Burney, P.; Forsberg, B.; Gauderman, J. W.; Hazenkamp, M. E.; Heinrich, J.; Jarvis, D.; Norback, D.; Payo-Losa, F.; Poli, A.; Sunyer, J.; Borm, P. J. A. *Environ. Health Perspect.* **2006**, *114*, 684.

(18) Kovarik, M. L.; Li, M. W.; Martin, R. S. *Electrophoresis* **2005**, *26*, 202.

(19) Jung, H.; Guo, B.; Anastasio, C.; Kennedy, I. M. *Atmos. Environ.* **2006**, *40*, 1043.

(20) Foucaud, L.; Wilson, M. R.; Brown, D. M.; Stone, V. *Toxicol. Lett.* **2007**, *174*, 1.

(21) Bernardoni, V.; Cuccia, E.; Calzolai, G.; Chiari, M.; Lucarelli, F.; Massabo, D.; Nava, S.; Prati, P.; Valli, G.; Vecchi, R. *X-Ray Spectrom.* **2011**, *40*, 79.

(22) Hu, S.; Polidori, A.; Arhami, M.; Shafer, M. M.; Schauer, J. J.; Cho, A.; Sioutas, C. *Atmos. Chem. Phys.* **2008**, *8*, 6439.

(23) Poschl, U. *Angew. Chem. Int. Edit* **2005**, *44*, 7520.

(24) Vidrio, E.; Phuah, C. H.; Dillner, A. M.; Anastasio, C. *Environ. Sci. Technol.* **2009**, *43*, 922.

(25) Ivanova, N. A.; Onischuk, A. A.; Vosel, S. V.; Purtov, P. A.; Kulik, L. V.; Rapatskiy, L. L.; Vasenin, N. T.; Anufrienko, V. F. *Appl. Magn. Reson.* **2009**, *35*, 625.
(26) Venkatachari, P.; Hopke, P. K. *Aerosol Sci. Technol.* **2008**, *42*, 629.
(27) Venkatachari, P.; Hopke, P. K.; Grover, B. D.; Eatough, D. J. *J. Atmos. Chem.* **2005**, *50*, 49.
(28) Li, Q. F.; Wyatt, A.; Kamens, R. M. *Atmos. Environ.* **2009**, *43*, 1037.
(29) Li, N.; Sioutas, C.; Cho, A.; Schmitz, D.; Misra, C.; Sempf, J.; Wang, M. Y.; Oberley, T.; Froines, J.; Nel, A. *Environ. Health Perspect.* **2003**, *111*, 455.
(30) Kumagai, Y.; Koide, S.; Taguchi, K.; Endo, A.; Nakai, Y.; Yoshikawa, T.; Shimojo, N. *Chem. Res. Toxicol.* **2002**, *15*, 483.
(31) Kam, W.; Ning, Z.; Shafer, M. M.; Schauer, J. J.; Sioutas, C. *Environ. Sci. Technol.* **2011**, *45*, 6769.
(32) Venkatachari, P.; Hopke, P. K. *J. Aerosol Sci.* **2008**, *39*, 168.
(33) Weber, R. J.; Orsini, D.; Daun, Y.; Lee, Y. N.; Klotz, P. J.; Brechtel, F. *Aerosol Sci. Technol.* **2001**, *35*, 718.
(34) Orsini, D. A.; Ma, Y. L.; Sullivan, A.; Sierau, B.; Baumann, K.; Weber, R. J. *Atmos. Environ.* **2003**, *37*, 1243.
(35) Beer, D.; Weber, J. *Opt. Commun.* **1972**, *5*, 307.
(36) Wang, Y.; Hopke, P. K.; Sun, L.; Chalupa, D. C.; Utell, M. J. *J. Toxicol.* **2011**, *2011*.
(37) Garcia, C. D.; Henry, C. S. *Anal. Chim. Acta* **2004**, *508*, 1.
(38) Noblitt, S. D.; Lewis, G. S.; Liu, Y.; Hering, S. V.; Collett, J. L.; Henry, C. S. *Anal. Chem.* **2009**, *81*, 10029.
(39) Hu, M.; Yan, J.; He, Y.; Lu, H.; Weng, L.; Song, S.; Fan, C.; Wang, L. *ACS Nano* **2010**, *4*, 488.
(40) Lee, J. H.; Song, Y. A.; Han, J. Y. *Lab Chip* **2008**, *8*, 596.
(41) Dishinger, J. F.; Kennedy, R. T. *Electrophoresis* **2008**, *29*, 3296.
(42) Xu, X. L.; Zhang, S.; Chen, H.; Kong, J. L. *Talanta* **2009**, *80*, 8.
(43) Sassa, F.; Morimoto, K.; Satoh, W.; Suzuki, H. *Electrophoresis* **2008**, *29*, 1787.
(44) Holcomb, R. E.; Kraly, J. R.; Henry, C. S. *Analyst* **2009**, *134*, 486.
(45) Sameenoi, Y.; Mensack, M. M.; Boonsong, K.; Ewing, R.; Dungchai, W.; Chailapakul, O.; Cropek, D. M.; Henry, C. S. *Analyst* **2011**, *136*, 3177.
(46) Jokerst, J. C.; Emory, J. M.; Henry, C. S. *Analyst* **2012**, *137*, 24.
(47) Huang, X. J.; Kok, W. T. *Anal. Chim. Acta* **1993**, *273*, 245.
(48) Shahrokhian, S.; Hamzehloei, A.; Thaghani, A.; Mousavi, S. R. *Electroanal.* **2004**, *16*, 915.
(49) Hennigan, C. J.; Miracolo, M. A.; Engelhart, G. J.; May, A. A.; Presto, A. A.; Lee, T.; Sullivan, A. P.; McMeeking, G. R.; Coe, H.; Wold, C. E.; Hao, W. M.; Gilman, J. B.; Kuster, W. C.; de Gouw, J.; Schichtel, B. A.; Collett Jr, J. L.; Kreidenweis, S. M.; Robinson, A. L. *Atmos. Chem. Phys. Discuss.* **2011**, *11*, 11995.
(50) Baumann, K.; Ift, F.; Zhao, J. Z.; Chameides, W. L. *J. Geophys. Res.-Atmos.* **2003**, *108*.
(51) Cho, A. K.; Sioutas, C.; Miguel, A. H.; Kumagai, Y.; Schmitz, D. A.; Singh, M.; Eiguren-Fernandez, A.; Froines, J. R. *Environ. Res.* **2005**, *99*, 40.
(52) Martin, R. S.; Gawron, A. J.; Fogarty, B. A.; Regan, F. B.; Dempsey, E.; Lunte, S. M. *Analyst* **2001**, *126*, 277.
(53) Siangproh, W.; Chailapakul, O.; Laocharoensuk, R.; Wang, J. *Talanta* **2005**, *67*, 903.
(54) Svancara, I.; Vytras, K.; Kalcher, K.; Walcarius, A.; Wang, J. *Electroanal.* **2009**, *21*, 7.

(55) Noh, H. B.; Lee, K. S.; Lim, B. S.; Kim, S. J.; Shim, Y. B. *Electrophoresis* **2010**, *31*, 3053.
(56) Halbert, M. K.; Baldwin, R. P. *Anal. Chem.* **1985**, *57*, 591.
(57) Korfhage, K. M.; Ravichandran, K.; Baldwin, R. P. *Anal. Chem.* **1984**, *56*, 1514.
(58) Pereira-Rodrigues, N.; Cofre, R.; Zagal, J. H.; Bedioui, F. *Bioelectrochemistry* **2007**, *70*, 147.
(59) Halbert, M. K.; Baldwin, R. P. *J. Chromatogr.* **1985**, *345*, 43.
(60) Oshea, T. J.; Lunte, S. M. *Anal. Chem.* **1994**, *66*, 307.
(61) Kuhnline, C. D.; Gangel, M. G.; Hulvey, M. K.; Martin, R. S. *Analyst* **2006**, *131*, 202.
(62) Leardi, R. *Anal. Chim. Acta* **2009**, *652*, 161.
(63) Sehlotho, N.; Griveau, S.; Ruille, N.; Boujtita, M.; Nyokong, T.; Bedioui, F. *Mater. Sci. Eng. C-Biomimetic Supramol. Syst.* **2008**, *28*, 606.
(64) Tam, J. P.; Wu, C. R.; Liu, W.; Zhang, J. W. *J. Am. Chem. Soc.* **1991**, *113*, 6657.
(65) Cookeas, E. G.; Efstathiou, C. E. *Analyst* **1994**, *119*, 1607.
(66) Cookeas, E. G.; Efstathiou, C. E. *Analyst* **2000**, *125*, 1147.
(67) Ntziachristos, L.; Froines, J.; Cho, A.; Sioutas, C. *Part. Fibre Toxicol.* **2007**, *4*, 5.
(68) Chow, J. C.; Doraiswamy, P.; Watson, J. G.; Antony-Chen, L. W.; Ho, S. S. H.; Sodeman, D. A. *J. Air Waste Manage. Assoc.* **2008**, *58*, 141.
(69) *CRC handbook of chemistry and physics*; CRC Taylor & Francis: Boca Raton, Fla. ;, 2009.
(70) Hansen, R. E.; Østergaard, H.; Nørgaard, P.; Winther, J. R. *Anal. Biochem.* **2007**, *363*, 77.
(71) Di Pietro, A.; Visalli, G.; Munaò, F.; Baluce, B.; La Maestra, S.; Primerano, P.; Corigliano, F.; De Flora, S. *Int. J. Hyg. Envir. Heal.* **2009**, *212*, 196.
(72) Rucinski, C.; Resource Technology Corporation, Laramie, WY: Certificate of Analysis: Trace metal-Industrial Incinerator Ash, 2008.
(73) Wise, S. A.; Watters, R. L. J.; National Institute of Standard & Technology: Gaithersburg, MD, 2009.

CHAPTER 5. MICROFLUIDIC ELECTROCHEMICAL SENSOR FOR ASSESSING AEROSOL OXIDATIVE STRESS VIA THE ABILITY TO GENERATE HYDROXYL RADICALS

CHAPTER OVERVIEW

This chapter discusses the development and testing of microfluidic electrochemical sensor developed as described in Chapter 3 for the analysis of the hydroxyl radical generation ability of aerosols. The ultimate goal of this system is to create an on-line monitoring system using a similar approach as described in Chapter 4. As a first step toward this goal, assay optimization and system characterization in an off-line format employing flow injection analysis and amperometric detection were carried out. All of the material presented in this chapter was collected and analyzed by the author. At present, the off-line system characterization has been performed. Submission of a manuscript on this topic is anticipated once on-line measurements are finished.

SYNOPSIS

Particulate matter (PM) air pollution has an important effect on human health; however, the mechanisms of toxicity caused by PM are still unclear. A leading hypothesis states that PM induces damage by generating reactive oxygen species (ROS) in cells, leading to oxidative stress.[1,2] Among the ROS, $^{\bullet}OH$ is well-known as the most reactive species. The measurement of $^{\bullet}OH$ generation by PM is helpful for the information of how the PM induces toxicity in cells. Traditional measurements of $^{\bullet}OH$ generated by PM rely on filter-based sampling methods and PM extracts for the analysis that may cause sample reactive losses prior to analysis. To overcome these sampling artifacts, we are applying a microfluidic electrochemical sensor that can be coupled to on-line PM sampling to directly measure the $^{\bullet}OH$ generated from the PM in real time. As a first step toward this goal, the microfluidic electrochemical sensor was tested for its off-line performance for measuring $^{\bullet}OH$ generated from the PM. The determination is based on a salicylic acid trapping assay where the $^{\bullet}OH$ generated by PM is trapped by salicylic acid, forming 2,3- and 2,5-dihydroxybenzoic acid (DHBA) products that can be easily detected using a microfluidic electrochemical sensor with flow injection analysis. Performance of the sensor against standard DHBA detection was evaluated with the linearity in the range of 5-100 μM, detection limit of 4.06 ± 0.10 μM (3×S/N) and relative standard deviation of 0.19-2.82 %. Next, analytical figures of merit against standard Fe^{2+} as $^{\bullet}OH$ generator in the SA assay to generate DHBA were also studied and linearity range of 1-15 μg Fe^{2+}, detection limit of 2.60 ± 0.04 μg Fe^{2+} and relative standard deviation of 1.03-5.89 % were obtained. Proof-of-principle of the method for detecting $^{\bullet}OH$ generated from a non-aerosolized fly ash sample was studied and a relatively high sample mass (1 mg/assay) is required to generate detectable DHBA signal presently.

INTRODUCTION

Atmospheric aerosols (airborne particulate matter (PM)) have been investigated for their effects as a prime candidate for creating toxicity in humans, causing various diseases such as premature deaths,[3] impaired pulmonary function,[4] neurodegenerative disorders,[5] and respiratory and cardiovascular diseases.[1,6,7] Various chemical compounds in ambient PM, including aromatic compounds and transition metals such as Fe, V, Cr, Mn, Co, Ni, Cu, Zn, and Ti, may contribute to these effects through the generation of reactive oxygen species (ROS), including hydrogen peroxide (H_2O_2), hydroxyl radical ($^{\bullet}OH$), nitric oxide (NO), peroxyl radical ($ROO^{\bullet}$), peroxylnitrite radical ($ONOO^{-}$), and superoxide anion ($O_2^{\bullet-}$).[4,8,9] The exact mechanism by which PM causes oxidative stress is not completely understood; however, PM-associated ROS have been implicated in pro-inflammatory effects and are known to cause damage to lipids, proteins, and DNA.[2,4,5,8-12] In normal biological systems, natural generation of ROS as a result of aerobic metabolism is balanced by endogenous antioxidants.[13] High levels of ROS cause a change in the redox status of the cell and its surrounding environment, thereby triggering a cascade of events associated with inflammation and, at higher concentrations, significant cellular damage.[14,15] Of these ROS, $^{\bullet}OH$ is the most reactive and it can react with most organic molecules at diffusion-controlled rate constants ($k = 1.3 \times 10^{10}$ M s^{-1}).[16] Aerosols can have ability to catalyze the formation of $^{\bullet}OH$ when mixed with a small amount of H_2O_2 oxidant. Unlike $O_2^{\bullet-}$ and H_2O_2, which can be quenched enzymatically by superoxide dismutase and catalase, respectively, $^{\bullet}OH$ cannot be detoxified by such process. Therefore, the determination of *in vitro* and *in vivo* $^{\bullet}OH$ production are useful as indicators of cell toxicity caused by PM.[17]

The determination of $^{\bullet}OH$ produced by PM is not straightforward since the $^{\bullet}OH$ is very reactive. Therefore, a technique employing reaction of $^{\bullet}OH$ with a probe molecule was used

instead of direct detection of ·OH. In general, H_2O_2 added to the PM sample can react with transition metals, PAHs, and quinones present in the aerosol to produce ·OH, and the ·OH was trapped by the probe to produce stable species that can be readily detected. Several techniques have been developed for measuring ·OH products. Electron spin resonance (ESR) spectroscopy is a technique for detecting molecules with unpaired electrons. By adding a probe molecule such as 5,5-dimethyl, 1-pyrroline *N*-oxide (DMPO), commonly referred to as a *spin trap*, the lone electron on ·OH can be captured (trapped) on the DMPO molecule. The resulting DMPO-OH has a sufficiently long half life so that it is possible to record its distinctive electron paramagnetic resonance (EPR) spectrum.[18] ESR instrumentation is large and expensive, however. Fluorescent probes such as 2',7'- dichlorofluorescein (DCFH) have also been used for evaluating ·OH production. The probe is oxidized by ·OH to produce an intensely fluorescent compound and then detected.[17] Benzoic acids[19,20] including salicylic acid[21] have been used to trap ·OH from PM to form mono-hydroxybenzoic and dihydroxybenzoic acids and the products can quantified by HPLC coupled with electrochemical detection (HPLC-ECD).[19-21] All techniques stated above provided a wealth of information for the ability of PMs to generate ·OH; however, they require filter-based PM sampling methods and high aerosol mass for detection.[19,22] They require long (up to 24 h) aerosol sampling durations (to capture sufficient mass for detection). The long sampling times not only reduce the temporal resolution of the measurement but also increase the potential for collected species to react and change composition prior to analysis.[23,24]

To overcome problems associated with sampling artifacts, a system for on-line monitoring of ·OH generated by the PM would be useful. As a first step to reach this goal, we present the measurement of aerosol ·OH using a microfluidic electrochemical sensor. This sensor has been demonstrated for its ability to measure aerosol oxidative activity in an on-line

format with high temporal resolution (3 min/sample).[25] The analysis of ·OH generation by PM by the sensor is based on the salicylic acid trapping assay (SA assay) where after generated by the reaction of PM and H_2O_2, the ·OH products react with salicylic acid to form the 2,3- and 2,5-dihydroxybenzoic acid (DHBA) which is then directly detected electrochemically. The following reactions demonstrate how the SA trapping assay works using Fe^{2+} as an ·OH generator:

$$Fe^{2+} + H_2O_2 \longrightarrow Fe^{3+} + {}^{-}OH + {}^{\bullet}OH \qquad (1)$$

$$Fe^{3+} + H_2O_2 \longrightarrow Fe^{2+} + {}^{\bullet}OOH + H^{+} \qquad (2)$$

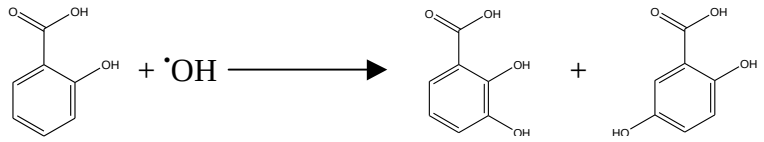

(3)

SA 2,3-DHBA 2,5-DHBA

Microfluidic devices can handle very small volumes (μL) of sample with a high degree of efficiency and minimal external equipment; thus, they are attractive for field-based measurements.[26,27] By reducing solution volumes from milliliters to microliters, similar reductions in the required PM mass can be achieved while still achieving quantitative measurements.[27] Furthermore, the analysis takes only 3 min per sample injection whereas the traditional HPLC-ECD method takes 30 min per injection. A flow injection system, coupled with amperometric detection, provide measurements of DHBA products. The sensor is also ready to couple with the on-line PM sampling system to create the on-line monitoring of ·OH generated from the PM. We have optimized the electrode composition and the results showed that unmodified carbon paste electrode (unmodified CPE) is suitable to detect the DHBA

products at 300 mV without interferences from background reagents. Reaction time, reaction pH, and reagent amount participating in the reaction were optimized. The analytical performance of the sensor was investigated to confirm that the system offers effective detection of DHBA. The working range and detection limit of the salicylic acid trapping chemistry were determined using a standard $^{\bullet}OH$ generator, Fe^{2+} and H_2O_2. Reactions were performed off-line and the DHBA products were directly injected into the flow system coupled to the microfluidic electrochemical sensor. Finally, method proof-of-concept for measuring $^{\bullet}OH$ produced from a non-aerosolized fly ash sample was studied and a relatively high sample mass (1 mg/assay) was required to create sufficient DHBA signal for the detection.

MATERIALS AND METHODS

Chemical and Materials

Unless otherwise stated, all chemicals were purchased from Sigma-Aldrich (St. Louis, MO, USA). Mineral oil was obtained from Fisher Scientific (Fair Lawn, NJ, USA). Poly(dimethyl siloxane) (PDMS) Sylgard 184 elastomer kit was purchased from Dow Corning (Midland, MI, USA). Silver paint was purchased from SPI supplies (West Chester, PA, USA). Copper wire was obtained from NTE Electronics (Bloomfield, NJ, USA). All electrochemical measurements were conducted using a commercially available potentiostat (QuadStat 164, eDAQ, Australia).

Carbon Paste Preparation

Carbon paste electrodes (CPE) were prepared using mixtures of graphite powder and the bonder. For unmodified CPE, graphite powder is mixed with the binder (1:1 PDMS: mineral oil)

in a 1:1 ratio. For carbon nanotube (CNT) modified CPE, CNT was acid washed by 6 M nitric acid to remove metal residuals prior to use.[28] Mixture of graphite and CNT (1:1 w:w) was combined with the binder (1:1 PDMS:mineral oil) in a ratio of 1:1. This mixture was used to fabricate electrodes as described below. Unmodified carbon paste electrodes were used as reference and auxiliary electrodes.

Electrode Fabrication

Electrode fabrication in microfluidic channels was performed using a method analogous to screen-printing as previously reported.[29] Channels were created in PDMS using soft lithography. Carbon paste was spread over the electrode channels within a PDMS slab (electrode dimensions: 500 μm wide by 50 μm deep; electrode spacing: 300 μm, center-to-center). Excess paste was removed by pressing and removing a piece of Scotch tape over the PDMS slab. The electrode chip slab was then hard baked for 30 min at 95 °C and taken out to clean using Kimwipe®. Further hard baking for 1 h at 120 °C was performed to cure the electrode on the PDMS chip. To create a microchip for flow injection analysis (FIA) a second piece of PDMS containing a flow channel (250 μm wide, 50 μm deep and 2.5 cm long) with 1.5 mm diameter inlet hole and outlet hole was sealed to the electrode layer. Electrodes were cleaned using air plasma (1 min, 150 W, 0.8 torr) prior to chip assembly to improve electrochemical performance.[30] The off-chip injection valve (6-port, fitted with a 10 μL injection loop) and syringe pump (PHD 4400, Harvard Apparatus, Holliston, MA, USA) for FIA system were connected to the inlet hole of the microfluidic device. The outlet hole of the chip was connected to the tube to direct the waste solution after the detection. A copper wire was attached to the electrode end using silver paint to create an electrical contact.

Assay Procedure

A standard reaction of metal-based catalysis of $^{\bullet}OH$ generation was performed using Fe^{2+} as a standard for PM solution to test the performance of the sensor for detection of DHBA products. Fly ash sample was employed to test the proof-of-principle of the assay. Fe^{2+} solution (mass range of 0-30 μg or 1 mg non-aerosolized fly ash sample) was mixed with SA (2.53 μmol) and H_2O_2 (1.47 μmol). Acetate buffer (100 mM, pH 3) was then added to reach the 2 mL reaction mixture and the reaction was allowed for 20 min. After reacting, the reaction mixture was stored at 4 °C until the analysis. The electrochemical analysis to quantify amount of DHBA products was performed by injecting the reaction mixture into a 10 μL injection loop within the FIA system in which phosphate buffer (100 mM, pH 7.4) was used as a running buffer.

RESULTS AND DISCUSSION

The ultimate goal of this project is to create a field-ready microfluidic electrochemical sensor for the measurement of $^{\bullet}OH$ generated from atmospheric aerosols. As the first step towards this goal, we have created a microfluidic electrochemical sensor with selectivity for DHBA products to allow assessment of $^{\bullet}OH$ generation by PM.

Electrode Composition Study

Carbon paste electrodes have been employed for on-chip analyte detection in this work. An electrode fabrication method analogous to screen-printing was used to produce on-chip electrodes using carbon paste with a custom designed binder previously reported.[29] We found that these electrode systems provided robustness and good electrochemical properties. The electrochemical sensor can be reused over a month by rising with de-ionized water after daily

use. As a first step, the composition of the electrode was studied. Performance of unmodified and CNT modified carbon paste electrode was compared toward the detection of DHBA and other background reagents. A good electrode should provide selective detection of DHBA without interferences at high potential. Figures 5.1 and 5.2 show hydrodynamic voltamograms of species associated with the salicylic acid trapping reaction to compare optimal potential for DHBA detection obtained from the two types of electrodes, unmodified CPE and CNT-modified CPE. Positive controls including DHBA solution and salicylic acid trapping assay using Fe^{2+} as a standard $^{\bullet}OH$ generator to produce DHBA (graph of Fe^{2+} + salicylic acid (SA) + H_2O_2) were studied. Negative controls including all individual reagents (H_2O_2, SA, Fe^{2+}) as well as combination of background reagents associated in the salicylic acid trapping assays (Fe^{2+} + SA, Fe^{2+} + H_2O_2, SA + H_2O_2) were also investigated for interferences. The optimal potential for detecting DHBA products without interferences from background reagents is 300 and 200 mV using unmodified CPE and CNT-modified CPE, respectively. At higher potentials, an interfering signal from H_2O_2 was observed. Since the use of unmodified CPE gave comparable DHBA signal detection in DHBA solution and reaction of standard salicylic acid trapping assay to CNT modified CPE, unmodified CPE was used for further experiment. Unmodified CPE is also cheaper and easier to prepare without the need of CNT preparation like acid wash prior to use.

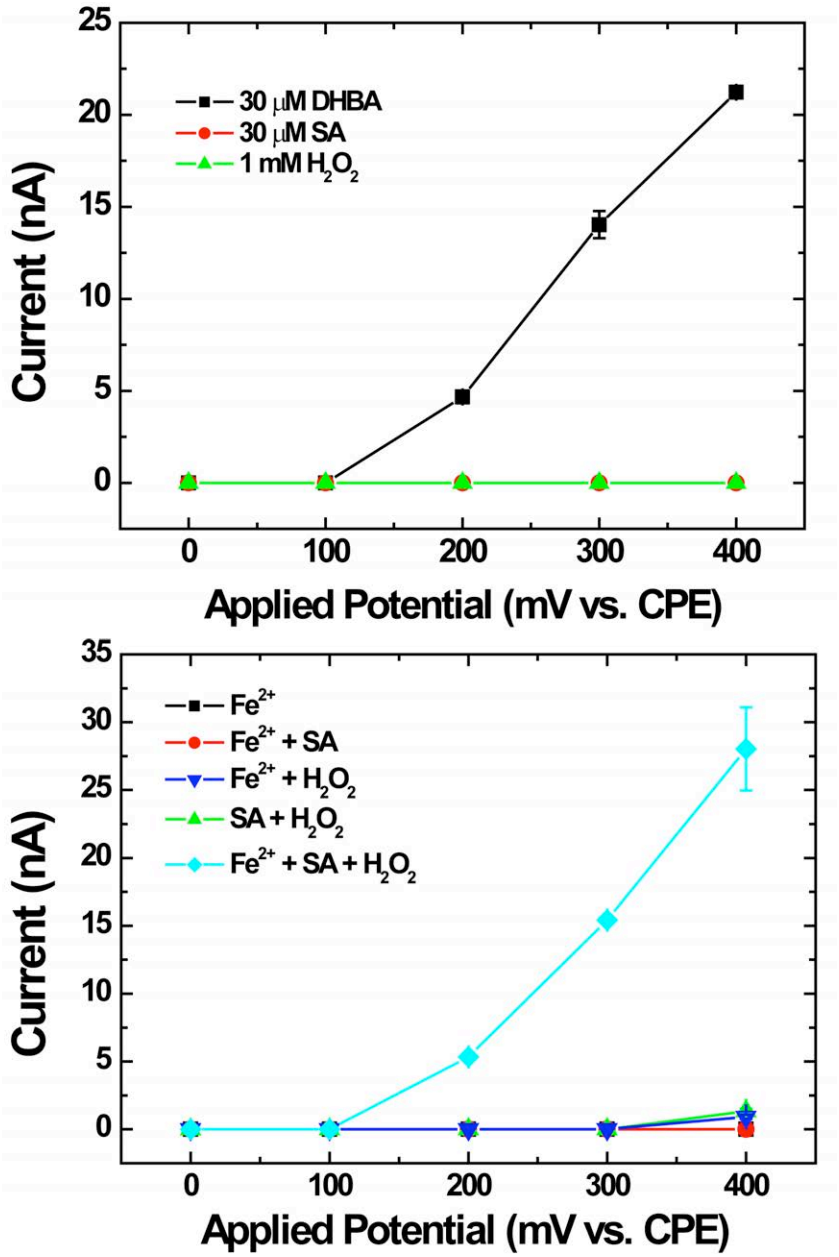

Figure 5.1. Unmodified CPE performance study on the detection of DHBA products. Hydrodynamic voltammogram plotted as signal current as a function of applied potential from the analysis of (A) individual species associated with the salicylic acid trapping assay and (B) individual, combination of background reagents, and positive control in the salicylic acid trapping assay using Fe (II) as a standard $^{\bullet}OH$ generator. Concentration of the reagents in Figure 5.1B is as follow; ■: Fe^{2+} (18 μM), ●: Fe^{2+} (18 μM) in SA (1. 81 mM), ▲: SA (1.81 mM, 1 mL) + H_2O_2 (2.94 mM, 1 mL), ▼: 18 μM Fe^{2+} (1 mL) + H_2O_2 (2.94 mM, 1 mL), ♦: 18 μM Fe^{2+} in SA (1.81 mM, 1 mL) + H_2O_2 (2.94 mM, 1 mL)

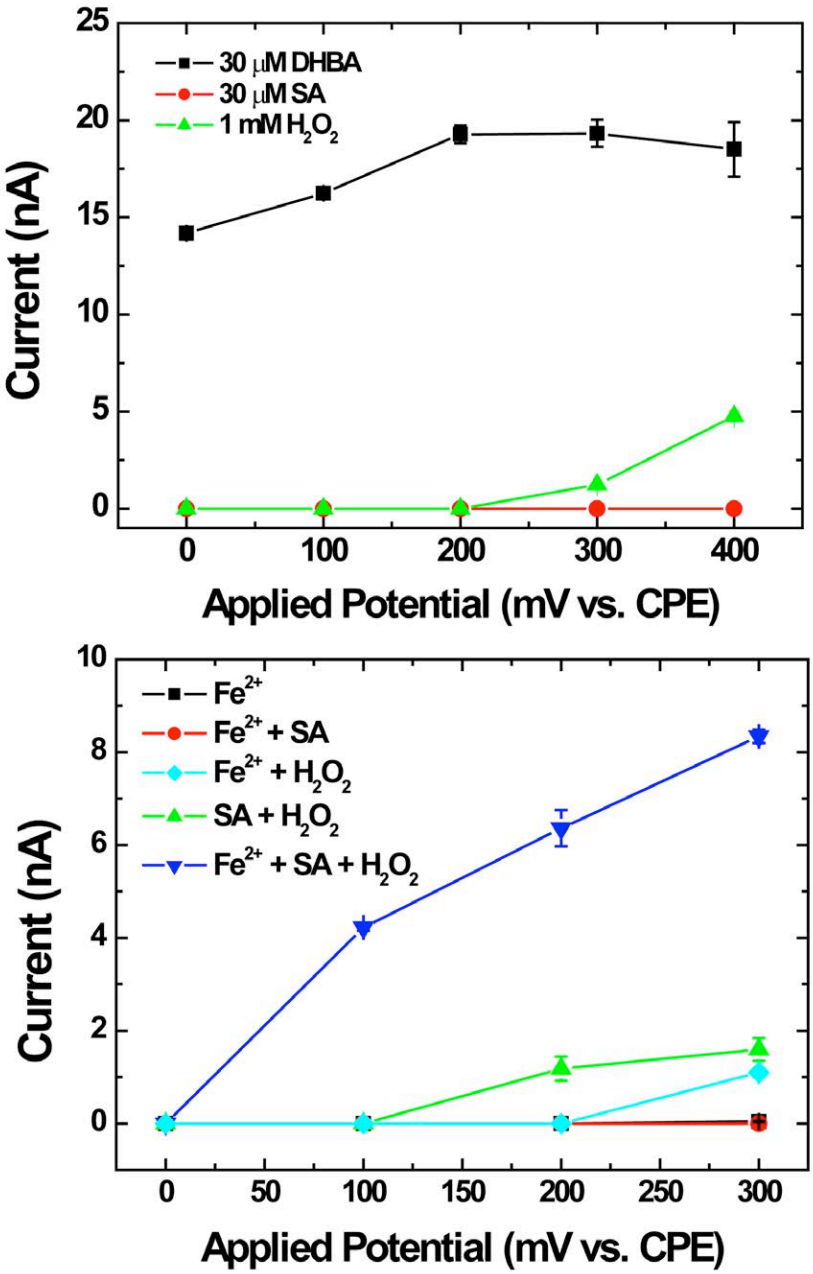

Figure 5.2. CNT-modified CPE performance study on the detection of DHBA products. Hydrodynamic voltammogram plotted as signal current as a function of applied potential from the analysis of (A) individual species associated with salicylic acid trapping assay and (B) individual, combination of background reagents, and positive control in the salicylic acid trapping assay using Fe^{2+} as a standard $^{\bullet}OH$ generator. Reagent concentrations are the same as provided in Figure 5.1.

Sensor Performance against DHBA

After determining the optimal electrochemical conditions, the analytical performance using 2,5-DHBA used as the standard for total DHBA was determined to ensure that the experimental conditions provided effective determination. Flow injection analysis was employed for detecting 2,5-DHBA in the concentration range of 5-100 μM. A plot (Figure 5.3) of average peak current (nA) (n=3) as a function of DHBA concentration (μM) showed a linear calibration curve from 5 to 100 μM ($y = 0.26x + 0.62$, $R^2 = 0.9996$). The relative standard deviations obtained from 3 times injection of the studied concentrations were in the range of 0.19-2.82%. The detection limit for DHBA defined as the concentration that gives a signal 3× larger than the baseline noise was 4.06 ± 0.10 μM (n=3) which is equivalent to 40.6 pmol for 10 μL injection loop. This is similar detection capability to the previously reported microfluidic electrochemical sensors.[31,32]

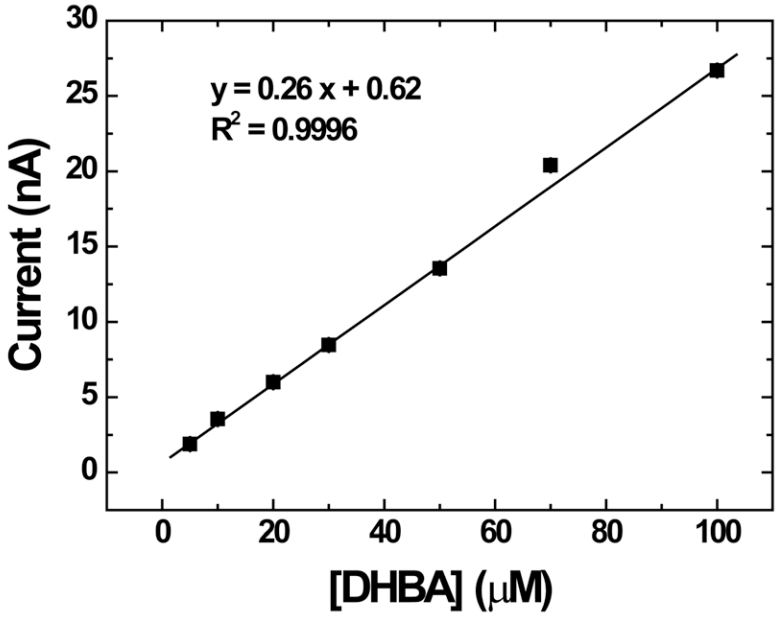

Figure 5.3. Response of the microfluidic electrochemical sensor to the 2,5-DHBA concentration range of 5-100 μM injected with a 10 μL injection loop of the flow injection analysis system.

Salicylic Acid Trapping Assay

After characterizing the response of the sensor, it was tested for the ability to detect DHBA products from the SA assay. The assay was optimized for suitable conditions. For this optimization purpose, Fe^{2+} and H_2O_2 were used as a standard $^{\bullet}OH$ generator. The reaction time of the assay was first studied to get an optimal reaction period for SA assay. Figure 5.4A demonstrates the plot of DHBA products signal of the SA assay at different reaction time. The DHBA signal increases as reaction time increases. These results are in agreement with previous reports where the DHBA increased until reaching a plateau at 35 min.[33] Since a 20 min reaction time provides sufficient DHBA signal and acceptable assay analysis time, it was selected for subsequent experiments. Reaction pH was next optimized since it plays an important role in reaction (1) (see above) in the production of $^{\bullet}OH$ via the Fenton chemistry and consequently affects the generation of DHBA products in reaction (3). Plot of DHBA signal from SA assay as a function of reaction pH is shown in Figure 5.4B. From pH 3-8, the DHBA signals decrease as reaction pH increases which is in agreement with the previously reported in the literature where the DHBA signal was seen to increase from pH 2-3.5 and then decreased.[33] Higher ^{-}OH amount at higher pH cause reaction (1) unfavorable and thus lower $^{\bullet}OH$ produced. Since the highest DHBA products were obtained at the reaction pH 3, this pH was used for further experiments. It should be note that a further two variable experiment (reaction time, reaction pH) should be carried out as a function of DHBA product signal to optimize the SA assay more fully since both reaction time and pH affect $^{\bullet}OH$ generation reaction.

Quantitative effects of H_2O_2 and SA in $^{\bullet}OH$ generation and trapping were studied. Different amounts of H_2O_2 added to the reaction were studied to find optimal amount to generate high sensitive response against Fe^{2+} as a standard $^{\bullet}OH$ generator. Obviously, 1.47 μmol H_2O_2

added to the reaction gave the highest sensitivity of the graph plotted of DHBA signal as a function of Fe^{2+} amount (Figure 5.5A). However, no additional DHBA signal was gained above 20 μg Fe^{2+}. Moreover, at higher H_2O_2, the DHBA signal increased at low Fe^{2+} amounts but decreased at higher Fe^{2+} amounts. For example, DHBA signals dropped at Fe^{2+} amount of 30 and 20 μg when H_2O_2 of 2.94 μmol and 5.88 μmol were used, respectively. These observations might be described by several mechanisms proposed previously.[34] After being produced by reaction (1), $^{\bullet}OH$ can undergo further reaction in the excess of Fe^{2+} as follow:[35]

$$Fe^{2+} + {}^{\bullet}OH \longrightarrow Fe^{3+} + {}^{-}OH \qquad (4)$$

This reaction competes with the DHBA formation reaction and thus lower DHBA signal was observed. Other mechanisms that might rationalize this situation is by considering the formation of an intermediate oxidant which is the ferryl ion, FeO^{2+} generated by reaction of ferrous ions and H_2O_2 at low pH:[36]

$$Fe^{2+} + H_2O_2 \longrightarrow FeO^{2+} + H_2O \qquad (5)$$

At excess H_2O_2:

$$FeO^{2+} + H_2O_2 \longrightarrow Fe^{2+} + H_2O + O_2 \qquad (6)$$

At excess Fe^{2+}:

$$FeO^{2+} + Fe^{2+} \xrightarrow{2H^+} 2Fe^{3+} + H_2O \qquad (7)$$

As shown via the ferryl ion intermediate pathway, no $^{\bullet}OH$ is produced in an excess of H_2O_2 and Fe^{2+}. This mechanism can compete with the DHBA formation reaction and consequently lower DHBA products were observed. Since the use of 1.47 μmol H_2O_2 in the assay gave us the highest sensitivity, this amount of H_2O_2 was used for subsequent experiments. Amount of SA was next optimized to provide effective trapping $^{\bullet}OH$ and generating DHBA

products. Figure 5.5B shows the plot of DHBA signals as a function of Fe^{2+} standard $^{\bullet}OH$ generator at different SA amounts added to the assay. At the three amounts of SA studied, the highest SA amount (2.53 μmol) added to the reaction provided highest sensitivity. This amount was thus used to trap the $^{\bullet}OH$ throughout the studies.

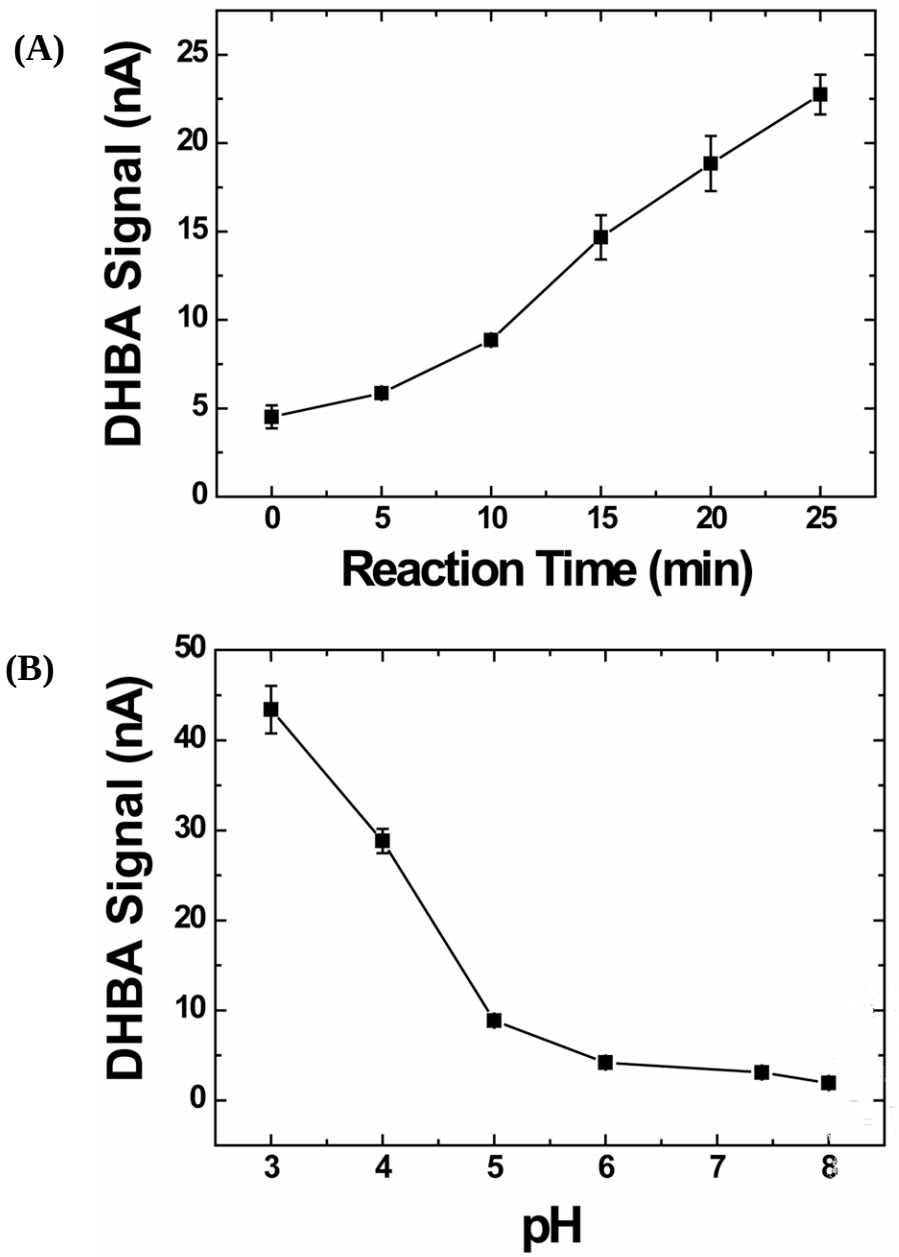

Figure 5.4. Optimization condition for SA assay. (A) DHBA product signal as a function of reaction time. $^{\bullet}OH$ were generated in 2 mL acetate buffer solution (pH 3) containing Fe^{2+} solution (15 μg), mixed with salicylic acid (2.53 μmol) and H_2O_2 (1.47 μmol) at different reaction times (B) a plot of DHBA product signal as a function of reaction pH. $^{\bullet}OH$ were generated in 1 mL of different buffer solution (pH 3-8) containing Fe^{2+} solution (15 μg), mixed with salicylic acid (2.53 μmol) and H_2O_2 (1.47 μmol). The reaction was allowed for 20 min.

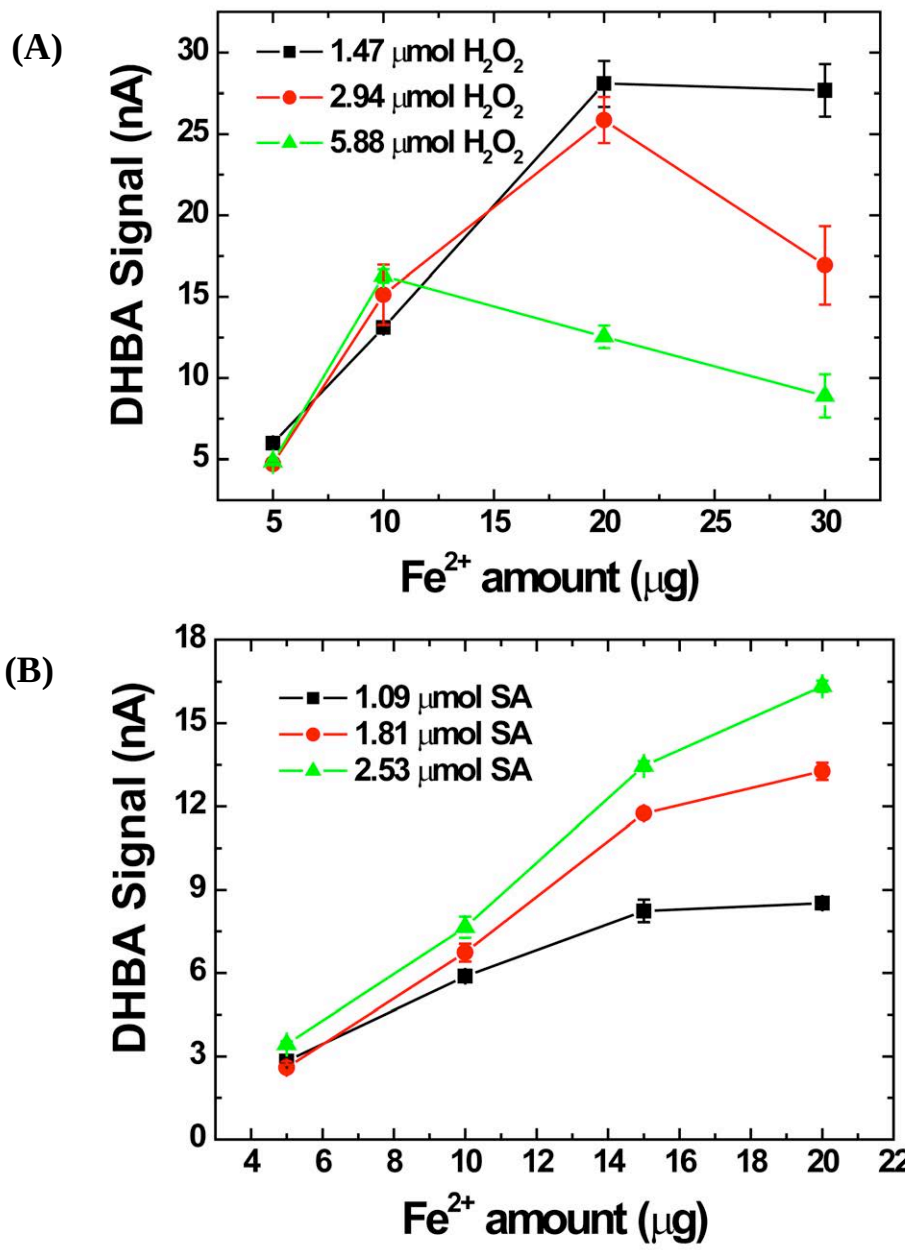

Figure 5.5. Key reagent amount optimization. (A) H_2O_2 amount optimization. Reaction mixture: 2 mL 100 mM acetate buffer pH 3 containing SA (1.81 μmol), Fe^{2+} (5-30 μg) and different amounts of H_2O_2 with the reaction time of 20 min. (B) SA amount optimization. Reaction mixture: 2 mL 100 mM acetate buffer pH 3 containing H_2O_2 (1.47 μmol), Fe^{2+} (5-20 μg) and different amounts of SA with the reaction time of 20 min.

Analytical Performance against Fe^{2+}

In order to test the ability of the sensor for quantitative determination of DHBA generated from the SA assay, analytical figures of merit against the Fe^{2+} standard $^{\bullet}OH$ generator were studied using the assay procedure described above. Figure 5.6 shows a plot of DHBA signal obtained from the SA assay as a function of Fe^{2+} used. The linearity range was found from 3-15 μg Fe^{2+}. The relative standard deviations obtained from 3 replicate injections of the DHBA product from Fe^{2+} studied amount participated in the SA assay were in the range of 1.03-5.89 %. Limit of detection, defined as the lowest Fe^{2+} amount used in the SA assay to produce DHBA signal 3× higher than the baseline noise, was 2.60 ± 0.04 μg.

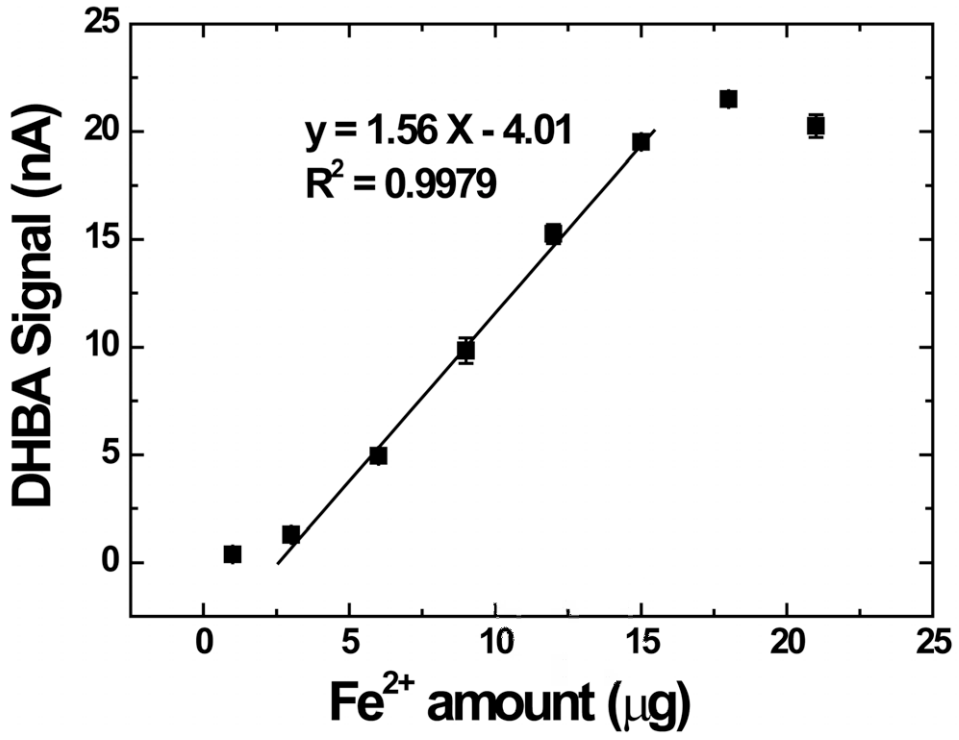

Figure 5.6. DHBA product signals as a function of Fe^{2+} amount used in the SA.

The possibility of the on-line SA assay to measure $^{\bullet}OH$ generated by PM can be approximated using the calculation of detection limit provided above. The lowest amount of Fe^{2+} used in the off-line assay that provides us the detectable signal is 2.60 μg. This amount is used in the reaction volume of 2 mL. In the on-line monitoring method proposed to operate similarly to our previously set up system[25], the injection loop is assumed as the reaction volume which is 10 μL. Therefore, the amount of Fe^{2+} required for 10 μL reaction volumes in an on-line system to get detectable DHBA signal is about 13 ng. In the PM samples such as a fly ash, Fe is present at 2.87% (w/w Fe/PM). Assuming Fe metal are in the reactive form of Fe^{2+} when generated as aerosols in the chamber, the lowest concentration of PM that can provide detectable DHBA signal from on-line SA assay is about 190 μg m^{-3}. This number was calculated using the particle-into-liquid-sampler (PILS) air-sampling rate (16.7 L min^{-1}), sample line flow rate (70 μL min^{-1}, time for a 10 μL injection loop is 1/7 min). Alternatively, Water Condensation Particle Counter (WCPC) might be employed as an on-line PM collector which offers higher PM collection efficiency than the PILS. This would lower the required ambient PM concentration 15 μg m^{-3} to get detectable DHBA signal based on SA assay (the calculation is based on 10 μL collection at 1.5 L/min for 20 min). Additionally, the amount of PM approximated here might be too high to find in the ambient air; however, in reality, lower concentration of PM might be enough to generate detectable DHBA signal from on-line SA assay. Other transition metals (e.g. Cr, V, Ni) or organic compounds (PAHs, quinones) can generate $^{\bullet}OH$ and produce DHBA products in SA assay.

Analysis of Fly Ash Samples

As a quick test to see if the developed off-line SA assay can analyze the DHBA products from the sample, a fly ash sample that is normally used for creating the artificial aerosols for testing on-line aerosol monitoring system was studied.[25,37] The sample that had not been aerosolized yet was used in the SA assay by reacting 1 mg of fly ash sample with SA (2.53 μmol) and H_2O_2 (1.47 μmol) in acetate buffer pH 3 and the total volume adjusted to 2 mL. After allowed to react for 20 min, the solution was then filtered and the DHBA products analyzed. The DHBA signal current from this analysis is 3.05 ± 0.09 nA (n=3). The $^{\bullet}OH$ generation ability of this amount of fly ash is equivalent to 3.83 ± 0.07 μg Fe^{2+}. Although a high fly ash amount was required in this experiment to create a detectable signal, in aerosol samples, lower amount PM at smaller particles sizes might be enough for the SA assay. Further studies employing several PM types for off-line assay testing are required to test the system performance more fully.

CONCLUSIONS

We demonstrate here for the first time the application of microfluidic electrochemical sensor for the determination of $^{\bullet}OH$ generation ability of PM using salicylic acid trapping assay. In this new approach, the DHBA products from reaction of H_2O_2 with PM and trapped by SA was measured directly using the electrochemical sensor. Flow injection analysis with amperometric detection was employed, and device coupling to provide continuous analysis and to be ready for the interfacing of the microfluidic device to an on-line aerosol sampler is our ultimate goal. Optimization of electrode composition and SA assay parameter were carried out to obtain effective conditions for measuring the activity of $^{\bullet}OH$ generation of the PM. Sensor

performance against DHBA detection was evaluated and efficient detection results were obtained. Analytical figures of merit of the SA assay with microfluidic electrochemical sensor for the detection of DHBA using a standard Fe^{2+} as $^{\bullet}OH$ generator were studied. This performance of the sensor shows promises as a tool for field studies of $^{\bullet}OH$ generation ability of the PM. Method validation of the sensor for SA assay against traditional SA assay using various PM samples is required to test the performance of the developed method more fully in an off-line format.

REFERENCES

(1) Gauderman, W. J.; Vora, H.; McConnell, R.; Berhane, K.; Gilliland, F.; Thomas, D.; Lurmann, F.; Avol, E.; Kunzli, N.; Jerrett, M.; Peters, J. *Lancet* **2007**, *369*, 571.

(2) Ghelfi, E.; Rhoden, C. R.; Wellenius, G. A.; Lawrence, J.; Gonzalez-Flecha, B. *Toxicol. Sci.* **2008**, *102*, 328.

(3) Hoek, G.; Meliefste, K.; Cyrys, J.; Lewne, M.; Bellander, T.; Brauer, M.; Fischer, P.; Gehring, U.; Heinrich, J.; van Vliet, P.; Brunekreef, B. *Atmos. Environ.* **2002**, *36*, 4077.

(4) de Kok, T. M.; Hogervorst, J. G.; Briede, J. J.; van Herwijnen, M. H.; Maas, L. M.; Moonen, E. J.; Driece, H. A.; Kleinjans, J. C. *Environ. Mol. Mutagen.* **2005**, *46*, 71.

(5) Verma, V.; Pakbin, P.; Cheung, K. L.; Cho, A. K.; Schauer, J. J.; Shafer, M. M.; Kleinman, M. T.; Sioutas, C. *Atmos. Environ.* **2011**, *45*, 1025.

(6) Ichoku, C.; Andreae, M. O.; Andreae, T. W.; Meixner, F. X.; Schebeske, G.; Formenti, P.; Maenhaut, W.; Cafmeyer, J.; Ptasinski, J.; Karnieli, A.; Orlovsky, L. *J. Geophys. Res.-Atmos.* **1999**, *104*, 24371.

(7) Ghelfi, E.; Rhoden, R.; Wellenius, G. A.; Lawrence, J.; Gonzalez-Flecha, B. *Toxicol. Sci.* **2008**, *102*, 328.

(8) Prahalad, A. K.; Soukup, J. M.; Inmon, J.; Willis, R.; Ghio, A. J.; Becker, S.; Gallagher, J. E. *Toxicol. Appl. Pharmacol.* **1999**, *158*, 81.

(9) Clarke, R. W.; Catalano, P.; Coull, B.; Koutrakis, P.; Murthy, G. G. K.; Rice, T.; Godleski, J. J. *Inhal. Toxicol.* **2000**, *12*, 73.

(10) Cho, A. K.; Sioutas, C.; Miguel, A. H.; Kumagai, Y.; Schmitz, D. A.; Singh, M.; Eiguren-Fernandez, A.; Froines, J. R. *Environ. Res.* **2005**, *99*, 40.

(11) Beck-Speier, I.; Dayal, N.; Karg, E.; Maier, K. L.; Schumann, G.; Schulz, H.; Semmler, M.; Takenaka, S.; Stettmaier, K.; Bors, W.; Ghio, A.; Samet, J. M.; Heyder, J. *Free Radic. Biol. Med.* **2005**, *38*, 1080.

(12) Kreyling, W. G.; Semmler, M.; Moller, W. *J Aerosol Med* **2004**, *17*, 140.

(13) Hatzis, C.; Godleski, J. J.; Gonzalez-Flecha, B.; Wolfson, J. M.; Koutrakis, P. *Environ. Sci. Technol.* **2006**, *40*, 2805.

(14) Xiao, G. G.; Wang, M. Y.; Li, N.; Loo, J. A.; Nel, A. E. *J. Biol. Chem.* **2003**, *278*, 50781.

(15) Li, N.; Kim, S.; Wang, M.; Froines, J.; Sioutas, C.; Nel, A. *Inhal. Toxicol.* **2002**, *14*, 459.

(16) Held, K. D.; Sylvester, F. C.; Hopcia, K. L.; Biaglow, J. E. *Radiat. Res.* **1996**, *145*, 542.

(17) Cohn, C.; Simon, S.; Schoonen, M. *Part. Fibre Toxicol.* **2008**, *5*, 2.

(18) Nawrot, T. S.; Kuenzli, N.; Sunyer, J.; Shi, T.; Moreno, T.; Viana, M.; Heinrich, J.; Forsberg, B.; Kelly, F. J.; Sughis, M.; Nemery, B.; Borm, P. *Atmos. Environ.* **2009**, *43*, 4595.

(19) Anastasio, C.; McGregor, K. G. *Atmos. Environ.* **2001**, *35*, 1079.

(20) Jung, H.; Guo, B.; Anastasio, C.; Kennedy, I. M. *Atmos. Environ.* **2006**, *40*, 1043.

(21) DiStefano, E.; Eiguren-Fernandez, A.; Delfino, R. J.; Sioutas, C.; Froines, J. R.; Cho, A. K. *Inhal. Toxicol.* **2009**, *21*, 731.

(22) Boogaard, H.; Janssen, N. A. H.; Fischer, P. H.; Kos, G. P. A.; Weijers, E. P.; Cassee, F. R.; van der Zee, S. C.; de Hartog, J. J.; Brunekreef, B.; Hoek, G. *Environ. Health. Perspect.* **2011**, *120*.

(23) Foucaud, L.; Wilson, M. R.; Brown, D. M.; Stone, V. *Toxicol. Lett.* **2007**, *174*, 1.

(24) Hu, S.; Polidori, A.; Arhami, M.; Shafer, M. M.; Schauer, J. J.; Cho, A.; Sioutas, C. *Atmos. Chem. Phys.* **2008**, *8*, 6439.

(25) Sameenoi, Y.; Koehler, K.; Shapiro, J.; Boonsong, K.; Sun, Y.; Collett, J.; Volckens, J.; Henry, C. S. *J. Am. Chem. Soc.* **2012**, *134*, 10562.
(26) Garcia, C. D.; Henry, C. S. *Anal. Chim. Acta* **2004**, *508*, 1.
(27) Noblitt, S. D.; Lewis, G. S.; Liu, Y.; Hering, S. V.; Collett, J. L.; Henry, C. S. *Anal. Chem.* **2009**, *81*, 10029.
(28) Pumera, M. *Langmuir* **2007**, *23*, 6453.
(29) Sameenoi, Y.; Mensack, M. M.; Boonsong, K.; Ewing, R.; Dungchai, W.; Chailapakul, O.; Cropek, D. M.; Henry, C. S. *Analyst* **2011**, *136*, 3177.
(30) Wang, S. C.; Chang, K. S.; Yuan, C. J. *Electrochim. Acta* **2009**, *54*, 4937.
(31) Kuhnline, C. D.; Gangel, M. G.; Hulvey, M. K.; Martin, R. S. *Analyst* **2006**, *131*, 202.
(32) Hansen, R. E.; Østergaard, H.; Nørgaard, P.; Winther, J. R. *Anal. Biochem.* **2007**, *363*, 77.
(33) Jen, J.-F.; Leu, M.-F.; Yang, T. C. *J. Chromatogr. A* **1998**, *796*, 283.
(34) González-Davila, M.; Santana-Casiano, J. M.; Millero, F. J. *Geochim. Cosmochim. Acta* **2005**, *69*, 83.
(35) Barb, W. G.; Baxendale, J. H.; George, P.; Hargrave, K. R. *Trans. Faraday Soc.* **1951**, *47*, 591.
(36) Bray, W. C.; Gorin, M. H. *J. Am. Chem. Soc.* **1932**, *54*, 2124.
(37) Rucinski, C.; Resource Technology Corporation, Laramie, WY: Certificate of Analysis: Trace metal-Industrial Incinerator Ash, 2008.

CHAPTER 6. MICROFLUIDIC PAPER-BASED ANALYTICAL DEVICE FOR AEROSOL OXIDATIVE ACTIVITY

CHAPTER OVERVIEW

This chapter discusses an alternative method developed for aerosol oxidative activity measurement that is suitable for personal exposure assessment. The analysis employed a microfluidic paper-based analytical device (μPAD) with DTT assay for oxidative activity of PM on filter samples. The system requires low PM mass for analysis without the requirement for lengthy sample extraction. The DTT assay was performed directly on a punched disk taken from the PM filter and after reacted for a specific time period, remaining DTT was analyzed on the μPAD. The system was applied for measurement of oxidative activity of samples collected by personal sampler from several events. This work is currently on a revision process to resubmit to the journal *Environmental Science and Technology*. Most of data collection and analysis in this Chapter was done by me. I wish to thank Dr. Jeffrey Collett, Jr. for providing the extracted aerosol samples and Ms. Taylor Carpenter for her assistance with gravimetric analysis of personal filter samples. Temperature and method validation study (Figure 6.4A and 6.6) were carried out by Pantila Panymeesamer and Natcha Supalakorn. They also performed initial study of the DTT assay on the μPAD.

SYNOPSIS

Human exposure to particulate matter (PM) air pollution has been linked with respiratory, cardiovascular, and neurodegenerative diseases, in addition to various cancers. Consistent among all of these associations is the hypothesis that PM induces inflammation and oxidative stress in the affected tissue. Consequently, a variety of assays have been developed to quantify the oxidative activity of PM as a means to characterize its ability to induced oxidative stress. The vast majority of these assays rely on high-volume, area-based sampling methods due to limitations in assay sensitivity and detection limit. As a result, our understanding of how personal exposure contributes to the intake of oxidative air pollution is limited. To further this understanding, we present a microfluidic paper-based analytical device (μPAD) for measuring PM oxidative activity on filters collected by personal sampling. The μPAD is inexpensive to fabricate and provides fast and sensitive analysis of aerosol oxidative activity. The oxidative activity measurement is based on the dithiothreitol assay (DTT assay), uses colorimetric detection, and can be completed in the field within 30 min following sample collection. The μPAD assay was validated against the traditional DTT assay using 13 extracted aerosol samples including urban aerosols, biomass burning PM, cigarette smoke and incense smoke. The results showed no significant differences in DTT consumption rate measured by the two methods. To demonstrate the utility of the approach, personal samples were collected to estimate human exposures to PM from indoor air, outdoor air on a clean day, and outdoor air on a wildfire-impacted day in Fort Collins, CO. Filter samples collected on the wildfire day gave the highest oxidative activity on a mass normalized basis, whereas typical ambient background air showed the lowest oxidative activity.

INTRODUCTION

Airborne particulate matter (PM) has a significant impact on human health.[1-4] The World Health Organization (WHO) estimates that indoor and urban outdoor air pollution causes 3 million premature deaths worldwide per year with about half of the deaths from pneumonia in children under 5 years of age.[5] The prevailing hypothesis around the toxic effects of PM centers on the ability of small particles to penetrate cells and induce oxidative stress through one of several pathways.[6-8] Furthermore, ultrafine PM (particles with diameters less than 0.1 μm) can readily penetrate into the circulatory system, affecting tissues distant from the lungs.[6-10] Because of the relationship between PM and oxidative stress, there has been significant interest in developing methods to measure the oxidative activity of aerosols. Historically, oxidative activity was estimated by measuring the presence of chemical species that could generate oxidative stress, such as transition metals, polycyclic aromatic hydrocarbons, and quinones. For example, several components of ambient PM (e.g., redox-active quinones) have been shown to catalyze the generation ROS in solution, which then react with tissues.[11] Unfortunately, speciation methods are expensive and time-consuming, requiring laboratory-based instruments with long sample preparation and analysis times (e.g., chromatography, spectrometry etc.).[2] Furthermore, these methods require a relatively large sample mass, and hence, a long sampling duration is needed to obtain sufficient sample for detection. Finally, the presence of chemicals capable of participating in oxidative reactions is a necessary but not sufficient criterion to determine overall PM oxidative activity.

As a result, there has been a push to develop improved, biologically-relevant approaches to estimate PM toxicity by measuring the *oxidative activity* rather than the *composition* of PM. The most common of these assays is the dithiothreitol (DTT) assay.[12-22] In this assay, PM

collected on a filter is extracted and reacted with reduced DTT. After a period of time, the remaining reduced DTT is reacted with Ellman's reagent [5,5′-dithiobis(2-nitrobenzoic acid), DTNB], releasing a chromogenic compound (2-nitro-5-thiobenzoate, NTB^{2-}) that can be measured using absorption spectroscopy. The DTT assay is considered biologically relevant because the rate of DTT consumption has been correlated with cellular oxidative stress both *in vitro*[23,24] and *in vivo.*[25] Although the DTT assay has provided a wealth of information on particle oxidative activity, it relies on time-integrated sampling methods and requires a relatively large PM sample; thus, it is not suitable for on-line measurements and/or personal exposure assessment (i.e., the use of a lightweight, portable device that samples air within an individual's breathing zone). We have recently addressed the need for on-line monitoring of aerosol oxidative activity by developing a microfluidic sensor coupled with a particle-into-liquid-sampler (PILS); this new system performs the DTT assay on-line and with a 3 min time resolution.[26] Although the on-line method represents an improvement over the traditional DTT method in terms of sensitivity and speed, it is still limited to area-based exposure assessment since the PILS and associated equipment are too large for personal sampling.

Personal exposure assessment is considered the gold-standard for quantifying an individual's risk from exposure. Personal samplers are designed to accompany an individual throughout their daily activities; these devices, therefore, can assimilate the dynamic exposures that an individual experiences as they move through various microenvironments each day.[27] Personal exposure assessment is important because individuals experience a wide range of local microenvironments (e.g., at home, at work, in transit, etc.) in any given 24-h period. Personal exposures may be assessed biologically (i.e., though biomarkers) or with the use of portable monitors worn within the breathing zone (personal samplers). The most common personal

samplers for PM use filter media as the collection substrate, where a known volume of air is drawn through a filter over specific time period (usually 8-24 h) and collected samples are analyzed optically, gravimetrically, or chemically. Chemical analyses of filter extracts are typically done using sensitive but expensive laboratory-based equipment such as GC-MS[28,29] and HPLC-ECD/Fluorescence.[30,31] As a result, the entire process (sample collection, handling, storage, extraction and analysis) can take 1-2 weeks and incur significant costs. This ultimately limits the number of samples collected and analyzed, leading to a smaller-than-desired data set. Furthermore, sample handling and storage prior to analysis can result in decomposition of short-lived species.

The ideal personal exposure assessment method for oxidative activity would require short sampling durations and provide an analysis that is fast, sensitive, inexpensive, portable and easy to perform. Here, in an attempt to accomplish this goal, we developed a method using a microfluidic paper-based analytical device (μPAD) for measuring the oxidative activity of PM collected on personal filter samples. First introduced in 2007,[32] μPADs are fabricated by creating hydrophobic barriers on paper using photolithography,[32,33] poly(dimethylsiloxane) printing,[34] and/or wax printing.[35-37] The barriers define hydrophilic channels designed to transport aqueous solutions by capillary action from a sample inlet to a detection zone. Detection is accomplished either colorimetrically[38,39] or electrochemically.[40] A typical μPAD analysis reduces the required sample volume from milliliters to microliters and also enables sample analysis in the field due to the size and portability of the device.[41] Most importantly, device fabrication is relatively simple and analysis costs can be very low (orders of magnitude less than traditional analytical methods), particularly when using wax printing and low cost

colorimetric reagents.[42] To date, μPADs have been used for quantitative and qualitative measurements in biological,[43] environmental,[42] and medical[44] applications.

The objective of this work was to develop a μPAD for assessing PM oxidative activity on personal air samples using a variant of the traditional DTT assay. The μPAD was designed to conduct the DTT assay on a 2.5×2.5 cm device containing both sample and detection zones as shown in Figure 6.1A (step c). Unlike the traditional DTT assay, where PM from the filter is extracted into solution for subsequent reaction (causing sample dilution), in the μPAD, reduced DTT reacts directly with PM on surface of an air sampling filter. The remaining DTT is then eluted off the filter and onto the μPAD to react with Ellman's reagent, forming a yellow product that is quantified by color intensity (Figure 6.1A, 6.1B). The μPAD DTT assay was optimized for reaction time and temperature using 1,4-naphthoquinone (1,4-NQ) as a standard oxidant. The sensitivity and detection limit of this assay (against the 1,4-NQ standard) may be modulated stoichiometrically by changing the level of DTT reactant presented to the sample. To test the μPAD performance for measuring aerosol oxidative activity, the device was validated against the traditional DTT assay with 13 extracted aerosol samples. No significant difference between the methods was observed for DTT consumption at the 95% confidence interval. Finally, to demonstrate that the μPAD can be applied for the measurement of aerosol oxidative activity for personal exposure, human exposures were assessed outdoors (a clean day and a smoky day, when ambient air quality was influenced by nearby wildfires, in Fort Collins, CO) and indoors (restaurant kitchen) using a personal filter sampler. Filters analyzed using the μPAD showed that samples collected on wildfire-impacted days gave higher relative oxidative activity than indoor samples and typical ambient background samples.

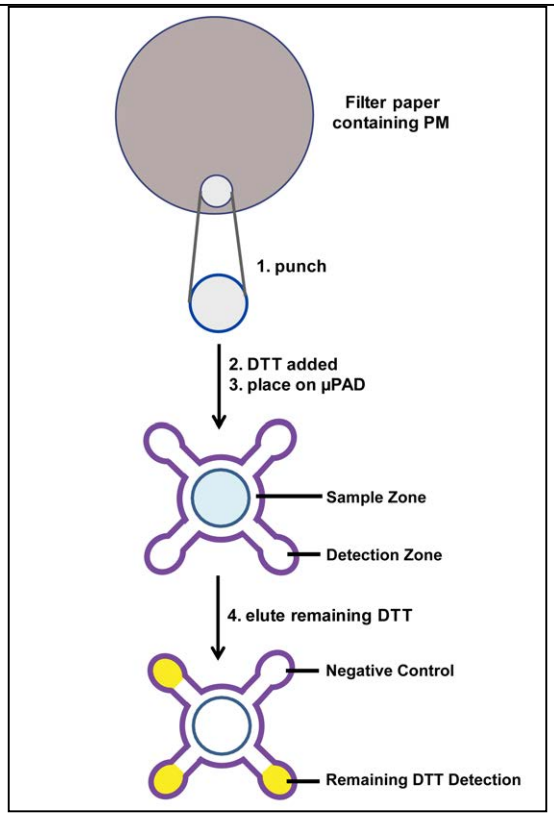

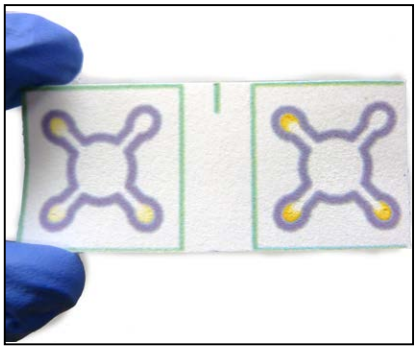

(A) **(B)**

Figure 6.1. (A) Steps to perform DTT assay on a microfluidic paper-based analytical device (µPAD). (B) Actual µPADs used for DTT detection. The left device measured high oxidative activity and, therefore, produced a low-intensity image (more DTT consumed); the right device measured low oxidative activity resulting in more color intensity at the detection zone (less DTT consumed). µPAD dimensions are 2.5×2.5 cm. The sample and detection zone diameters are 10 and 4 mm, respectively.

MATERIALS AND METHODS

Chemicals and Materials

Unless otherwise stated, all chemicals were purchased from Sigma-Aldrich (St. Louis, MO). Ellman's reagent [5,5'-dithiobis-(2-nitrobenzoic acid), or DTNB] was obtained from Alfa-Aesar (Ward Hill, MA). Poly(dimethyl siloxane) (PDMS) Sylgard 184 elastomer kit was purchased from Dow Corning (Midland, MI). A Xerox Phaser 8860 wax printer and Scanner

Documate 3220 were purchased from Xerox (Norwalk, CT) for device printing and scanning, respectively. Whatman filter paper #1 was used as the base material for all μPAD devices. Phosphate buffer (100 mM pH7.4) was used to prepare standard 1,4-Naphthoquinone (1,4-NQ) and DTT solutions as well as elution buffer. The 1,4-NQ powder was dissolved in dimethyl sulfoxide prior to use.

Microfluidic Paper Analytic Device (μPAD) Fabrication

There are two key steps associated with the DTT assay: the catalytic reaction of DTT with PM-generated ROS and the quenching reaction of remaining DTT with DTNB to produce a yellow product (NTB^{2-}) for detection. The μPAD was designed to allow both reaction steps on a single device (step c in Figure 6.1A). The pattern was created using Corel Draw (Corel Corporation, Mountain View, CA), and the device was fabricated by wax printing according to previously described methods.[35] The wax printing fabrication technique is fast and inexpensive and does not require additional solvents or polymers.[45] Following printing, wax-treated paper was placed on a hotplate at 110 ºC for 2 min to allow the wax melt through the paper creating a hydrophobic barrier for directed sample flow. Each μPAD measures approximately 2.5×2.5 cm. The device includes a central sample zone connected to four detection zones via capillary flow channels. The sample zone (10 mm diameter) was designed to allow sufficient area to accommodate a 6 mm sample punch taken from a personal sampling filter. Four smaller areas (4 mm diameter) are each connected to the sample zone; three of these areas act as detection zones (for replicate measurement) and the fourth acts as a negative control. Immediately after fabrication, one side of the patterned paper was covered with Scotch® packing tape. This last step prevents any solution from leaking through the backside of the device during sample analysis.

Violet-colored ink was used for the hydrophobic barrier around the detection zone because violet is complementary to yellow, providing increased contrast for subsequent DTT detection. The violet color in the area around detection zone was subtracted during image analysis using a color threshold adjustment with the imaging software. This process leaves only yellow product color for subsequent image intensity analysis.

Method Validation Using Filter Extracts

Method validation was carried out using extracted filter samples from biomass burning aerosol, urban PM, incense, and cigarette smoke. Filter extracts were chosen since they are amenable to both μPAD and traditional DTT assay analysis techniques. A total of 13 samples, representative of different PM sources and exposures were tested. Three $PM_{2.5}$ samples were collected from the combustion of common vegetation found in North American wildfires using a high-volume filter sampler as part of the USDA's third Fire Lab at Missoula Experiment study.[46] Four $PM_{2.5}$ samples of urban aerosol were collected on quartz filters over separate, integrated three-day sampling periods in Cleveland, OH during the winter of 2008 using a Thermo Anderson Hi-Volume Air Sampler (Windsor, NJ). The quartz filters were pre-baked in an oven at 550 °C for 12 h and wrapped in aluminum foil before use. Six samples of cigarette and incense aerosols were created in an aerosol chamber as described previously.[26] Briefly, aerosol was generated in a ~1 m^{-3} chamber by burning the cigarette or incense for approximately 10 seconds. Filter holders (47 mm diameter) were placed in the chamber and sampled the aerosol for 4 hours at a flow of 10 L min^{-1}. After sampling, all filters were stored at -20 °C prior to extraction.

The filter extraction procedure was described previously.[47] Briefly, two 20-mm diameter punches from each filter sample were extracted in 5 mL of deionized water in a Nalgene Amber High Density Polyethylene (HDPE) bottle using sonication with heat (70 ± 5 °C) for 75 min. The aerosol extracts were syringe filtered (0.2 μm PTFE membrane, Millipore, Billerica, MA, USA) to remove insoluble materials. The filtered samples were kept in the dark at 4 °C until analysis.

The traditional DTT assay was performed according to previously described methods,[20,48] except that EDTA was not added to the reaction buffer for reasons described by Charrier et al.[22] One milliliter of 0.1 M phosphate buffer (pH 7.4) was used as the reaction buffer. A 50 μL aliquot of 0.5 mM DTT was added to the buffer followed by 50 μL of the filtered aqueous aerosol extract. After mixing, the solution was incubated at 37 °C for 25 min. Then, 100 μL of 100 mM Ellman's reagent was added to the reaction mixture to consume the remaining reduced DTT, forming a yellow colored solution of 2-nitro-5-thiobenzoate (NTB^{2-}). Levels of NTB^{2-} were then quantified by absorption at 412 nm using a Genesys UV10 spectrometer (Thermo Scientific, Waltham, MA).

Personal PM Exposure Sampling

Field validation was carried out using μPADs to analyze filter samples collected via personal sampling. Volunteers were asked to carry a backpack containing personal samplers for $PM_{2.5}$ (PM size ≤ 2.5 μm) and PM_{10} (PM size ≤ 10 μm). Personal sampling was conducted across a 24 h period and for three distinctly different events: an 8 h work shift in a restaurant kitchen, an 8 h outdoor exposure on a clean day, and an 8 h outdoor exposure on a smoky day, when the city of Fort Collins was impacted by the High Park wildfire of 2012. The remaining 16 h of each sampling day was spent indoors at the volunteer's home in a relatively clean

environment (free of other combustion or cooking sources). For each event, $PM_{2.5}$ and PM_{10} samples were collected onto Teflon-coated glass fiber filters (Pallflex® T40A60, 37 mm, Pall Corporation, Ann Arbor, MI) using personal impactors (Personal Environmental Monitors, 761-203A or 761-200A, SKC, Inc.). A miniature sampling pump (Omni-400, BGI Incorporated, Waltham, MA) was used to draw air through each sampler at 4 L min^{-1}. Filters were equilibrated at low relative humidity (RH< 40%) and weighed with a microbalance (Mettler-Toledo, model MX5) before and after sampling to determine collected aerosol mass prior to μPAD analysis of oxidative activity. The mass of PM collected on each filter is provided in Table 6.1.

Table 6.1. PM mass on filters collected using personal sampler at the events investigated.

Event	PM Size on Filter (μm)	Mass on 37 mm Diameter Filter (mg)
Outdoor (Clean Day)	2.5	0.0970
	10	0.2560
Outdoor (Smoky Day)	2.5	0.1540
	10	0.2480
Indoor (Restaurant Kitchen)	2.5	0.1565
	10	0.1655

DTT Assay on μPAD

Steps to perform the DTT assay on the μPAD for aerosol oxidative activity analysis are shown in Figure 1A. Samples for method validation (aerosol extract samples) and assay optimization (1,4-NQ solutions) were pipetted onto a 6 mm disk of standard filter paper

(Whatman #1) that was created using a biopsy punch (Robbins Instruments, Chatham, NJ) from a larger sheet. A five microliter aliquot of aerosol extract or 1,4-NQ was added to the 6 mm punch followed by five microliters of DTT solution (0.5 mM in 100 mM phosphate buffer pH 7.4). The filter disk was then placed inside a Petri dish at room temperature (22 ± 2 ºC) and allowed to react for 25 min. Next, the disk was placed in the sample zone of a μPAD and DTNB (5 mM, three aliquots of 0.4 μL at each detection zone) was pipetted onto three of the detection zones, while phosphate buffer (100 mM, pH 7.4) was deposited on the fourth zone as a negative control. The remaining reduced DTT from the punched filter paper was eluted with phosphate buffer (100 mM pH 7.4, three aliquots of 10 μL) allowing the remaining reduced DTT to flow into the detection zones and react with the DTNB to generate a yellow color. To prevent leakage and provide a uniform flow of a solution through the channel, a piece of polydimethylsiloxane (PDMS, Dow Corning) the same size as the paper device containing holes at the center and the detection zones was placed over the device prior to elution.[42] A DTT calibration curve was constructed by adding varying DTT concentrations (0.1-0.7 mM, 5 μL) and phosphate buffer (5 μL) to the 6 mm filter disk. After 25 min, the remaining DTT was analyzed using the method described above. Quantification of the final yellow product was done by scanning the device using a desktop scanner (Xerox DocuMate 3220 Scanner, color photo setting, 600 dpi resolution) and analyzing the spot for yellow intensity using NIH ImageJ software as described previously.[42,43]

Assay Optimization

For temperature optimization, 1,4-NQ was used as a standard oxidant. Two temperatures were compared: room temperature (22 ± 2 °C) and 37 °C. DTT (0.5 mM, 100 μL), 1,4-NQ (0-6

μg/mL, 50 μL) and phosphate buffer (350 μL) were mixed in a culture tube (5 mL, Fisher Scientific, Pittsburgh, PA) and allow to react for 25 min at either room temperature or 37 °C. An aliquot of the solution was then pipetted onto a 6 mm filter disk and analyzed using the μPAD as described above. For optimizing reaction time, different concentrations of 1,4-NQ (2-8 μg/mL, 5 μL) and DTT (0.5 mM, 5 μL) were pipetted onto a filter disk and allowed to react for 10, 20, or 25 min at room temperature. After the specified time, the DTT remaining on the filter punch was analyzed on the μPAD using the method described above.

Analysis of Personal Sampling Filters

As described above, a 6 mm punch was taken from each personal sampling filter. However, prior to analysis, each filter disk was treated with sodium dodecyl sulfate (1 mM SDS, 10 μL) to increase the hydrophillicity of the Teflon filter surface. After 15 minutes of SDS treatment, DTT (0.5 mM, 5 μL) and phosphate buffer (3 μL) were added to the filter disk. The reaction of DTT with PM was carried out for 25 min and then the remaining DTT was measured using the method described above. For each sample, a negative control was performed where the PM filter disk was analyzed without reacting with DTT. A DTT calibration curve for these samples was constructed in a similar manner to that for the extracted samples except that the SDS-modified blank Pallflex® filter was used as a filter disk instead of Whatman#1 filter.

RESULTS AND DISCUSSION

μPAD Performance for DTT Detection

The ability of a μPAD to quantify DTT consumption was determined first. The linearity, reproducibility, sensitivity and detection limit were studied to demonstrate that the system

provided effective analysis of reduced DTT. A plot of gray intensity for the DTT signal as a function of deposited DTT mass as well as apparent color obtained at different quantities of DTT is shown in Figure 6.2. Linearity in the range of 0 to 12.5 nmol DTT was obtained ($y = 8.66x + 0.36$, $R^2 = 0.99$). The relative standard deviation from the analysis of all concentrations was in the range of 0.43-12.50 % (n=3). The DTT detection limit, defined as the concentration giving a signal three times larger than the standard deviation of the blank (phosphate buffer), was 0.27 ± 0.05 nmol. These results demonstrate the ability to measure very low amounts of reduced DTT using a μPAD.

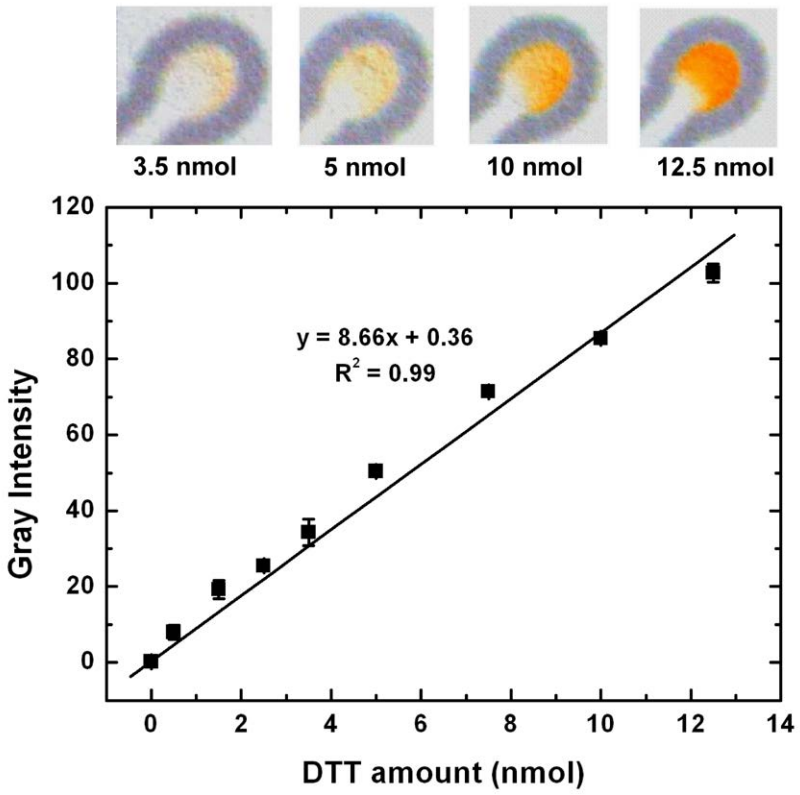

Figure 6.2. Standard calibration for DTT detection generated in the range of 0-12.50 nmol by measuring the color intensity (converted to grayscale) formed at the detection zones (above).

Optimization of DTT Assay

A typical dose-response curve for the μPAD DTT assay using 1,4-NQ as the oxidant is shown in Figure 6.3. Error bars in the curve represent within-sample replicates across the three detection zones on a single device. A linear signal decrease was observed, correlating with previously published colorimetric and electrochemical assays for DTT consumption.[26] The optimal reaction time and temperature conditions for performing the μPAD DTT assay were also determined. As reported in the literature, the DTT assay is typically carried out at 37 °C. In this work, the DTT assay was performed at room temperature (22 ± 2 °C), in an effort to simplify the method. The comparison of assay results at room temperature (22 ± 2 °C) and 37 °C is shown in Figure 6.4A. At both temperatures, DTT reacts with 1,4-NQ at a similar rate.

The reaction duration was also studied. Method sensitivity increased as a function of reaction time with 25 min giving the steepest slope (Figure 6.4B). Further improvements at longer durations were not observed, primarily because the devices dried out consistently between 25 and 30 min. As a result, a 25 min reaction time was selected for further experiments. Longer drying times would be expected for more humid environments but no attempt was made to control this variable.

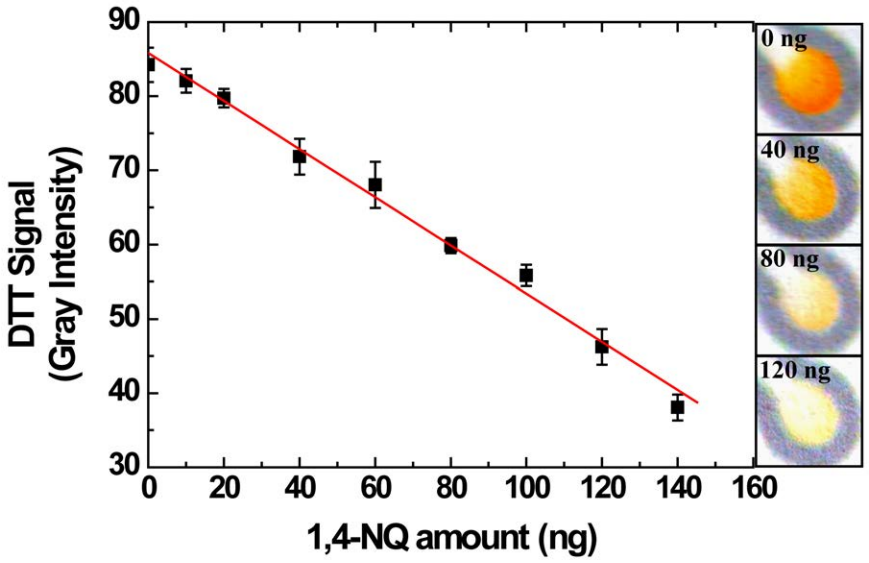

Figure 6.3. Typical dose response curve obtained from DTT assay plotted remaining DTT signal (gray intensity) as a function of 1,4-NQ model oxidant added to the assay (n=3).

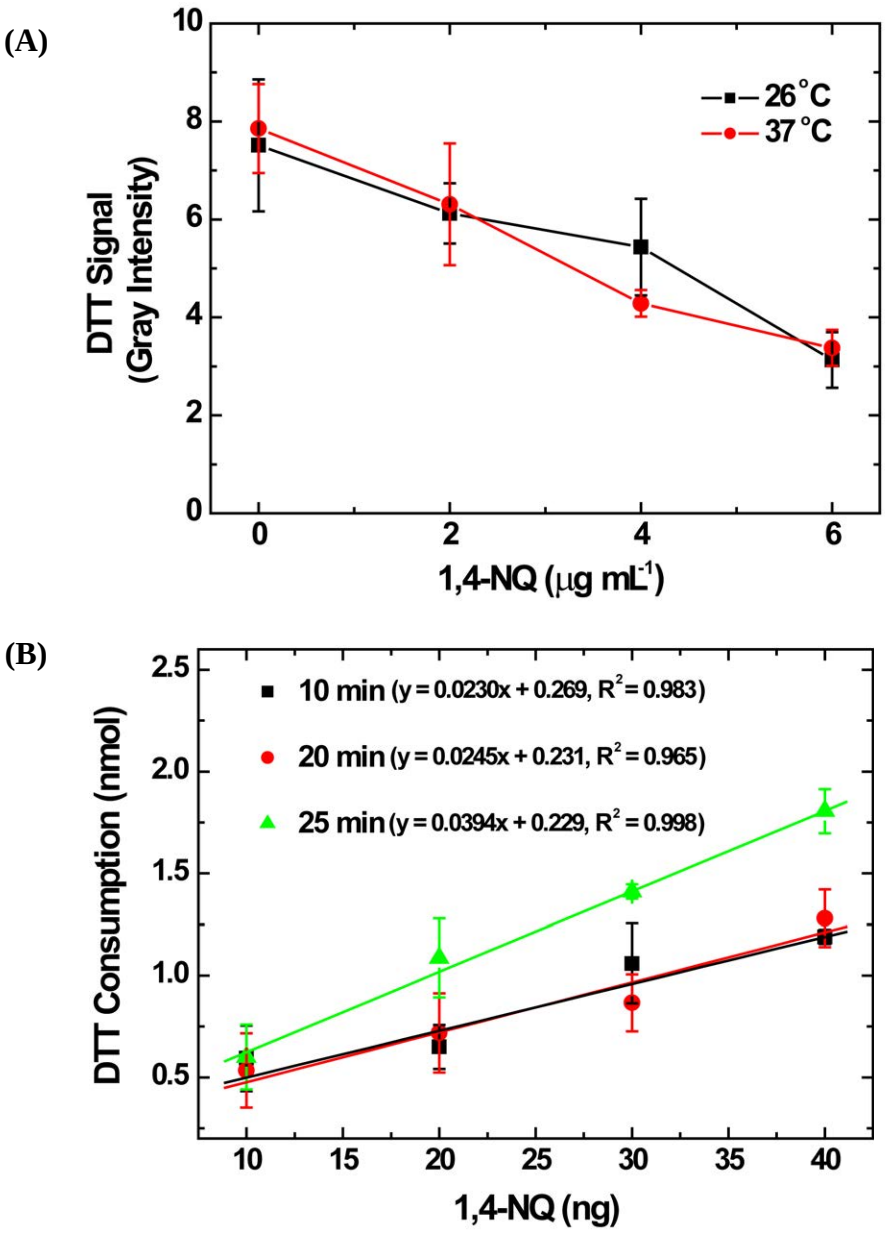

Figure 6.4. Optimization of DTT assay for analysis by μPAD using 1,4-NQ as a PM model oxidant (a) Reaction temperature study (b) Reaction time study.

Analytical Figures of Merit for 1,4-NQ

Once an optimized protocol was obtained, the analytical figures of merit for the device were determined, again using 1,4-NQ as a standard oxidant. Changing the initial proportion of DTT shifted the dose response curve as shown in Figure 6.5. At low initial DTT (2.5 nmol),

signal dropped quickly as a function of 1,4-NQ applied, providing the highest sensitivity of three conditions investigated. Unfortunately, this high sensitivity came at the cost of a small working range (0-20 ng of 1,4-NQ). Higher initial DTT (10 nmol) gave a lower sensitivity but provided a larger working range (0-140 ng of 1,4-NQ). The limit of detection, defined as the 1,4-NQ mass causing a decrease in the DTT signal three times the signal to noise ratio relative to the control, was found to depend on the starting amount of DTT. A lower initial DTT concentration provided a lower detection limit. Analytical figures of merit for DTT consumption are summarized in Table 1. Results shown here demonstrated that performance of the μPAD DTT assay can be adjusted by the choice of initial DTT amount. The assay sensitivity can also be modulated by changing the size of filter disk (from 3 to 10 mm diameter) and consequently changing PM mass on the filter as an alternative to varying the amount of DTT added.

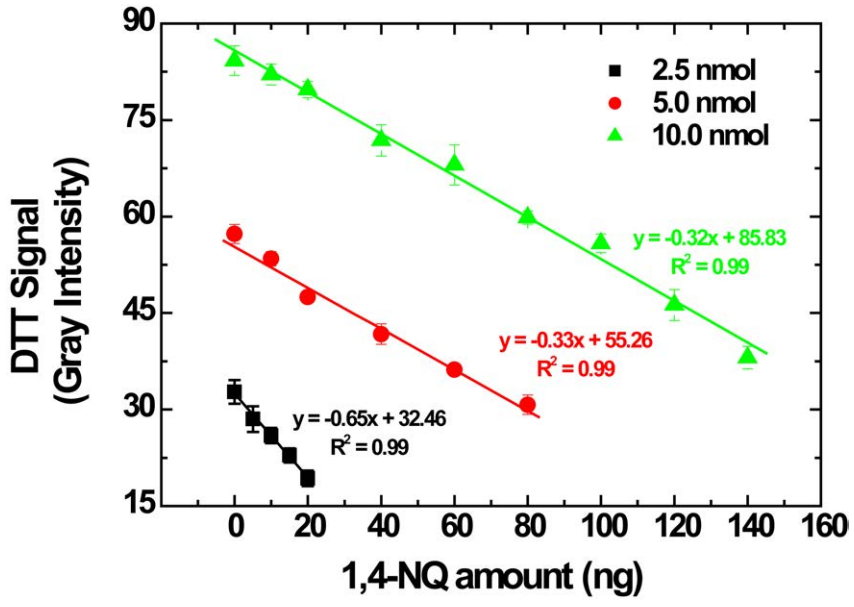

Figure 6.5. The impact of initial DTT amount on the assay sensitivity using 1,4-NQ as a model oxidant (n=3).

Method Validation

The μPAD was validated against the traditional DTT assay using 13 PM extracts taken from representative samples of urban dust, biomass burning, cigarette smoke and incense smoke. DTT consumption was measured using both methods and compared using linear regression (Figure 6.6). There was no significant difference in DTT consumption rate between the two methods based on a 95% confidence interval where the intercept and slope are not significantly different from 0 and 1, respectively (y = 1.105 (±0.159) x + 0.002 (±0.007), R^2 = 0.98).[49] The high degree of equivalence between the two methods shows that the μPAD DTT assay is appropriate for the analysis of oxidative activity from PM samples collected on filters. More importantly, however, the μPAD method requires approximately 10 times less aerosol mass and 100 times less reagent volume than the traditional DTT assay.[7,20,48,50] These improvements enable the analysis of PM oxidative activity on personal filter samples, which typically collect far less mass than area-samples or other high-volume techniques.

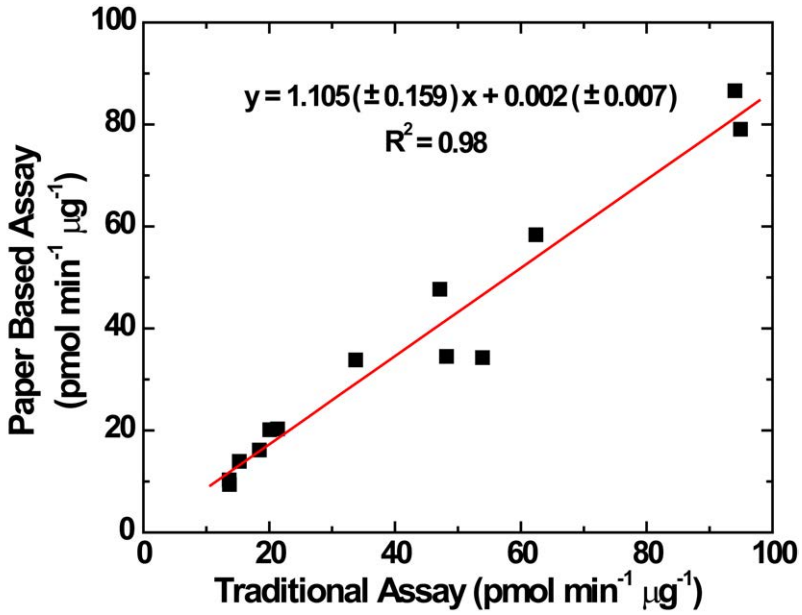

Figure 6.6. Comparison of PM oxidative activity (DTT consumption rate, pmol min^{-1} μg^{-1}) between the traditional DTT assay and paper based DTT assay. Data represent aqueous extracts of 13 different aerosol samples.

Personal Exposure Assessment

A final evaluation of this new technology was conducted using real-world, personal filter sampling. Three sampling periods were selected, each representing a different aerosol source: ambient outdoor air (a typical clean day in Fort Collins, CO), a wildfire-impacted day (smoky day), and indoor aerosol from a restaurant kitchen. For these tests, Teflon-coated glass-fiber filters (Pallflex® T60A20) filters were used in place of Whatman #1 filter paper, since the former provide a lower pressure drop to accommodate the personal sampling pump at 4 L min^{-1} of flow. However, SDS treatment was required to increase the hydrophilicity of the Teflon filter coating to promote sample mixing and subsequent elution. Without SDS, aqueous sample surface tension prevented capillary flow through the Teflon-coated glass-fiber matrix. We compared SDS-treated Pallflex® filters and standard Whatman#1 filters and saw no significant difference in

measured remaining DTT at the 95% confidence level using 11 different aerosol extracts (Figure 6.7).

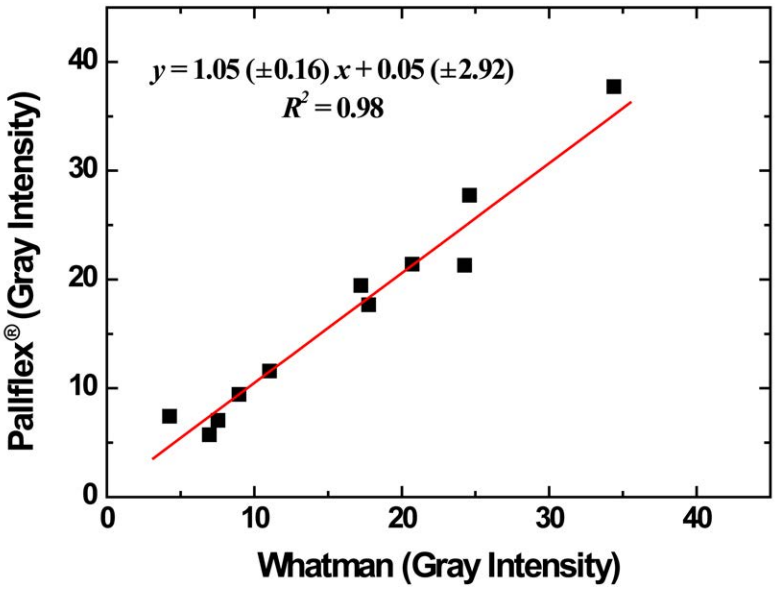

Figure 6.7. Comparison of the performance between Whatman#1 and Pallflex filter punches for aerosol oxidative activity by μPAD DTT assay. Shown are data from 11 different aerosol extracts. Filter handing and analysis procedures were identical, except that the Pallflex filter punch was treated with SDS prior to sample elution to increase filter hydrophilicity. No significant differences were detected between the two filter types at a 95% confidence interval (intercept: 0.05±2.92, slope: 1.05±0.16).

PM oxidative activity was quantified on all personal filter samples (Figure 6.8). Aerosol oxidative activity tended to be higher in the $PM_{2.5}$ size fraction (vs. PM_{10}), but these differences were not statistically significant. This is likely because $PM_{2.5}$ (a component of PM_{10}) constituted the majority of collected sample mass.[20,51,52] Typically, $PM_{2.5}$ is more reactive than PM_{10} because it has higher surface area per unit mass. Also, $PM_{2.5}$ is more likely to originate from anthropogenic sources (i.e., combustion) whereas PM_{10} has both anthropogenic and biogenic sources.[53] Relative aerosol reactivity (DTT consumption rate normalized by filter mass gain) was highest from samples collected on a smoky day in Fort Collins during the 2012 High Park

wildfire.[54] This finding coincided with the poor air quality reported throughout the Rocky Mountain region during this time when the air quality index in Fort Collins was reported as unhealthy for sensitive groups. In comparison to outdoor samples from other cities, the oxidative activity of PM collected on a clean day Fort Collins (5.5-6.3 pmol min^{-1} μg^{-1}) was substantially lower than values reported for ambient air in Los Angeles and in Mexico City (~20-50 pmol min^{-1} μg^{-1}). The oxidative activity on the smoky day Fort Collins (31.6-43.5 pmol min^{-1} μg^{-1}) was comparable to these urban environments, all of which are known to contain relatively higher levels of air pollution.[15,20]

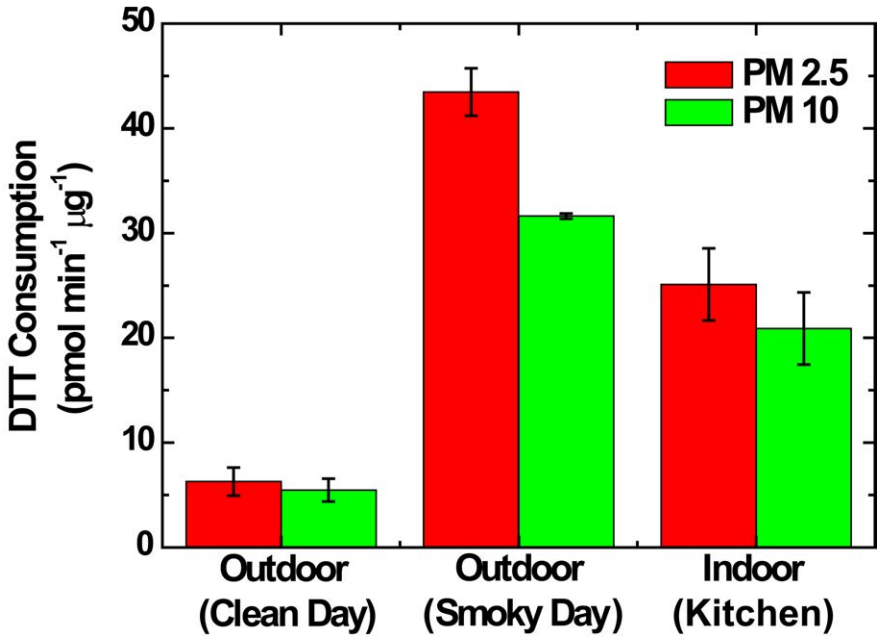

Figure 6.8. Oxidative activity of personal $PM_{2.5}$ (red bar) and PM_{10} (green bar) samples collected in various environments. Outdoor (clean day): PM collected on a typical day in Fort Collins, CO. Outdoor (smoky day): PM collected on a smoky day when the High Park wildfire (10 miles from Fort Collins, CO) was active. Indoor (Kitchen): PM collected in a restaurant kitchen.

Samples collected from the restaurant kitchen had higher oxidative activity than for samples collected outdoors on a relatively pollution-free day. This result was also expected, since cooking is a known source of indoor air pollution that can produce toxic PAHs, aldehydes,

and organic acids.[55-58] Outdoor PM levels in Fort Collins are typically below national ambient air quality standards set by the U.S. EPA.[59] However, for each of the personal samples, we cannot rule out the contribution from the air in each volunteer's home for these comparisons. Although we attempted to reduce sources of indoor air pollution that may be encountered at home (e.g., volunteers were asked to refrain from cooking and cleaning), we did not eliminate or control these exposures. Rather, the intent of the personal sampling campaign was to demonstrate applicability of the μPAD method for personal sampling and to investigate potential variability in 24-hr measures of PM oxidative activity when measured within the breathing-zone of individuals. Further investigation into how specific sources contribute to the inhalation of aerosol on a personal level is a promising avenue of future research (which has been enabled by the development of the μPAD technology described here).

These results clearly show our ability to use the inexpensive μPAD DTT assay to measure differences in PM reactivity based on personal sampling. Additionally, application of this technology is not limited to personal sampling but can also be applied to any filter-based method (e.g., area or high-volume sampling).

CONCLUSIONS

A microfluidic paper-based analytical device was developed to measure aerosol oxidative activity in the context of personal exposure assessment. Unlike current methods for PM oxidative activity that require whole-filter extracts and expensive laboratory equipment, the μPAD DTT assay was able to analyze oxidative activity directly from a filter without substantial handling and extraction steps. The μPAD analysis can be carried out in approximately 30 minutes using dramatically reduced sample mass and reagent volumes (compared to the

traditional DTT assay). When compared to the traditional DTT assay using 13 extracted aerosol samples, the μPAD DTT assay showed no significant difference. Application of the μPAD DTT assay to personal aerosol samples showed the highest oxidative activity on a wildfire-impacted day samples. The least reactive aerosol (by mass) was found when sampling outdoor air on a relatively pollution-free day in Fort Collins, CO. The μPAD developed here shows promise as a device for personal exposure studies of aerosol oxidative activity where a high number of samples are needed to better understand the impacts of PM on human health. The low-cost and ease-of-use of this μPAD technology shows promise for greater sample throughput (i.e., to support larger sample sizes given fixed resources) and also for application in more challenging sampling environments (i.e., the developing world).

REFERENCES

(1) Nel, A. *Science* **2005**, *308*, 804.
(2) Poschl, U. *Angew. Chem. Int. Edit.* **2005**, *44*, 7520.
(3) Sioutas, C.; Delfino, R. J.; Singh, M. *Environ. Health Perspect.* **2005**, *113*, 947.
(4) Mills, N. L.; Donaldson, K.; Hadoke, P. W.; Boon, N. A.; MacNee, W.; Cassee, F. R.; Sandstrom, T.; Blomberg, A.; Newby, D. E. *Nat. Clin. Prac. Cardiovasc. Med.* **2009**, *6*, 36.
(5) In *World Health Organization Fact Sheets*; http://www.who.int/mediacentre/factsheets/fs313/en/: Geneva, 2011; Vol. 2011.
(6) Araujo, J. A.; Barajas, B.; Kleinman, M.; Wang, X. P.; Bennett, B. J.; Gong, K. W.; Navab, M.; Harkema, J.; Sioutas, C.; Lusis, A. J.; Nel, A. E. *Circ. Res.* **2008**, *102*, 589.
(7) Li, N.; Sioutas, C.; Cho, A.; Schmitz, D.; Misra, C.; Sempf, J.; Wang, M. Y.; Oberley, T.; Froines, J.; Nel, A. *Environ. Health Perspect.* **2003**, *111*, 455.
(8) Limbach, L. K.; Wick, P.; Manser, P.; Grass, R. N.; Bruinink, A.; Stark, W. J. *Environ. Sci. Technol.* **2007**, *41*, 4158.
(9) Li, N.; Xia, T.; Nel, A. E. *Free Radic. Biol. Med.* **2008**, *44*, 1689.
(10) Rahman, I.; MacNee, W. *Am. J. Physiol.-Lung C.* **1999**, *277*, L1067.
(11) Vidrio, E.; Phuah, C. H.; Dillner, A. M.; Anastasio, C. *Environ. Sci. Technol.* **2009**, *43*, 922.
(12) Chung, M. Y.; Lazaro, R. A.; Lim, D.; Jackson, J.; Lyon, J.; Rendulic, D.; Hasson, A. S. *Environ. Sci. Technol.* **2006**, *40*, 4880.
(13) Hu, S.; Polidori, A.; Arhami, M.; Shafer, M. M.; Schauer, J. J.; Cho, A.; Sioutas, C. *Atmos. Chem. Phys.* **2008**, *8*, 6439.
(14) McWhinney, R. D.; Gao, S. S.; Zhou, S. M.; Abbatt, J. P. D. *Environ. Sci. Technol.* **2011**, *45*, 2131.
(15) Mugica, V.; Ortiz, E.; Molina, L.; De Vizcaya-Ruiz, A.; Nebot, A.; Quintana, R.; Aguilar, J.; Alcantara, E. *Atmos. Environ.* **2009**, *43*, 5068.
(16) Rattanavaraha, W.; Rosen, E.; Zhang, H. F.; Li, Q. F.; Pantong, K.; Kamens, R. M. *Atmos. Environ.* **2011**, *45*, 3848.
(17) Verma, V.; Ning, Z.; Cho, A. K.; Schauer, J. J.; Shafer, M. M.; Sioutas, C. *Atmos. Environ.* **2009**, *43*, 6360.
(18) Verma, V.; Pakbin, P.; Cheung, K. L.; Cho, A. K.; Schauer, J. J.; Shafer, M. M.; Kleinman, M. T.; Sioutas, C. *Atmos. Environ.* **2011**, *45*, 1025.
(19) Verma, V.; Polidori, A.; Schauer, J. J.; Shafer, M. M.; Cassee, F. R.; Sioutas, C. *Environ. Sci. Technol.* **2009**, *43*, 954.
(20) Cho, A. K.; Sioutas, C.; Miguel, A. H.; Kumagai, Y.; Schmitz, D. A.; Singh, M.; Eiguren-Fernandez, A.; Froines, J. R. *Environ. Res.* **2005**, *99*, 40.
(21) Wang, Y.; Arellanes, C.; Curtis, D. B.; Paulson, S. E. *Environ. Sci. Technol.* **2010**, *44*, 4070.
(22) Charrier, J.; Anastasio, C. *Atmos. Chem. Phys. Discuss* **2012**, *12*, 11317.
(23) Li, N.; Hao, M.; Phalen, R. F.; Hinds, W. C.; Nel, A. E. *Clin. Immunol.* **2003**, *109*, 250.
(24) Li, N.; Sioutas, C.; Cho, A.; Schmitz, D.; Misra, C.; Sempf, J.; Wang, M.; Oberley, T.; Froines, J.; Nel, A. *Environ. Health Perspect.* **2003**, *111*, 455.
(25) Li, N.; Wang, M. Y.; Bramble, L. A.; Schmitz, D. A.; Schauer, J. J.; Sioutas, C.; Harkema, J. R.; Nel, A. E. *Environ. Health Perspect.* **2009**, *117*, 1116.

(26) Sameenoi, Y.; Koehler, K.; Shapiro, J.; Boonsong, K.; Sun, Y.; Collett, J.; Volckens, J.; Henry, C. S. *J. Am. Chem. Soc.* **2012**, *134*, 10562.
(27) *Air pollution, the automobile, and public health*; National Academy Press: Washington, D.C., 1988.
(28) Jeng, H. A.; Pan, C. H.; Diawara, N.; Chang-Chien, G. P.; Lin, W. Y.; Huang, C. T.; Ho, C. K.; Wu, M. T. *Occup. Environ. Med.* **2011**, *68*, 653.
(29) Wei, Y.; Han, I.-K.; Hu, M.; Shao, M.; Zhang, J.; Tang, X. *Chemosphere* **2010**, *81*, 1280.
(30) Ruchirawat, M.; Navasumrit, P.; Settachan, D.; Tuntaviroon, J.; Buthbumrung, N.; Sharma, S. *Toxicol. Appl. Pharm.* **2005**, *206*, 207.
(31) Ruchirawat, M.; Mahidol, C.; Tangjarukij, C.; Pui-ock, S.; Jensen, O.; Kampeerawipakorn, O.; Tuntaviroon, J.; Aramphongphan, A.; Autrup, H. *Sci. Total Environ.* **2002**, *287*, 121.
(32) Martinez, A. W.; Phillips, S. T.; Butte, M. J.; Whitesides, G. M. *Angew. Chem.-Int. Edit.* **2007**, *46*, 1318.
(33) Martinez, A. W.; Phillips, S. T.; Carrilho, E.; Thomas, S. W.; Sindi, H.; Whitesides, G. M. *Anal. Chem.* **2008**, *80*, 3699.
(34) Bruzewicz, D. A.; Reches, M.; Whitesides, G. M. *Anal. Chem.* **2008**, *80*, 3387.
(35) Lu, Y.; Shi, W. W.; Jiang, L.; Qin, J. H.; Lin, B. C. *Electrophoresis* **2009**, *30*, 1497.
(36) Carrilho, E.; Martinez, A. W.; Whitesides, G. M. *Anal. Chem.* **2009**, *81*, 7091.
(37) Lu, Y.; Shi, W. W.; Qin, J. H.; Lin, B. C. *Anal. Chem.* **2010**, *82*, 329.
(38) Dungchai, W.; Chailapakul, O.; Henry, C. S. *Anal. Chim. Acta* **2010**, *674*, 227.
(39) Martinez, A. W.; Phillips, S. T.; Butte, M. J.; Whitesides, G. M. *Angew. Chem. Int. Ed. Engl.* **2007**, *46*, 1318.
(40) Dungchai, W.; Chailapakul, O.; Henry, C. S. *Anal. Chem.* **2009**, *81*, 5821.
(41) Zhao, W. A.; van den Berg, A. *Lab. Chip* **2008**, *8*, 1988.
(42) Mentele, M. M.; Cunningham, J.; Koehler, K.; Volckens, J.; Henry, C. S. *Anal. Chem.* **2012**, *84*, 4474.
(43) Jokerst, J. C.; Adkins, J. A.; Bisha, B.; Mentele, M. M.; Goodridge, L. D.; Henry, C. S. *Anal. Chem.* **2012**, *84*, 2900.
(44) Vella, S. J.; Beattie, P.; Cademartiri, R.; Laromaine, A.; Martinez, A. W.; Phillips, S. T.; Mirica, K. A.; Whitesides, G. M. *Anal. Chem.* **2012**, *84*, 2883.
(45) Martinez, A. W.; Phillips, S. T.; Whitesides, G. M.; Carrilho, E. *Anal. Chem.* **2010**, *82*, 3.
(46) Hennigan, C. J.; Miracolo, M. A.; Engelhart, G. J.; May, A. A.; Presto, A. A.; Lee, T.; Sullivan, A. P.; McMeeking, G. R.; Coe, H.; Wold, C. E.; Hao, W. M.; Gilman, J. B.; Kuster, W. C.; de Gouw, J.; Schichtel, B. A.; Collett Jr, J. L.; Kreidenweis, S. M.; Robinson, A. L. *Atmos. Chem. Phys. Discuss.* **2011**, *11*, 11995.
(47) Baumann, K.; Ift, F.; Zhao, J. Z.; Chameides, W. L. *J. Geophys. Res.-Atmos.* **2003**, *108*.
(48) Li, Q. F.; Wyatt, A.; Kamens, R. M. *Atmos. Environ.* **2009**, *43*, 1037.
(49) Miller, J. C. *Statistics for analytical chemistry*; E. Horwood Halsted Press: Chichester, England, 1988.
(50) Kumagai, Y.; Koide, S.; Taguchi, K.; Endo, A.; Nakai, Y.; Yoshikawa, T.; Shimojo, N. *Chem. Res. Toxicol.* **2002**, *15*, 483.
(51) Wallace, L. A.; Emmerich, S. J.; Howard-Reed, C. *Environ. Sci. Technol.* **2004**, *38*, 2304.
(52) Li, C. S.; Lin, W. H.; Jenq, F. T. *Environ. Int.* **1993**, *19*, 147.
(53) Koike, E.; Kobayashi, T. *Chemosphere* **2006**, *65*, 946.

(54) *FAQ ON HOW TO PROTECT YOUR RESPIRATORY HEALTH IN FORT COLLINS DURING HIGH PARK FIRE INCIDENT*, http://www.fcgov.com/airquality/pdf/_20120611_FAQ_FINAL_HighParkFire.pdf (accessed on 06/21/12).
(55) Fullana, A.; Carbonell-Barrachina, A. A.; Sidhu, S. *J. Agric. Food Chem.* **2004**, *52*, 5207.
(56) Hung, H. S.; Wu, W. J.; Cheng, Y. W.; Wu, T. C.; Chang, K. L.; Lee, H. *Mutat. Res.-Gen. Tox. En.* **2007**, *628*, 107.
(57) Lin, J. M.; Liou, S. J. *B. Environ. Contam. Tox.* **2000**, *64*, 817.
(58) Yang, S. C.; Jenq, S. N.; Kang, Z. C.; Lee, H. *Chem. Res. Toxicol.* **2000**, *13*, 1046.
(59) *Fort Collins Air Quality Report 2010*, http://www.fcgov.com/airquality/pdf/AAQR-2010.pdf?1312821338 (acessed on 06/03/12).

CHAPTER 7. DISSERTATION SUMMARY AND FUTURE DIRECTIONS

CHAPTER OVERVIEW

The last chapter of this doctoral dissertation presents a research summary as well as future directions for the projects presented in Chapters 2-6. The majority of research in this dissertation has generally focused on the development of methods for assessing oxidative stress caused by atmospheric aerosols, which contributed to the understanding of how air pollution affects human health. The first chapter focused on the development of a biological assay for multianalyte oxidative stress biomarkers using cleavable tag immunoassays (CTI) chemistry for assessing oxidative stress caused by particulate matter (PM) in cells as the ultimate goal. Chapter 3-5 described the development toward on-line monitoring of aerosol oxidative activity using a microfluidic electrochemical sensor. Chapter 6 presented the discussion of method development for aerosol oxidative activity for personal exposure studies by employing a microfluidic paper-based analytical device. Synopses of this research as well as short-term, intermediate, and long-term directions of this work are given in the following text.

SUMMARY AND FUTURE DIRECTIONS

The success of method development for assessing oxidative stress caused by atmospheric aerosols would contribute to the better understanding of mechanisms for how air pollution causes adverse human health. Chapter 2 describes a biological assay developed called cleavable tag immunoassay (CTI) for the ultimate goal of measuring multiple oxidative biomarkers in a single run. As a first step toward this goal, CTI in competitive, non-competitive, and mixed competitive/non-competitive formats were evaluated for the detection of inflammation

biomarkers. Thyroxine (T4) and 3-nitrotyrosine (3-NT) were analyzed to demonstrate for the first time the proof-of-principle for multi-analyte competitive CTI. C-reactive protein (CRP) was successfully analyzed by non-competitive CTI. Finally, analysis of CRP and 3-NT were conducted in mixed mode competitive/non-competitive CTI to demonstrate that CTI can be applied for measuring proteins and small molecules simultaneously. This assay gives a promising method for screening small molecules and protein oxidative stress biomarkers. Its application is not limited to only a small class of biomarkers but can be used for any applications that require a multi-analyte analysis screening system. This novel assay provides much lower analysis time, sample consumption, and cost of analysis compared to the traditional immunoassays.

Future direction for the CTI project would be the analysis of a higher number of oxidative stress biomarkers including small molecules and proteins simultaneously to demonstrate the performance of the CTI more fully. The oxidative stress makers of interest would be, for example, F2-isoprostanes, malondialdehyde, 8-hydroxy-2-deoxyguanosine (8-OHdG), 3-nitrotyrosine (3-NT), glutathione (GSH), catalase (CAT), glutathione peroxidase (GPx), and superoxide dismutase (SOD). The higher the number of analytes investigated, the larger cleavable tag library needed. These tags would be in the FRB (structure provided in Chapter 2) analogues tags where homo-bifunctional amines can be used to generate various spacers. These differences in spacers allow the separation by MCE after cleavage from the analytes for the detection. Possible homobifunctional amines that can create different spacers of the fluorescent tags would be, for example, *m*-xylene diamine, 1,4-diaminobutane, 1,3-diaminopropane, and *trans*-1,2-diaminocyclohexane. MCE separation conditions of these tags need to be evaluated to provide effective separation. Then, to apply the developed CTI for real

sample analysis, cells/tissues that has been exposed to the PM will be analyzed for oxidative stress biomarkers. Exposure experiments and cell sample preparations for analysis of the markers have been described previously.[1-5] Some sample preparation artifacts might still be found here. The long term goal for this project would be the integration of all steps in the CTI procedure in one device including cell culture, cell exposure to the PM and detection of oxidative stress makers released from the cells by CTI chemistry. This sampling, exposure, and analysis system would provide the on-line analysis of oxidative stress biomarkers in cell culture without the need of complicated sample preparation resulting in the decomposition of oxidative stress markers. To do this, briefly, the cell line such as C6 Glial cell line normally used to study neurological tumors and relatively easy to be grown and maintained in culture will be grown in the microfluidic chamber.[6,7] A procedure to grow the cells in the microfluidic device has been reported in the literature.[8-10] After culturing, the chip chamber will be exposed to the artificial PM created in the aerosol chamber. The CTI assay will be perform on chip by directing fluorescently tagged antibodies over the cells and then analyzing the cleaved tag and by on-chip MCE. Major work for this proposed system will be the chip design and testing process to accommodate all steps mentioned above. If successful, this would significantly impact our understanding of how PM affects biological samples and provide a direct link to understand the effect of PM on human health.

Chapters 3-5 described steps of method development toward on-line monitoring instrument for aerosol oxidative activity by a microfluidic electrochemical sensor. Chapter 3 described a novel fabrication method as well as a new electrode composition employing a mixed PDMS-mineral oil binder for low cost, patternable, highly robust, carbon paste electrodes to create the microfluidic electrochemical sensor. This sensor has been extensively used for on-line

monitoring of aerosol oxidative activity as described in Chapters 4 and 5. The robustness of the electrode was achieved from the cross-linking of PDMS between the electrode and PDMS microfluidic chip. Selectivity of the sensor can be tuned for detection of interested analytes by modifying the carbon paste with dopants. Both chemical (CoPC) and physical (MWCNT) modified carbon paste electrodes (CPE) were demonstrated for increasing the detection capability for thiols and catecholamines (dopamine), respectively. Furthermore, the mixed binder CPEs did not exhibit electrode fouling when performing analysis in complex biological matrices including RBC lysate (thiol detection) and PC12 cell supernatant (detection of catecholamine release). This electrochemical chip is readily adaptable, can be applied to various electrode materials and is amenable to chemical and physical modification to improve electrochemical properties.

Future direction for this sensor would be both improvement of electrode performance and expanding application of the sensor to other areas besides measuring aerosol oxidative activity. Increasing electrode area by designing bigger channel on the PDMS slab would increase the signal response of the analyte as shown in the Randles-Sevcik equation. To create more robust electrodes on the microfluidic device, the fabricated electrode on chip might need to be hard baked to facilitate the crosslinking to the PDMS chip. Chemical and physical modifications from various materials might need to be employed depending on the applications to enhance the performance of the electrode for specific electrochemical species. Long term, the applications would included environmental, clinical, and biological fields.

Chapters 4-5 described the application of the invented microfluidic electrochemical sensor for the analysis of oxidative activity caused by atmospheric aerosols in an on-line format as an ultimate goal. Chapter 5 dealt with the application of the sensor for the analysis of aerosol

oxidative activity based on the dithiothreitol (DTT) assay. This work presented for the first time demonstrated the highest temporal resolution on-line sampling/analysis system for aerosol oxidative activity using a microfluidic electrochemical sensor coupled with the PILS as an on-line PM collection system. The determination of aerosol oxidative activity was based on the widely reported DTT assay but used electrochemical detection instead of absorption detection to detect the remaining DTT after catalytically oxidized by the PM for a specific time period. Analysis of PM samples created in the chamber was carried out and showed high correlation between aerosol concentration and DTT consumption rate (oxidative activity) for two representative test aerosols, fly ash and urban dust aerosol samples. This on-line sampling/analysis system showed potential as an ultimate tool for field studies of aerosol oxidative activity. Chapter 6 described the application of the microfluidic electrochemical sensor to measure aerosol activity to generate hydroxyl radicals, one of the most potent free radicals causing oxidative stress in affected cells. The analysis is based on a salicylic acid trapping method in which hydroxyl radicals generated from the PM, typically via Fenton chemistry, react with salicylic acid and produce dyhydroxybenzoic acid (DHBA), which is detected electrochemically by the microfluidic electrochemical sensor. The ultimate goal of this work is to create an on-line sampling/analysis system similar to what was demonstrated in the Chapter 5. As an initial step toward this goal, this chapter described optimization steps using off-line analysis as described in Chapter 5. Optimization parameters, including electrode material composition, reaction pH, reaction time, and key reagent amounts to participate in the reaction using iron (II) as standard hydroxyl radical generators, were investigated to improve sensitivity and the detection limit for the analysis. Further investigation in the short term needs to be conducted for real PM sample analysis as well as method validation against HPLC detection

methods to study the performance of the system for analyzing hydroxyl radicals generated from aerosols.[11,12]

Intermediate directions for this on-line sampling/analysis system to more fully assess aerosol oxidative activity would be to combine the two assays described in Chapter 4 and 5 to perform in an on-line format. This system will provide us information on aerosol oxidative activity (DTT assay) and aerosol ability to generate hydroxyl radicals (salicylic acid trapping assay) simultaneously. To do this, briefly, the PM created in the chamber is collected by the PILS and directed to the two sample lines connected to the impaction plate of the PILS. In one sample line, a syringe pump is used to direct the DTT to mix with the PM in the sample line through the T-valve. In the other sample line, a mixture of salicylic acid and H_2O_2 is added using a similar approach as on-line DTT assay. In one of these sampling lines, the internal standard (LiF) is collected at the end of the line and analyzed off-line by ion chromatography. After reacted for a specific time period through the sample line, the products will be detected using microfluidic electrochemical sensors, one for remaining DTT detection (DTT assay) and the other for DHBA detection (salicylic acid trapping assay). If successful, this would provide extremely useful system for information of oxidative activity and hydroxyl radicals generated from aerosol with high temporal resolution. Long-term direction of this work would be the application of this system for on-site aerosol oxidative activity analysis in the area of interest. Collaboration with aerosol scientists, environmental public health scientists, and analytical chemists should be done to conduct studies of the mechanisms of how PM affected human health using this proposed system.

The last project of this dissertation, described in Chapter 6, presented the development of microfluidic paper-based analytical devices (μPAD) for assessing oxidative activity caused by

atmospheric aerosols based on the DTT assay applied for personal exposure assessment. Unlike current methods that require high amount of PM mass, whole-filter extracts, and expensive laboratory equipment, the μPAD DTT assay was able to analyze oxidative activity directly from a filter without extensive handling and extraction steps, thus reducing sampling artifacts. The analysis time using μPAD is approximately 30 minutes using dramatically reduced sample mass and reagent volumes (compared to the traditional DTT assay). The performance of μPADs was evaluated against the traditional DTT assay using 13 different aerosol types and no significant differences were found. Application to personal exposure samples collected from 3 different events including an outdoor clean-air day, a wildfire-impacted day, and an indoor restaurant kitchen were accomplished, where the wildfire-impacted day samples showed the highest aerosol oxidative activity. The μPAD developed here shows promise as a device for personal exposure studies of aerosol oxidative activity where a high number of samples are needed to better understand the impacts of PM on human health. Furthermore, the device is not limited to only PM filter collected from personal sampler but it can be applied for any studies that use filter-based PM collection methods. With a high volume collector, higher temporal resolution for the analysis of area-based study can be obtained using this low-mass analytical device.

Future direction of this work would incude the application of the μPAD for analysing PM samples collected by filter-based sampling methods from specific events of interest. The study of aerosol oxidative activity in samples collected by a personal sampler during the High Park wildfire period in Colorado during summer 2012 is currently being conducted in our lab. Aerosol oxidative activity analyzed by μPAD together with the analysis of PM compositions (e.g. levoglucosan, potassium ion, transition metals) will help us to better understand the toxicity of PM from wildfire burning. Long-term direction would be the application of the μPAD for

aerosol oxidative activity assessment of the polluted atmospheres in Thailand including Bangkok (traffic affected), Chiangmai (wildfire burning affected) and some industrial sites (power plants, oil refinery affected).[13]

REFERENCES

(1) Li, N.; Sioutas, C.; Cho, A.; Schmitz, D.; Misra, C.; Sempf, J.; Wang, M.; Oberley, T.; Froines, J.; Nel, A. *Environ. Health Perspect.* **2003**, *111*, 455.

(2) Donaldson, K.; Brown, D.; Clouter, A.; Duffin, R.; MacNee, W.; Renwick, L.; Tran, L.; Stone, V. *J. Aerosol Med.-Depos. Clear. Eff. Lung* **2002**, *15*, 213.

(3) Donaldson, K.; Stone, V.; Borm, P. J. A.; Jimenez, L. A.; Gilmour, P. S.; Schins, R. P. F.; Knaapen, A. M.; Rahman, I.; Faux, S. P.; Brown, D. M.; MacNee, W. *Free Radic. Biol. Med.* **2003**, *34*, 1369.

(4) Foucaud, L.; Wilson, M. R.; Brown, D. M.; Stone, V. *Toxicol. Lett.* **2007**, *174*, 1.

(5) Halliwell, B.; Whiteman, M. *Brit. J. Pharmacol.* **2004**, *142*, 231.

(6) Sak, K.; Illes, P. *Neurochem. Int.* **2005**, *47*, 401.

(7) Grobben, B.; De Deyn, P. P.; Slegers, H. *Cell Tissue Res.* **2002**, *310*, 257.

(8) Tourovskaia, A.; Figueroa-Masot, X.; Folch, A. *Lab Chip* **2005**, *5*, 14.

(9) Hung, P. J.; Lee, P. J.; Sabounchi, P.; Aghdam, N.; Lin, R.; Lee, L. P. *Lab Chip* **2005**, *5*, 44.

(10) Hung, P. J.; Lee, P. J.; Sabounchi, P.; Lin, R.; Lee, L. P. *Biotechnol. Bioeng.* **2005**, *89*, 1.

(11) Gruber, M.; Wiesner, G.; Burger, R.; Lindner, R. *J. Chromatogr. B Analyt. Technol. Biomed. Life Sci.* **2006**, *831*, 320.

(12) Liu, J.; Steinberg, S. M.; Johnson, B. J. *Chemosphere* **2003**, *52*, 815.

(13) Vichit-Vadakan, N.; Vajanapoom, N. *Environ. Health Perspect.* **2011**, *119*.